CLIMATE DRIVERS AND LANDSCAPE RESPONSE: HOLOCENE FIRE, VEGETATION, AND EROSION AT CITY OF ROCKS NATIONAL RESERVE, IDAHO

By

Kerrie N. Weppner

A thesis

submitted in partial fulfillment

of the requirements for the degree of

Master of Science in Hydrologic Sciences

Boise State University

May 2012

BOISE STATE UNIVERSITY GRADUATE COLLEGE

DEFENSE COMMITTEE AND FINAL READING APPROVALS

of the thesis submitted by

Kerrie N. Weppner

Thesis Title: Climate Drivers and Landscape Response: Holocene Fire, Vegetation, and Erosion at City of Rocks National Reserve, Idaho

Date of Final Oral Examination: 07 March 2012

The following individuals read and discussed the thesis submitted by student Kerrie N. Weppner, and they evaluated her presentation and response to questions during the final oral examination. They found that the student passed the final oral examination.

Jen Pierce, Ph.D.	Chair, Supervisory Committee
Julio Betancourt, Ph.D.	Member, Supervisory Committee
Doug Shinneman, Ph.D.	Member, Supervisory Committee
David Wilkins, Ph.D.	Member, Supervisory Committee

The final reading approval of the thesis was granted by Jen Pierce, Ph.D., Chair of the Supervisory Committee. The thesis was approved for the Graduate College by John R. Pelton, Ph.D., Dean of the Graduate College.

DEDICATION

I dedicate this thesis to my husband, Justin Nielsen, and to my daughter, Leidy. Thank you for your love and encouragement.

ACKNOWLEDGEMENTS

First and foremost, I would like to express my sincere gratitude to my advisor, Dr. Jen Pierce, who provided guidance, excellent instruction, and constant encouragement. I would also like to thank my committee members; Dr. Julio Betancourt, Dr. Dave Wilkins and Dr. Doug Shinneman, who dedicated time to this project and offered invaluable insight.

I would like to acknowledge Boise State University and the Department of Geosciences for accepting me into the Hydrologic Sciences program, offering me financial support through a teaching assistantship, and equipping me with necessary tools to successfully conduct this research. This project was also supported by the Idaho EPSCoR Program and by the National Science Foundation under award number EPS-0814387, the Bureau of Land Management, the United States Geological Survey, and, City of Rocks National Reserve.

Special thanks to everyone at the City of Rocks National Reserve, Wallace Keck, Superintendant at the City of Rocks National Reserve, for supporting and facilitating this research, Kristen Bastis for research assistance and companionship, and Juanita Jones for taking care of all of my camping needs!

I would also like to thank Dr. Lesley Morris, for her great advice and my field assistant, Austin Hopkins, for his strong back and excellent shoveling skills. Lastly, I must thank my family who helped with child care and supported me in many other ways.

ABSTRACT

Climate exerts primary control over vegetation and fire occurrence but landscape structure, vegetation type, and density determine fire pattern, frequency and severity (i.e., fire regime), and the nature of fire-related geomorphic response. To explore these relationships, we compare alluvial charcoal records of fire and fire-related sedimentation with a woodrat midden reconstruction of vegetation at the northern migration front for single-leaf pinyon and Utah juniper at City of Rocks National Reserve (CIRO), south-central Idaho.

Radiocarbon ages from 37 charcoal macrofossils sampled from discrete fire-related deposits indicate five episodes of increased fire activity over the past ~11 ka. Fires burned following deglaciation (10,700-9500 cal yr BP), and later during prolonged drought (7200-6700 cal yr BP). A moderate fire interval (2400-2000 cal yr BP) followed arrivals of Utah juniper (~3800 cal yr BP) and single-leaf pinyon (~2800 cal yr BP). Fire activity increased as pinyon-juniper expanded (850-700 and 550-400 cal yr BP), and fire peaks during this interval correspond to decadal droughts. No fires were recorded during extended wetter conditions (~9500-7200 cal yr BP) and fires were also infrequent during an interval of dry but relatively stable climate (~6700-4700 cal yr BP), suggesting a fire regime shift from a moisture-limited system to a fuel-limited system likely occurred during the mid-Holocene.

Characteristics of Holocene fire-related deposits also provide information about past fire severity and landscape characteristics. Gently sloping terrain (mean slope <16°) and clay-poor colluvium at CIRO make debris flow development unlikely; rather, sediment-rich, low-volume sheetfloods from unburned basins dominate the modern response to storm events. Alluvial stratigraphic sections also record small sheetflooding events ~6500-2500 cal yr BP, which account for only 4% of measured alluvial stratigraphic thickness. This suggests a prolonged interval of minimal erosion, when drier, warmer mid-Holocene climate and low vegetation densities suppressed both severe fires and colluvial storage of sediment needed for debris flow development. However, our record indicates large fire-related debris flows were common during early and late Holocene. After ~4000 cal yr BP, higher vegetation densities (inferred from midden radiocarbon ages) re-stabilized hillslopes and increased colluvial storage, as indicated by post ~2200 cal yr BP soil horizon development. This, combined with frequent fires of expanding pinyon-juniper woodlands, likely triggered episodic post-wildfire debris flows.

TABLE OF CONTENTS

LIST OF TABLES

LIST OF FIGURES

INTRODUCTION

In recent decades, extreme droughts, decreasing snowpacks, earlier snow melts and earlier onset of plant growth (Stewart et al., 2004; Mote et al., 2006; Kunkel and Pierce, 2010; Pederson et al., 2011) have intensified fire frequency, severity, and size across a range of ecosystems in the western U.S. (e.g., Flannigan et al., 2000; Westerling et al., 2006). Climate models forced by projected increases in greenhouse gases suggest 2-5° C mean spring temperature increases in the western U.S. by 2100 (Abatzoglou and Redmond, 2007). Predicted increases in spring temperatures and summer droughts and the subsequent increase in occurrences of large fires will likely increase post-fire flooding and erosion, incur costly damages to property and infrastructure, undermine conservation efforts, impact water resources and forest products, and possibly transform ecosystems (Westerling et al., 2006, 2011). Our ability to predict and prepare for such changes hinges on our understanding of how climate drives shifts in vegetation, fire regimes, and fire-related erosion. Most fire studies have focused on forested ecosystems since fire records from semiarid ecosystems are limited due to sparse trees for fire scar records and a paucity of lakes with charcoal sediments. Paleoecological studies of past vegetation and fire regimes from a range of ecosystems can help elucidate likely effects of projected changes in climate on fire regime shifts and vegetation dynamics.

While climate ultimately governs vegetation and fire occurrence (Westerling et al., 2006), vegetation type, fuel availability, and continuity primarily control fire frequency and severity (i.e., fire regime; Baker, 2009). These complex relationships vary

temporally (e.g., Pierce et al., 2004; Whitlock et al., 2010), and across ecosystems (Littell et al., 2009). Over annual timescales, climate controls fuel availability and moisture content (Swetnam and Betancourt, 1998; Heyerdahl et al., 2002; Westerling et al., 2006), while over decadal to multi-centennial timescales, climate modulates the composition and structure of plant populations, and the associated fire regime (Grissino-Mayer and Swetnam, 2000; Whitlock et al., 2003; Mensing et al., 2006).

Wildfire is a primary driver of enhanced hillslope erosion in both modern (e.g., Cannon et al., 2001; Jackson and Roering, 2009) and paleo-records (e.g., Meyer et al., 1995; Pierce et al., 2004). The nature of the fire-related erosional response is controlled by basin geomorphic features (topography and slope), basin lithology (Cannon and Reneau, 2000; Cannon et al., 2001, 2010), and vegetation type and density (e.g., Wilcox et al., 2011). Fire removal of vegetation, addition of fine-grained ash, and development of hydrophobic soil layers (DeBano, 2000) likely push the erosional responses past geomorphic thresholds. In granitic terrain, fire may shift the erosional response from frequent sheetflooding (Blair, 1999) to episodic, and more catastrophic, debris flows.

The relationship between large fires and drought for many ecosystem types is evident in both historic and Holocene-scale records (e.g., Meyer et al., 1995; Flannigan et al., 2000; Westerling et al., 2006). Likewise, modern and historic relationships between vegetation type, associated fire regime (as summarized in Baker, 2009), and geomorphic response (Cannon et al., 2001, 2010) are also generally understood. However, a key research question about the influence of vegetation change on fire regimes remains unresolved. Specifically, which comes first, the shift in fire regime or the change in vegetation? How are these dynamics manifested in the stratigraphic record? How can

these past relationships be extrapolated to the future? To answer these questions, this study employs a novel combination of geomorphology and paleoecology. We use alluvial charcoal records and woodrat midden records to reconstruct contemporaneous changes in vegetation, fire, and alluvial histories along the leading edge of a relatively recent (~4-2 ka) plant species migration at the City of Rocks National Reserve (CIRO) in south-central Idaho.

CIRO is located in the transition between woodland and steppe, at or near the northern limits of single-leaf pinyon (*Pinus monophylla*) and Utah juniper (*Juniperus osteosperma*; Little, 1971), and between north-south opposing precipitation responses to Pacific climate variability (Dettinger et al., 1998). Granitic bedrock at CIRO has weathered to form majestic domes and spires. Incision of the easily-mobilized, grussy colluvium affords excellent exposure of stratigraphy that incorporates both the fire history from alluvial charcoal and the related alluvial process, including the occurrence of sheetfloods and debris flows (e.g., Meyer et al., 1995; Pierce et al., 2004). Woodrat middens preserved in numerous rock crevices and shelters at CIRO contain fossilized vegetation and pollen collected from around the animals' nests. Middens allow detailed reconstruction of vegetation and plant migration history (e.g., Betancourt et al., 1991). The main hypothesis tested in this study is that Holocene vegetation changes, and specifically local colonization and expansion by single-leaf pinyon and Utah juniper, triggered shifts in both fire occurrence and fire-related sedimentation. This study provides useful insight about the response of fire and erosion to projected plant migrations under changing climate.

STUDY AREA

Description, Modern Climate, and Geology

The City of Rocks National Reserve and nearby Castle Rocks State Park are located in the Albion Range of south-central Idaho in the northeastern Great Basin Desert Region, approximately 60 km northwest of the Great Salt Lake, Utah (Figure 1). The study area is characterized by gentle to moderate slopes, with a mean slope of 15.6°, and spans an elevation range of 1600-2700 m.

Geologically, CIRO is comprised predominantly of Oligocene (29 Ma) Almo Pluton granite, which has eroded to form magnificent fins, domes, and spires. The pluton intruded Proterozoic (1.6 Ga) Green Creek Complex metasediments and Archean (2.5 Ga) granitic gneiss. The pluton and uplifted basement rocks are ringed by exposures of Proterozoic Elba quartzite and sparsely capped with Miocene rhyolitic tuff (Miller and Bedford, 1999; Miller et al., 2008; Pogue and Katz, 2008; Figure 2). Mechanical and chemical weathering and erosion of the Almo Pluton granite has blanketed much of the gently sloping terrain with a thick grussy mantle (Pogue and Katz, 2008). Active incision reveals excellent exposures of fire-related alluvial stratigraphy.

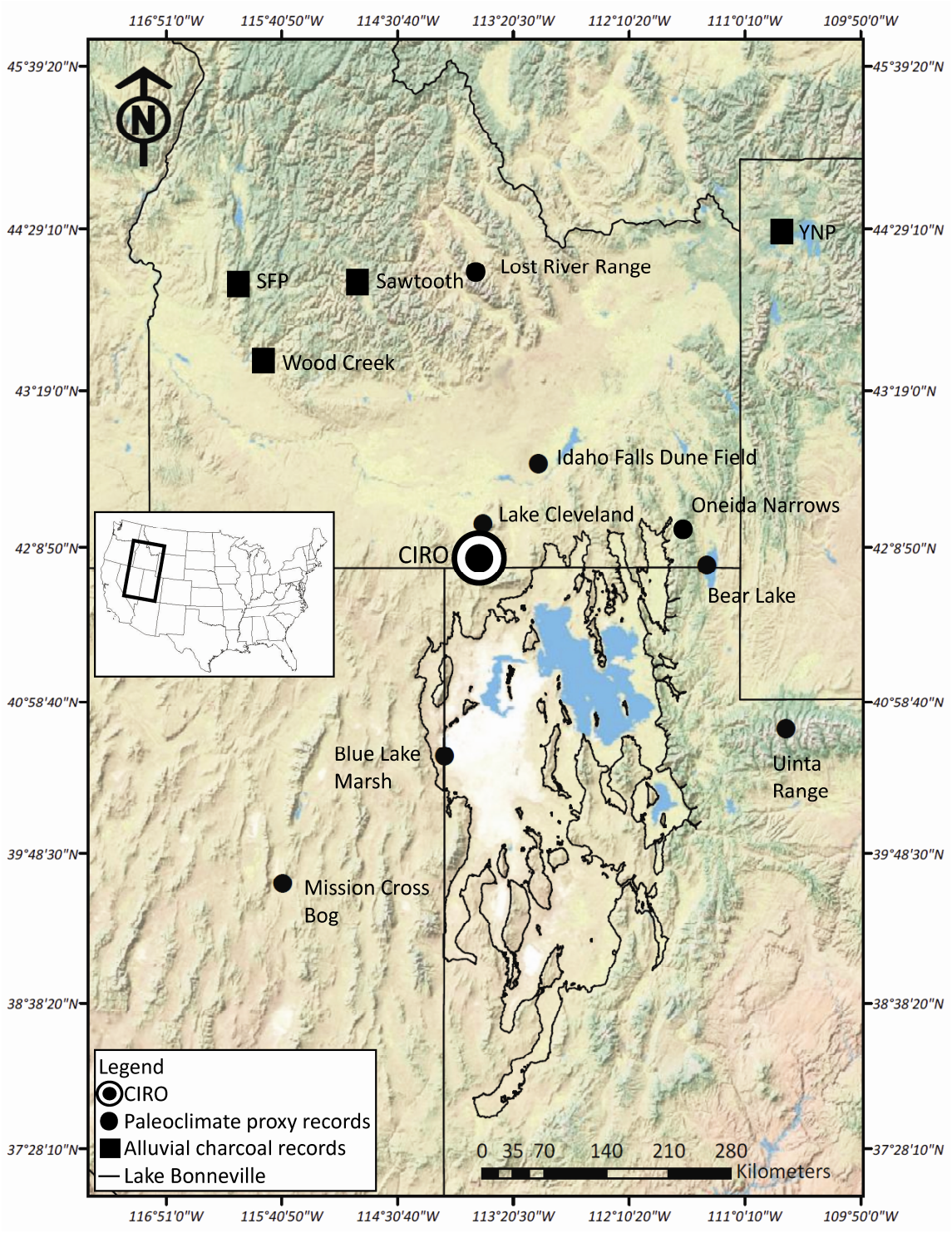

Figure 1: Map showing location of CIRO relative to the Bonneville Basin, regional paleoclimate proxy record sites and alluvial charcoal record sites used for comparison in this study. The Lake Bonneville outline shows the approximate extent of the Bonneville highstand (20,000-16,000 yrs BP; Automated Georeference Center, 2001).

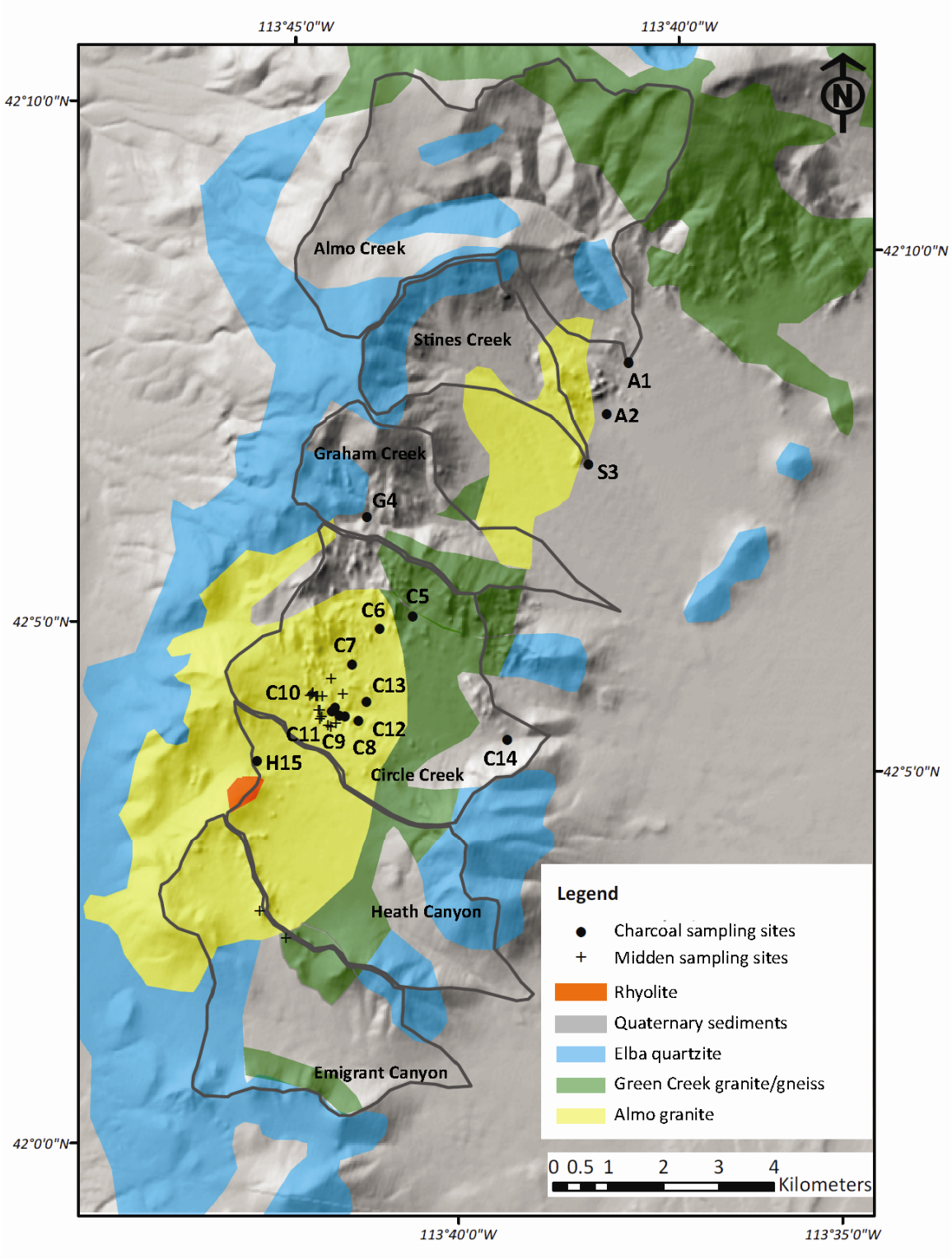

Figure 2: Geologic map of CIRO (Miller and Bedford, 1999; Ludington et al., 2006).

The study area consists of six headwater basins of varying lithologies that drain into the Raft River, a tributary of the Snake River, Idaho. The basins are shown in Figure 3 and are oriented north to south as follows:

1. Almo Creek drains 57.9 km^2 and is composed of quartzite to the west and gneiss to the east.
2. Stines Creek drains 6.9 km^2 and is composed of quartzite to the west and granite to the south.
3. Graham Creek drains 8 km^2 and is composed of quartzite to the west, granite to the east, and gneiss to the south.
4. Circle Creek drains 17.4 km^2 and is composed of granite and a fin of gneiss to the east.
5. Heath Canyon drains 13.9 km^2, and is composed of granite to the north and quartzite to the south.
6. Emigrant Canyon drains 13.3 km^2, and is composed of quartzite.

Mean annual precipitation at CIRO is 280 mm, peaking in April through June (Western Regional Climate Center). The majority (60%) of annual precipitation falls as snow (Western Regional Climate Center). Located at 42° N, CIRO lies in the transition between opposing modes of precipitation responses to Pacific variability (El Nino Southern Oscillation and Pacific Decadal Oscillation). Using both instrumental and tree-ring data from the western U.S., Dettinger et al. (1998) identified a north-south seesaw of precipitation that pivots near 40-42° N and manifests at many timescales (e.g., Brown and Comrie, 2004; Pederson et al., 2011).

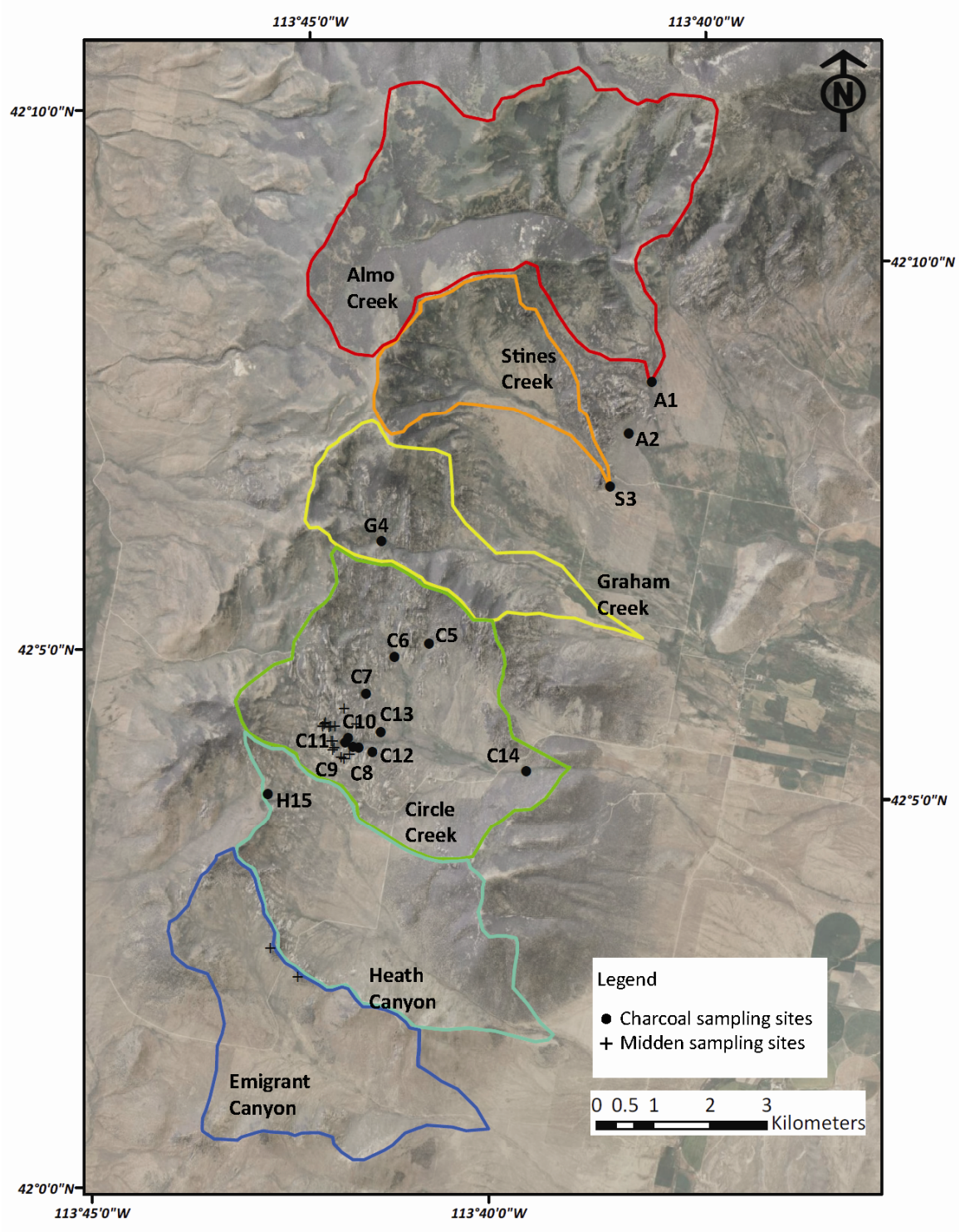

Figure 3: Study area map showing the six drainage basins at CIRO, charcoal sampling sites, and midden sampling sites.

Vegetation

CIRO is a floristically diverse woodland-steppe ecotone, with over 450 documented plant species (John, 1993). Lower elevations (<1800 m) are dominated by big sagebrush (*Artemisia tridentata)* and antelope bitterbrush (*Purshia tridentata*) with an understory of several native and non-native bunch grasses. Single-leaf pinyon (*Pinus monophylla*) dominates lower to middle elevations (1600-2000 m), along with Utah juniper *(Juniperus osteosperma)*, and Rocky Mountain juniper *(Juniperus scopulorum).*

Co-occurrence of single-leaf pinyon and limber pine (*Pinus flexilis*) at CIRO is unusual in the Great Basin (Thomas and Packham, 2007) and probably represents late Holocene pinyon colonization of intermediate elevations (1600-2000 m) gradually being vacated by postglacial contraction of limber pine (Thompson, 1990). In this location, limber pine may represent a relict species from the Last Glacial Maximum (LGM), a time when modeled projections indicate that average regional temperatures were ~5° C cooler (Schmittner et al., 2011) and average regional precipitation was increased by ~100-200 mm/year (Braconnot et al., 2007). Figure 4 illustrates the maximum and minimum mean annual precipitation and temperatures where these trees and shrubs are found today (Thompson et al., 1999) and the modern vs. modeled LGM temperature and precipitation at CIRO.

Patches of mountain mahogany *(Cercocarpus ledifolious)* and aspen groves *(Populus tremuloides)* grow at middle to upper elevations (>1800 m). At upper elevations (>2000 m), in the northern portion of CIRO, subalpine fir *(Abies lasiocarpa),* lodgepole pine *(Pinus contorta),* limber pine, and Douglas fir *(Pseudotsuga menziesii)* are found. The reserve is dissected by riparian habitat that includes Rocky Mountain maple *(Acer*

glabrum), box elder *(Acer negundo),* redosier dogwood *(Cornus sericea),* and narrow leaf cottonwood *(populus angustifolia).*

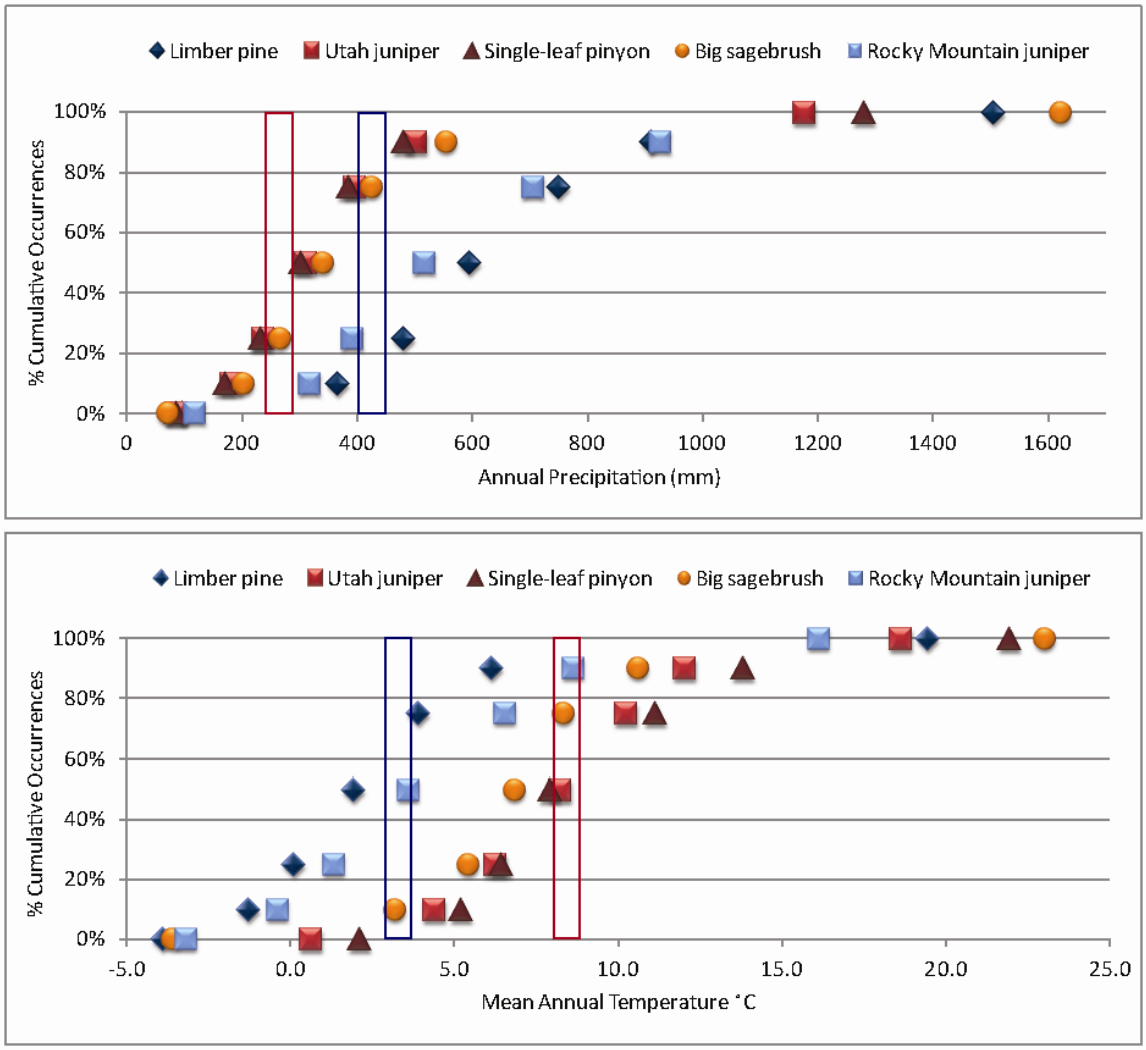

Figure 4: Percent cumulative occurrences of vegetation plotted against mean annual precipitation (upper) and temperature (lower). Limber pine and Rocky mountain juniper typically occur in colder, wetter climates compared to single-leaf pinyon, big sagebrush, and Utah juniper (Thompson et al., 1999). Red boxes show modern mean annual precipitation and temperature at CIRO, while blue boxes show modeled mean annual precipitation (Braconnot et al., 2007) and temperature (Schmittner et al., 2011) from the Last Glacial Maximum.

FIRE REGIMES AND POST-FIRE RECOVERY IN PINYON-JUNIPER, SAGEBRUSH, AND LIMBER PINE COMMUNITIES

Most forested ecosystems have "moisture-limited" fire regimes, where fire is limited by too much moisture. Although these ecosystems may contain sufficient fuels, moist conditions inhibit fuel flammability, and ignition depends on the drying of fuels during fire season drought (Westerling et al., 2003). Arid to semiarid shrublands and grasslands are typically "fuel-limited" systems, where fire extent is limited by fuel availability. These ecosystems typically do not experience widespread fire unless fuels have accumulated during wetter conditions 10-18 months prior to the current fire season (Westerling et al., 2003). "Ignition-limited" systems have abundant accumulated fuels that are often dried and ready for ignition, but fire occurrence is restricted by climate conditions that may limit ignition, such as infrequency of convective storm events (Romme et al., 2009; Gedalof, 2011). However, with recent invasions of annual grasses such as cheatgrass (*Bromus tectorum*), a cool-season grass that matures early, lengthens fire seasons and provides a continuous fine fuel source (Keane et al., 2008), the term "fuel-limited" may no longer be applicable in many modern Great Basin plant communities. For example, in 2007, the Murphy Complex fire burned over 2600 km^2 of cheatgrass-dominated rangeland in southern Idaho, making it the third largest wildfire in Idaho since 1910 (National Interagency Fire Center).

Fire rotation is the average projected time it takes to burn an entire area of a given size, and is calculated by dividing the time period of observation by the summation of

burned area (fire patches) and expressed as a proportion of a defined area of interest (i.e., a watershed; Baker, 2009). Fire rotations typically span decadal to centennial timescales and vary according to ecosystem (Baker, 2009). Figure 5 demonstrates these fire-ecosystem relationships, and compares CIRO mean fire rotation with estimated fire rotations for other alluvial charcoal records referred to in this study.

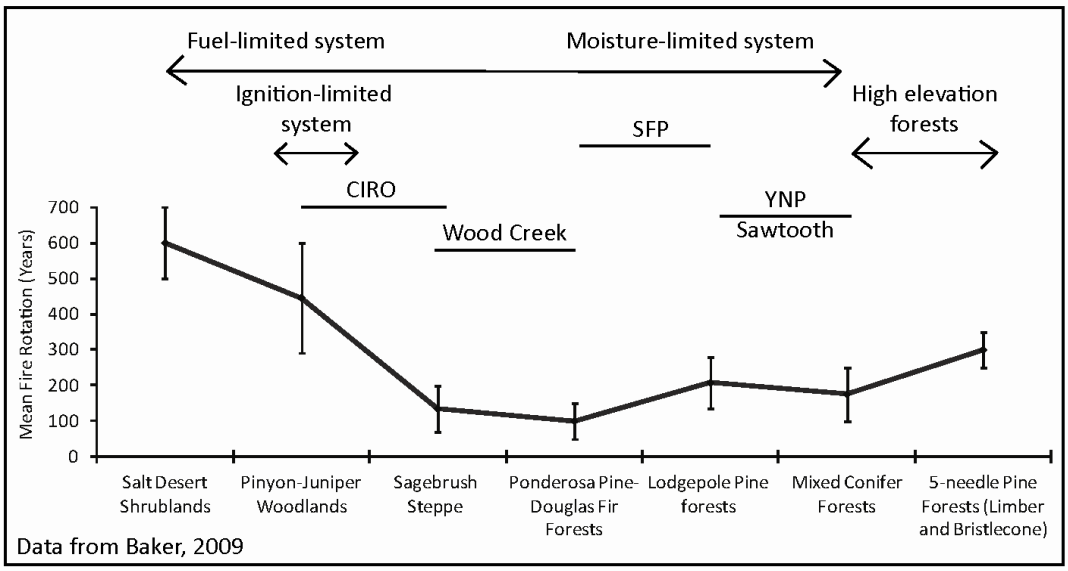

Figure 5: Fire rotation time (yrs) plotted against ecosystem type. CIRO and other alluvial charcoal records used for comparison in this study are also plotted and include; the South Fork of the Payette, Idaho (SFP; Pierce et al., 2004), Wood Creek in the Danskin Mountains, southern Idaho (Nelson and Pierce, 2010), Yellowstone National Park (YNP; Meyer et al., 1995) and the Sawtooth Mountains, central Idaho (Svenson, 2010). Ecosystems that fall on the left side of the graph are typically semiarid, fuel-limited systems, transitioning to ignition-limited systems, while ecosystems on the right side of the graph are typically cooler, wetter, moisture-limited systems and high-elevation ecosystems. Some sparsely-vegetated, high-elevation forests (e.g., 5-needle pine forests) may also be relatively fuel-limited.

Studies in pinyon-juniper woodlands estimate fire rotations that range from 290-600 years (Floyd et al., 2000; Huffman et al., 2008; Shinneman and Baker, 2009) and post-fire regeneration can take 150-200 years (Goodrich and Barber, 1999). Evidence of low-severity fires in pinyon-juniper woodlands is scarce (Baker and Shinneman, 2004). It is unlikely that these woodlands experience low-severity, surface fires because of a fuel

structure that is characterized by discontinuous fine fuels (Baker and Shinneman, 2004), and trees with thin, fire-intolerant barks (Miller and Rose, 1999; Romme et al., 2009) and low crowns (Romme et al., 2009). In general, fires destroy all of the trees in a pinyon-juniper ecosystem, and top-kill shrubs and understory vegetation within the burned area (Romme et al., 2009). Pinyon-juniper woodlands can become quite dry and flammable during a fire season. However, fire occurrence is not necessarily controlled by availability and continuity of fine fuels because closed canopy conditions can limit understory plant growth. Instead fires in these systems depend on climate conditions conducive to ignition (i.e., ignition-limited; Romme et al., 2009; Gedalof, 2011). However, when ignition occurs, fires in pinyon-juniper systems are more common where more fine fuels are accumulated (Floyd et al., 2000; Romme et al., 2009; Bauer and Weisberg, 2010).

In big sagebrush communities, fire is characteristically stand-replacing and kills all aboveground biomass (Kauffman and Sapsis, 1989). Fires are more likely during wetter than average years or following years with above average precipitation (Miller and Tausch, 2001; Mensing et al., 2006). Post-fire recovery can take 35-100 years and mean fire rotations are estimated between 70-200+ years (Baker, 2006).

Limber pine forests typically occupy drier, rocky, and nutrient-poor sites at subalpine elevations (>1500 m), where fires are likely rare due to sparse canopy cover and limited fine fuels at these locations (Schoettle, 2004). Although fire regimes are poorly understood in these ecosystems, fire regimes and surface fire occurrences likely varied over time with climate (Brown and Schoettle, 2008). Regeneration following fire can be slow, taking as long as 450-700 years (Rebertus et al., 1991).

REGIONAL HOLOCENE CLIMATE AND VEGETATION

Located in the eastern Great Basin and 75 km south of CIRO, the Great Salt Lake is the Holocene descendent of Pleistocene Lake Bonneville (Figure 1). The Bonneville Basin has been extensively studied and paleoclimate conditions have been reconstructed from geomorphic evidence and radiocarbon dating of charcoal and organic material deposited on past shorelines (Murchison, 1989; Oviatt et al., 2003; Miller et al., 2005; Patrickson et al., 2010), pollen records (Davis et al., 1986; Madsen et al., 2001; Louderback and Rhode, 2009) and faunal evidence (Broughton et al., 2000; Grayson, 2000). These records are important for comparison because of the geographic proximity of the Bonneville Basin to CIRO.

Bear Lake straddles the Idaho-Utah border and is located at the same latitude 190 km east of CIRO (Figure 1). Diatom and isotopic records (Moser and Kimball, 2009) and pollen records (Doner, 2009) reconstruct climate and vegetation from the late Pleistocene to present. Bear Lake climate and vegetation records are important for comparison because it is located at the same latitude as CIRO, within the north-south hydroclimate transition zone (Dettinger et al., 1998) and likely experienced similar climate forcings during the Holocene.

Most climate records agree (e.g., Davis et al., 1986; Murchison, 1989; Broughton et al., 2000; Grayson, 2000; Madsen et al., 2001; Oviatt et al., 2003; Louderback and Rhode, 2009) that the Bonneville Basin and Great Basin were colder and wetter than

today during the Younger-Dryas cool interval (12.8-11.2 ka; Berger, 1990), when Lake Bonneville shorelines reached the maximum Holocene elevation, known as the Gilbert shoreline (Oviatt, 1997; Benson et al., 2011). Between ~11-9.5 ka, warming climate drove Lake Bonneville shorelines elevations downward (Murchison, 1989, Madsen et al., 2001) and pushed subalpine fir upward in elevation in the Albion Range (Davis et al., 1986). Regionally, vegetation populations were changing in response to warming climate. At Blue Lake Marsh on the western margin of the Bonneville Basin, warmer taxa replaced sagebrush (Louderback and Rhode, 2009), and sagebrush steppe replaced cold tolerant vegetation at Bear Lake (Doner, 2009).

Between ~9.5-8 ka, Lake Bonneville shorelines rose once more (Murchison, 1989; Louderback and Rhode, 2009). A record from Stansbury Island, located on the southern shore of the Great Salt Lake, estimates that shorelines peaked at ~8.3 ka and may have exceeded the earlier Gilbert shoreline (Patrickson et al., 2010). Warming resumed after ~8.2 ka, when Blue Lake Marsh dried up between ~8-6.5 ka (Louderback and Rhode, 2009), single-leaf pinyon migrated to the Bonneville basin (Madsen et al., 2001), and some small animal species became locally extinct in the Great Basin (Grayson, 2000).

Warming and drying persisted during the middle Holocene in the Bonneville Basin (Murchison, 1989; Schmitt et al., 2002; Louderback and Rhode, 2009) and throughout the Rocky Mountain Region (Shuman et al., 2009). Evidence of low lake levels in the Rocky Mountains between ~7-4 ka (Shuman et al., 2009), in the Uinta Range between 6-3 ka (Corbett and Munroe, 2010), and isotopic evidence for higher

evaporation between 7.6-5.9 ka at Bear Lake (Moser and Kimball, 2009) suggest region-wide, extended drought.

Pollen, midden, and lake records indicate that between ~4-2 ka climate shifted from middle Holocene drought to cooler and wetter conditions in both the Great Basin (Miller and Tausch, 2001) and in the Bonneville Basin (Madsen et al., 2001; Louderback and Rhode, 2009). Several accounts estimate a Lake Bonneville highstand occurred between 3.8 ka and 3.5 ka (Murchison, 1989; Broughton et al., 2000; Miller et al., 2005), which supports evidence of cooler and wetter conditions beginning ~4 ka. This return to wetter, cooler climate was documented earlier at Bear Lake, when vegetation shifted to a conifer-dominant forest by ~5.3 ka (Doner, 2009) and isotopic evidence suggests reduced evaporation (Moser and Kimball, 2009).

After ~3.5 ka, Lake Bonneville records do not agree well (Murchison, 1989; Broughton et al., 2000; Miller et al., 2005). Although it seems likely that lake records should exhibit lowstands during the warm and droughty Medieval Climatic Anomaly (MCA) between ~1.1-0.7 ka (Stine, 1994), only the Murchison (1989) record indicates a lowstand at ~1 ka, and fish remains from the Homestead Cave indicate a highstand only 100 years later at ~0.9 ka (Broughton et al., 2000). Nearby lake level reconstructions from the Great Basin, however, indicate both high and low lake levels during the MCA (Adams, 2003), suggesting this was a time of both multidecadal droughts and wet intervals in this region. This MCA variability is supported by Palmer Drought Severity Index (PDSI) reconstructions from tree ring records which indicate variable climate between ~1-0.6 ka (Cook et al., 2004), and rapidly shifting lake levels might reflect such variability. Lake records were also discordant during the cooler and wetter Little Ice Age

(LIA) between 0.6-0.1 ka (Grove, 2001). The Murchison (1989) record shows a highstand ~0.5 ka, while the Locomotive Springs record indicates that shorelines were dropping ~0.5 ka (Miller et al., 2005). However, dune activation in the Snake River Plain (Rittenour and Pearce, 2011) and droughts reconstructed from tree rings in the Uinta Range (Gray et al., 2004) agree with dropping lake levels reported by the Locomotive Springs record (Miller et al., 2005). Furthermore, locally reconstructed PDSI (within 100 km of CIRO) during this period indicates that conditions were drier than average (Cook et al., 2004), suggesting that although the LIA was regionally cooler and wetter (Grove, 2001), conditions may not have been cooler and wetter at CIRO.

METHODS

Field Methods

We sampled charcoal from fire-related deposits exposed in arroyos, stream terraces, and one incised alluvial fan within the study area. We identified depositional characteristics and inferred depositional process from stratigraphic units (e.g., sheetflood, debris flow, overbank flood, channel flood), and recorded deposit thickness and depth within the profile. We described units according to clast size, sorting, clast orientation, and imbrication, and identified soil properties, color, and texture according to Birkeland et al. (1991).

Clast-supported, moderately-well sorted deposits that alternate between fine-grained and coarse-grained couplets are defined as sheetflood deposits. Textures of fine units in sheetflood couplets are loam, sandy-loam, and silty-loam with <20% of clasts coarser than 2 mm. Textures of coarse-grained units in sheetflood couplets are sandy, loamy-sand, and sandy-loam with 20-50% of clasts coarser than 2 mm. Individual couplets vary in thickness 0.25 cm to 6 cm. Maximum clasts sizes are typically 3 mm in fine-grained units and 10 mm in coarse-grained units.

Matrix-supported and poorly sorted fine-grained units with 30% of clasts coarser than 2 mm that consist of randomly oriented fine to coarse gravel-sized clasts are identified as debris flow deposits. Textures of matrix material in debris flow deposits are typically loam and silty-loam, and sometimes silty-clay-loam. Deposits vary in depth but

can reach 100+ cm thicknesses. Debris flow deposits are more cohesive than sheetflood deposits and form more vertical, sometimes overhanging faces in stratigraphic profiles. Clasts in both sheetflood and debris flow deposits at CIRO are composed of grussy gravels that are relatively small (1-20 cm), and rarely exceed 20 cm.

Well-sorted, fine-grained units with 5-40% of clasts coarser than 2 mm but finer than 10 mm are identified as overbank flood deposits. Textures are typically loam, silty-loam, and silty-clay loam. Clast-supported, poorly to moderately-sorted deposits with imbricated sand to boulder-sized clasts are identified as channel flood deposits.

Charcoal-rich deposits are termed "fire-related" and the geomorphic response to fire is inferred from the type of depositional process (e.g., sheetflood vs. debris flow). Charcoal preserved in overbank deposits suggests hydrodynamic separation of charcoal during flood events. Regardless of the depositional event, charcoal, and its associated radiocarbon age, records the timing of a past fire. We interpret laterally continuous burned surfaces that are stratigraphically below fire-related debris flow deposits or fire-related sheetflood deposits, as likely representing the burn surface that is associated with the subsequent overlying fire-related deposit.

Analytical Methods

Annually produced wood, such as, twigs, branches, and seeds were prioritized for radiocarbon dating to decrease "inbuilt age" error, which is the difference between the age of wood formation and the date of fire (Gavin, 2001). Angular versus rounded wood fragments were selected to avoid dating re-worked charcoal that can produce ^{14}C ages that are inverted stratigraphically (e.g., Meyer et al., 1995). Charcoal macrofossils were dated with Accelerator Mass Spectrometry (AMS) ^{14}C, and dates were calibrated into

calendar years before 1950 A.D. (cal yr BP) using the CALIB 6.0.1 program (Stuiver and Reimer, 1993). All results are presented in this paper as the median age of the 1σ error, although 2σ age errors are also provided. Individually calibrated fire ages are summed and presented as a cumulative probability density distribution of fires plotted against time. Our record begins at 0 cal yr BP (equivalent to 1950 A.D.), and progresses backward in time to 13,000 cal yr BP.

Fire frequency is calculated by dividing the number of dated alluvial charcoal samples in the study area by number of years that make up a cluster of radiocarbon ages. Alluvial charcoal fire frequency is reported as a minimum recorded frequency because we cannot be sure that every fire is preserved or exposed in fire-related stratigraphy. For example, not all fires produce a fire-related erosional response (i.e., sheetfloods or debris flows) and some fire-related deposits remain buried in the subsurface.

We summed the total measured alluvial thickness (as measured and recorded in the field) to estimate erosional trends during the Holocene. We used radiocarbon ages for dated units combined with stratigraphically inferred ages for undated units based on location within the profile, upper and lower age constraints, and deposit characteristics. We binned the thickness of depositional units by process into 500-year time interval bins. The percentage of total measured Holocene thickness per depositional process is plotted backward in time to 13,000 cal yr BP.

We identified charcoal macrofossils under a microscope through comparison with magnified images and descriptions of burned wood (Adams and Murray, 2011). Charcoal was classified as “pine,” “juniper,” or “sagebrush,” and characteristics of each vegetation type are described in Table 1. We used general categories for “pine” and “juniper”

because differentiation between different species of pine and different species of juniper is difficult, and beyond the scope of this project. The midden record documents the presence of limber pine and Rocky Mountain juniper at CIRO since the late Pleistocene. The midden record documents the arrival of single-leaf pinyon and Utah juniper, (Betancourt, unpublished data) before which we assume that all burned "pine" was limber pine and all burned "juniper" was Rocky Mountain juniper. After colonization, "pine" includes limber pine and single-leaf pinyon, and "juniper" includes Rocky Mountain juniper and Utah juniper.

Table 1: Characteristics used for macrofossil vegetation identification (Adams and Murray, 2011).

Vegetation type		Vegetation Characteristics			
Common name	Scientific name	Ring patterns	Ring boundaries	Vessels	Resin Canals
Juniper	Includes: *J. osteosperma, J. scopulorum*	Distinct; rings consist of parrallel rows of very small fibertracheids	Distinct; narrow latewood boundary and wide earlywood boundary	Absent	Absent
Pine	Includes: *P. flexilis, P. monophylla*	Distinct; variable width rings	Distinct; abrupt boundary between earlywood and latewood	Absent	Abundant
Big sagebrush	*Artemisia tridentata*	Semi-ring porous; vessels concentrated at earlywood and latewood boundaries	Distinct	Abundant; distributed within the ring in "flamelike" patterns	Absent

We compared our fire record to calibrated radiocarbon ages of woodrat midden vegetation reconstructions, sampled from many of the same drainage basins as alluvial charcoal sampling locations (Figure 3; Betancourt, unpublished data). We include midden radiocarbon ages from the Oneida Narrows in southeastern Idaho and the Lost River

Range in south-central Idaho with the CIRO midden record as a regional measure of ecosystem productivity (Betancourt, unpublished data; Smith and Betancourt, 2003). Relative abundances of midden radiocarbon ages can be used to infer periods of past ecosystem productivity. During times of high ecosystem productivity, packrat populations flourish and are reflected by increased nest (midden) construction (Webb and Betancourt, 1990).

We graphically compared our fire record with independent paleoclimate records from the Bonneville Basin, and Northern Great Basin. We selected lake paleoshoreline reconstructions from Lake Bonneville, Utah (Murchison, 1989; Miller et al., 2005; Patrickson et al., 2010), pollen-inferred reconstructions of subalpine fir forest elevational shifts from nearby Lake Cleveland sediments in the Albion Range (Davis et al., 1986), and pollen-inferred temperature reconstructions from the Blue Lake Marsh region in the Western Bonneville Basin (Louderback and Rhode, 2009; Figure 1). We used the 2000-year dendrochronological reconstruction of the Palmer Drought Severity Index (PDSI), offered on a 2.5 degree grid point plot that covers the U.S and Canada (Cook et al., 2004). CIRO is located at the same latitude and approximately equidistant between grid points 70 and 89, so we averaged these values.

The CIRO record was also compared to data from four regional alluvial charcoal records, which are important because they employ the same methods as this study. We used two records from more xeric regions: the Wood Creek record, a semiarid ponderosa forest-sagebrush ecotone in the Danskin Mountains of south-central Idaho (Nelson and Pierce, 2010), and the South Fork of the Payette record (SFP), a ponderosa pine and Douglas fir dominated region of central Idaho (Pierce et al., 2004). We used two records

from cooler, higher elevation ecosystems: the Sawtooth record, a Douglas fir, lodgepole Pine forest of central Idaho (Svenson, 2010), and the Yellowstone record (YNP) a lodgepole pine forest ecosystem in northeastern Yellowstone National Park, Wyoming (Meyer et al., 1995).

Correcting for the Fading Record and Limitations of the Method

We used a stratigraphically-based model put forth by Surovell et al. (2009) to correct for "taphonomic bias," which is defined as the tendency for over-representation of younger macrofossils relative to older macrofossils due to destructive processes such as weathering and erosion. The model represents the rate of geologic (or archeological) sample loss through time by comparison of a temporal frequency distribution of radiocarbon ages for volcanic events preserved in ice cores with a temporal frequency distribution of radiocarbon ages for terrestrial records of volcanism. The model attempts to correct for the fading geologic record using the following equation:

$$n_t = 5.73 \times 10^6 (t + 2176.4)^{-1.39}$$

where n_t is the number of radiocarbon dates surviving from time t.

Another form of sampling bias is governed by the Law of Superposition, where stratigraphic exposures are sampled from top to bottom, and deposits that are lower in the profile and therefore older in age may not be exposed at the time of sampling (Surovell et al., 2009). This bias, like "taphonomic bias," can bias the data towards younger versus older radiocarbon ages.

Not all fires produce a fire-related erosional deposit. Alluvial charcoal deposition is episodic in nature because it occurs following episodic fire events in response to

complex interactions among climate, fire, vegetation, and the geomorphic response. Such geomorphic processes are further controlled by lithology, topography, and slope.

Lastly, radiocarbon ages do not produce annually resolved records, like tree ring chronologies (e.g., Grissino-Mayer and Swetnam, 2000). Instead, radiocarbon ages have an associated error of ~ ±100 years; therefore, we cannot resolve the timing of fire to the year of fire but rather provide a period of time in which the fire likely occurred.

Geomorphic Analytical Methods

Drainage basin delineation provides an estimate of the extent of the potential charcoal source area. Comparison of similarly aged fires that burned in multiple basins can help distinguish between smaller and larger fire events. Drainage basins were delineated upstream of each charcoal sampling site using a 30 meter Digital Elevation Model (DEM; Gesch et al., 2002; Gesch, 2007). In ArcGIS, basin delineation was conducted using hydrology tools (flow accumulation > flow direction) and the reclassify tool to identify pixels that drain 300+ upslope pixels from which basin areas were calculated.

Incised alluvial exposures are present throughout the study area; however, not all exposures contain fire-related stratigraphy. We used ArcGIS geomorphic analysis methods to better understand geomorphic and lithologic controls on fire-related erosion. We delineated six headwater drainage basins to identify trends between lithology, mean slope, ruggedness, and the absence or presence of fire-related stratigraphy across basins.

Slopes steeper than 30% (16.7°) have been correlated to debris flow initiation in burned basins (Cannon et al., 2010). Skewness of slope frequency histograms per basin have been used as a metric for the type of diffusive processes that dominate a basin. For

example, creep-dominated basins exhibit positively-skewed slope frequency histograms and landslide-dominated basins exhibit negatively-skewed slope frequency histograms (Wolinsky and Pratson, 2005). We used DEM-extracted slope values to calculate mean slopes per basin and to create slope frequency histograms per basin.

Debris flow initiation in burned basins has been correlated to higher ruggedness values, i.e., high topographic variability (Cannon and Reneau, 2000), and standard deviation of slope has been shown to accurately identify terrain ruggedness (Grohmann et al., 2011). We created slope rasters for each basin using ArcGIS (surface>slope) and used the standard deviation of slope reported in classification statistics to identify relative ruggedness between basins.

RESULTS

Alluvial Charcoal

We dated 37 charcoal samples preserved in 18 sheetflood deposits, 17 debris flow deposits, one overbank deposit, and one channel flood deposit that were collected from sites exposed in arroyos, streambanks, and one alluvial fan at CIRO (Figure 6; Table 2; Appendix). Arroyo sites include: A2, C5, C8, C9, C11, C12, C13, and H15 (Figure 3: Figure 6). These sites are typically incised 1-6+ m and drain small areas (0.01-0.5 km^2; Figure 7). Arroyo stratigraphy is characterized by abundant sheetflood deposits, some debris flow deposits, and occasional buried soils. Active channel sites include: A1, G4, C6, C7, C10 and C14 (Figure 3; Figure 6). All active channel sites are incised <4m and typically drain larger areas (0.5-24 km^2; Figure 7). Streambank stratigraphy is characterized by debris flow deposits, fine-grained overbank deposits, some sheetflood deposits, and occasional channel flood deposits. Site S3 is exposed in a 1.5 m deep incised alluvial fan that contains the oldest dated deposit (12,740 cal yr BP) and consists of debris flow deposits, sheetflood deposits, and buried soils (Figure 3: Figure 6).

We applied the correction for "taphonomic bias" (loss of geologic samples over time; Surovell et al., 2009) to the fire radiocarbon ages. To see how the correction impacts the data over time, we applied the method during different timeframes (Figure 8). Surovell et al. (2009) suggest that the method should not be applied to ages <750 cal yr BP because these ages are least likely to be impacted by taphonomic bias.

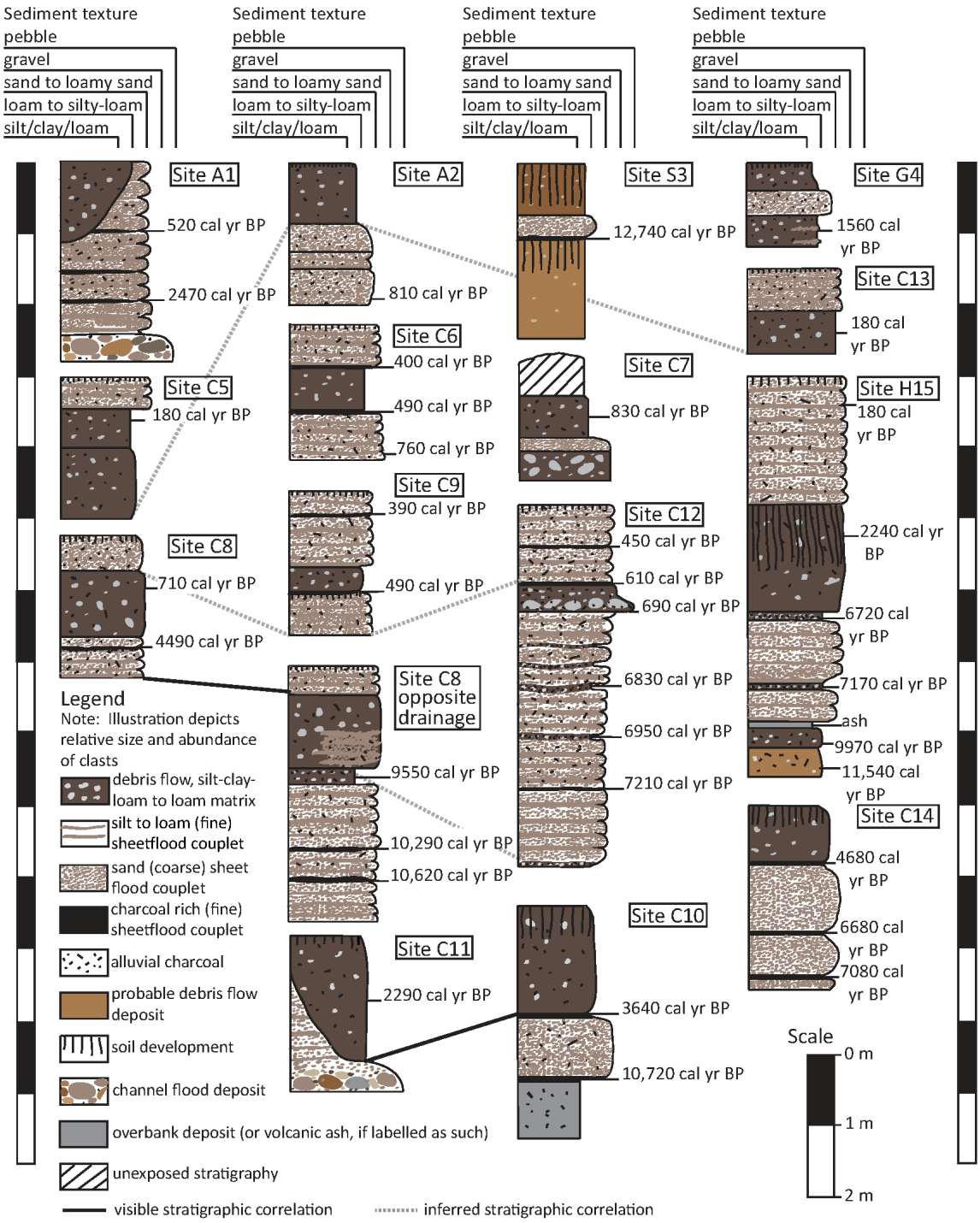

Figure 6: Summary illustration of the stratigraphic characteristics of each charcoal sampling site and the stratigraphic correlations between sites.

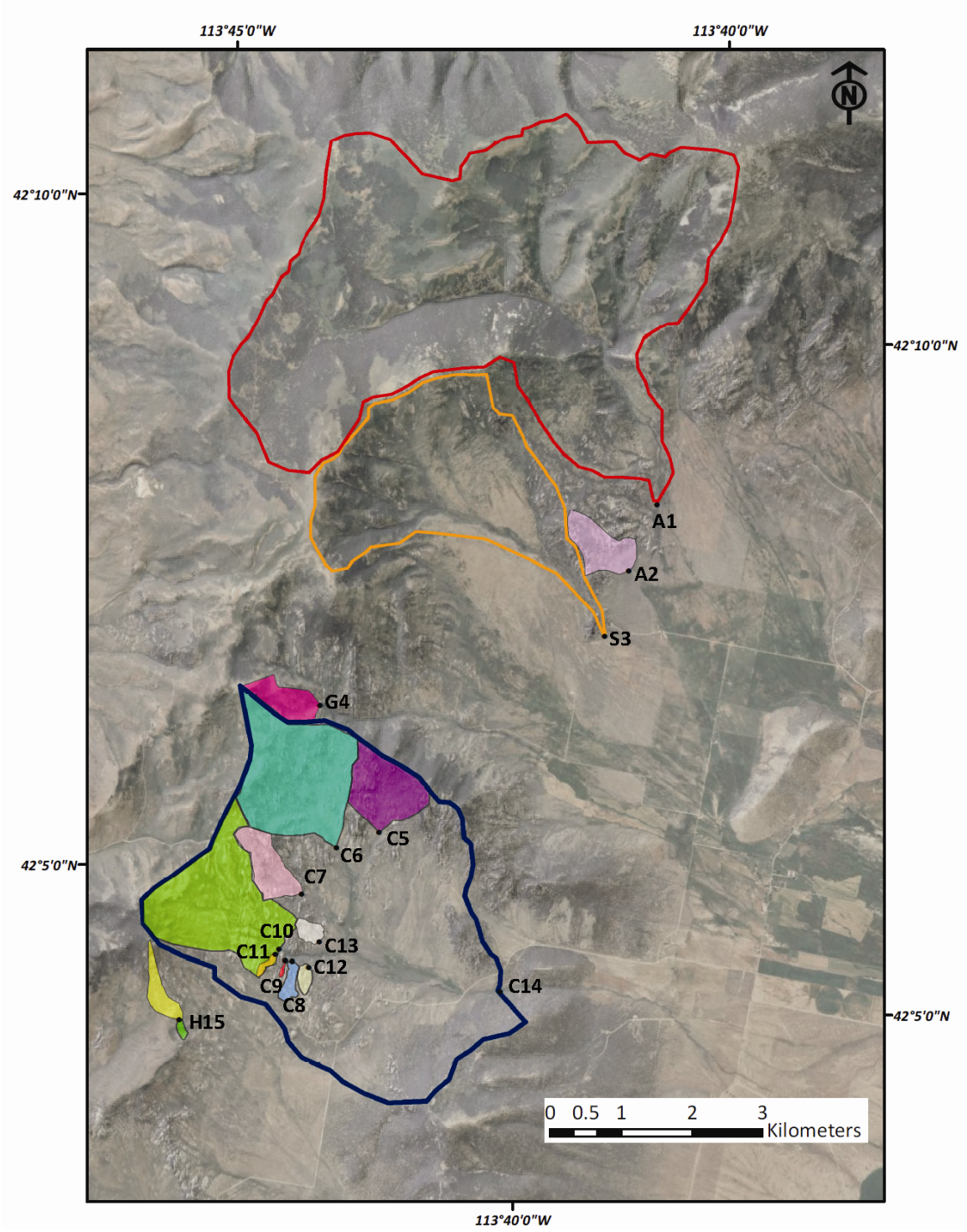

Figure 7: Map of CIRO showing delineated contributing drainage basins upslope of each charcoal sampling site.

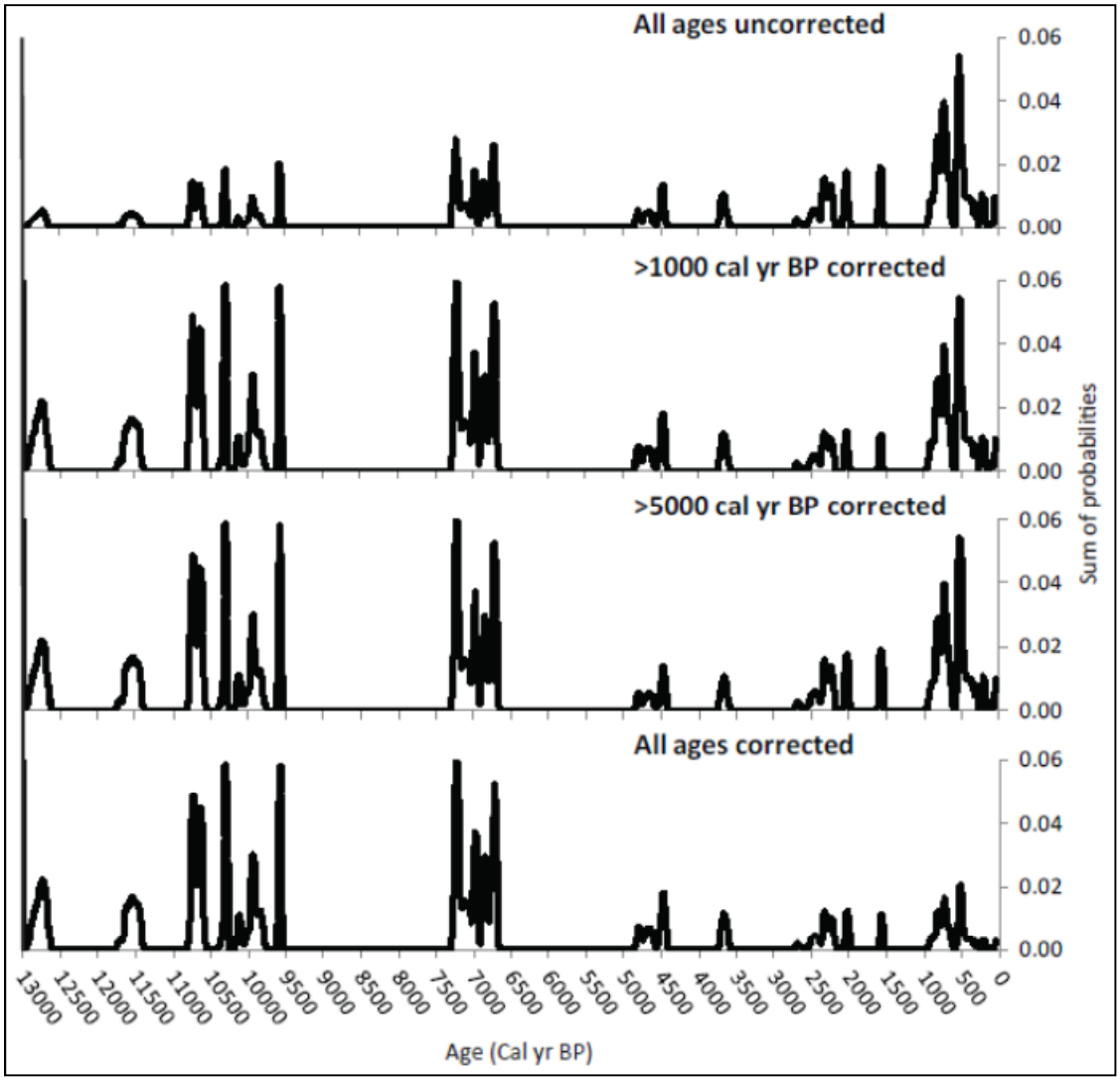

Figure 8: The top graph shows the uncorrected summed probability distribution of charcoal radiocarbon ages. Moving downward, the next graph shows the correction applied to all ages older than 1000 cal yr BP, next the method is applied to all ages older than 5000 cal yr BP and the bottom graph shows all ages corrected.

It is likely that the fading record at CIRO is primarily a function of depth of incision, where fire-related deposits deeper than natural exposures are not exposed and therefore not sampled. Figure 9 plots median radiocarbon ages against depth of sample in profile. The majority (96%) of macrofossil radiocarbon ages younger than 5000 cal yr BP were sampled from the uppermost 200 cm of stratigraphy, while 77% of samples older than 5000 cal yr BP are exposed between 200-600 cm depth. All but one of the stratigraphic

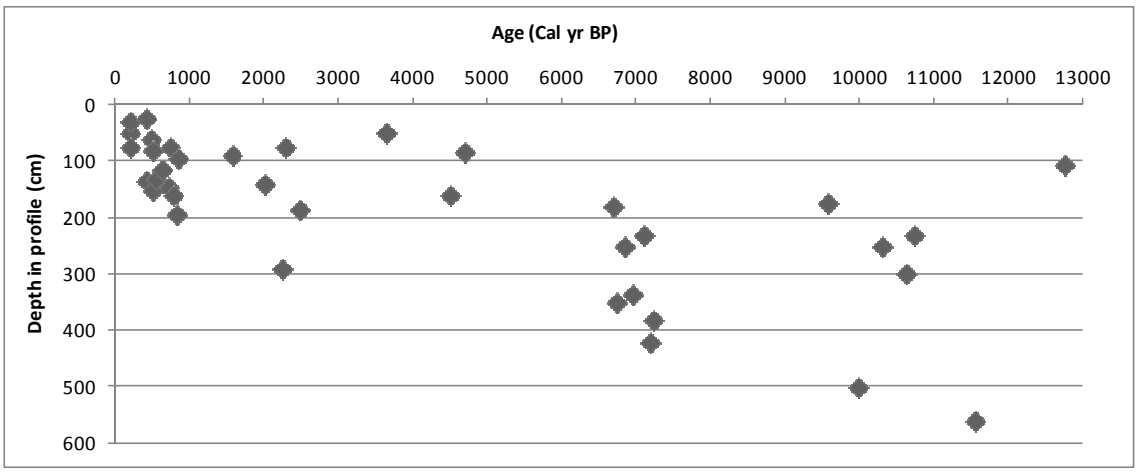

Figure 9: Median radiocarbon age for each charcoal sample plotted against depth of sample location within the stratigraphic profile.

exposures at CIRO are 200 cm or greater in depth (Figure 6), which suggests that depth of incision likely contributes to sampling bias, especially for samples >5000 years old. Charcoal preservation over time (i.e., taphonomic bias; Surovell et al., 2009), where buried charcoal macrofossils decompose over time, likely plays a secondary role in the fading record at CIRO. One debris flow deposit containing sparse charcoal was dated 12,700 cal yr BP. However, several fire-related deposits older than ~9000 cal yr BP contain abundant charcoal, suggesting either that charcoal preservation is not as important as stratigraphic exposure, or that charcoal preservation varies on a site-by-site basis (Table 2). Based on the age-depth relationships at CIRO, we therefore believe the Surovell et al. (2009) correction model provides the most accurate representation when applied to all radiocarbon ages older than 5000 cal yr BP (where ages are under-represented due to lack of exposure), but not applied to ages <5000 cal yr BP (Figure 8).

Radiocarbon ages show five episodes of enhanced fire activity during the Holocene (Figure 10c). The earliest period of fire activity, between 10,700-9500 cal yr BP, is recorded in four debris flow deposits (H15, S3, C8), two sheetfloods (C8), and one overbank deposit (C10; Figure 6; Figure 10; Table 2; Appendix). The second fire interval

occurred between 7200-6700 cal yr BP and charcoal is preserved in three sheetflood deposits (C12, C14) and in four thin (<10 cm), fine-grained debris flow deposits that are interbedded with fire-related sheetflood deposits and charcoal-poor sheetflood deposits (C12, H15; Figure 6; Figure 10; Table 2; Appendix). The third period of moderate fire activity, between 2400-2000 cal yr BP, is preserved in two debris flow deposits (C11, H15), one sheetflood deposit (A1), and one channel flood deposit (C11; Figure 6; Figure 10; Table 2; Appendix). The two most recent fire intervals are represented by fire peaks between 850-700 and ~550 cal yr BP. These recent fire-related sedimentation events are the most geographically widespread, and charcoal is preserved throughout the study area in nine sheetflood deposits (C9, C12, A1, A2, C6, H15), four debris flow deposits (C6, C8), and in one overbank deposit (C7; Figure 6; Figure 10; Table 2; Appendix).

Two stratigraphic profiles (C6 and C11) yielded stratigraphically inverted radiocarbon ages. At site C6, a twig macrofossil dated ~490 cal yr BP was sampled from a sheetflood deposit at a depth of 80 cm, and a wood macrofossil dated ~400 cal yr BP was sampled from a debris flow deposit at a depth of 135 cm. The two units are preserved in distinctly separate fire-related deposits with clear boundaries, and 1σ and 2σ age errors do not overlap (Table 2), so we infer that the upper sheetflood deposit likely transported older charcoal from an earlier fire. While the upper deposit cannot be interpreted as the geomorphic response to a fire dated ~490 cal yr BP, the radiocarbon age does date the timing of fire, and the fire-related deposit indicates post ~400 cal yr BP.

Table 2: Summary of sampled charcoal ages, calibrated ages including 1σ and 2σ error ranges, associated depositional processes, location in stratigraphic profile, type of macrofossil, and charcoal abundance.

Site ID	Lab ID	Sample ID	^{14}C age BP	Ana-lytical error ±	Median calibrated age (cal yr BP)	Error (1 σ)	Error (2 σ)	Deposit type [1]	Depth (cm)	Char-coal type	Burned vegetation-type (%) (J)(SB)(P)[2]	Charcoal abundance [3]
Drainage Basin: Almo Creek												
A1	80536	KWCA02-2-3A	485	20	520	512-527	506-535	SF	130	twig	(17) (67) (17)	abundant
	AA88400	KWCA02-5	2428	39	2470	2370-2514	2362-2582	SF	185	wood	(40) (40) (20)	present
A2	80537	AHCA06B-3	900	20	810	767-839	756-886	SF	195	wood	(0) (100) (0)	scarce
Drainage Basin: Stines Creek												
S3	80538	AHCA04	10875	35	12740	12656-12803	12626-12887	BS/DF	105	wood	not identified	scarce
Drainage Basin: Graham Creek												
G4	AA88389	KWCR06-3	1655	37	1560	1521-1609	1486-1629	DF	90	twig	(50) (7) (43)	abundant
Drainage Basin: Circle Creek, Location: North Fork of Circle Creek												
C5	AA88388	SPCR03-1	180	35	180	132-208	103-300	DF	50	wood	(38) (25) (38)	present
C6	AA88390	NCCR01-1	415	35	490	485-495	480-500	SF	80	twig	(40) (50) (10)	present
	AA88391	NCCR01-4	356	35	400	377-427	314-435	DF	135	wood	(28) (40) (32)	abundant
	AA88397	NCCR04-5B	846	42	760	708-790	681-802	SF	160	twig	(0) (89) (11)	present
Drainage Basin: Circle Creek, Location: Middle Fork of Circle Creek												
C7	AA88398	KWCR15-1	913	36	830	788-837	782-873	DF	95	wood	(15) (69) (15)	abundant
Drainage Basin: Circle Creek, Location: South Fork of Circle Creek												
C8	AA88396	TRCR02-2B	786	36	710	699-711	694-718	DF	75	wood	(40) (60) (0)	present
	80524	TRCR02-4A	3990	20	4490	4483-4512	4418-4450	SF	160	branch	(35) (35) (41)	present
	80525	TRCR05A-1	8605	25	9550	9535-9567	9519-9588	DF	175	wood	not identified	scarce
	80526	TRCR05C-4	9155	25	10290	10250-10319	10240-10319	SF	250	wood	(67) (11) (22)	abundant
	80527	TRCR05B-5	9390	25	10620	10572-10657	10549-10702	SF	300	wood	(100) (0) (0)	scarce

[1] Deposit type abbreviations: SF = sheetflood, DF = debris flow, OB = overbank and CF = channel flood.

[2] Burned vegetation type abbreviations: J = juniper, SB = sagebrush and P = pine.

[3] Charcoal abundance: abundant indicates fire-related deposit, present = likely a fire-related deposit, and scarce = probably a fire-related deposit.

Table 2 continued: Summary of sampled charcoal ages, calibrated ages including 1σ and 2σ error ranges, associated depositional processes, location in stratigraphic profile, type of macrofossil, and charcoal abundance.

Site ID	Lab ID	Sample ID	^{14}C age BP	Analytical error ±	Median calibrated age (cal yr BP)	Error (1 σ)	Error (2 σ)	Deposit type [1]	Depth (cm)	Charcoal type	Burned vegetation-type (%) (J)(SB)(P)[2]	Charcoal abundance [3]
Drainage Basin: Circle Creek, Location: South Fork of Circle Creek												
C9	AA88384	KRCR01-1A	308	35	390	358-430	298-469	SF	25	needle	(47) (27) (27)	abundant
	AA88385	KRCR01-7B	425	35	490	499-505	494-509	SF	150	seed pod	(7) (57) (36)	abundant
C10	AA88387	KWCR04-1	3393	41	3640	3591-3688	3495-3736	SF	50	twig	(50) (50) (0)	scarce
	AA88392	KWCR11-1	9469	56	10720	10598-10783	10553-10869	OB	230	wood	(100) (0) (0)	present
C11	80534	KWCR03-2-1A	2250	20	2290	2288-2327	2182-2331	DF	75	wood	(33) (0) (67)	abundant
	80535	KWCR03-2-2	2050	20	2010	1988-2019	1972-2033	CF	140	wood	not identified	abundant
C12	80518	TRCRO4-1C	375	20	450	446-490	410-495	SF	60	seed	(32) (32) (37)	abundant
	80519	TRCRO4-2B	660	20	610	567-584	562-594	SF	115	branch	(33) (67) (0)	abundant
	80520	TRCR04-3B	770	20	690	687-709	677-734	DF	145	seed	(23) (46) (31)	abundant
	80521	TRCR04-5	5995	20	6830	6805-6849	6783-6873	DF	250	wood	(0) (33) (67)	present
	80522	TRCR04-6A	6090	20	6950	6939-6970	6923-6983	DF	335	wood	(8) (46) (46)	abundant
	80523	TRCR04-7B	6280	60	7210	7203-7231	7193-7249	SF	380	wood	(0) (45) (55)	abundant
C13	80539	AHCR19-3	175	20	184	150-189	268-282	DF	75	twig	(40) (40) (20)	abundant
Drainage Basin: Circle Creek, Location: Main Fork of Circle Creek												
C14	80528	CCCR01-2-1	4135	20	4680	4602-4684	4580-4801	SF	83	wood	(0) (100) (0)	scarce
	AA88386	CCCR01-2B	5864	45	6680	6674-6700	6658-6710	SF	180	wood	(0) (43) (57)	present
	80529	CCCR02-4	6165	20	7080	7017-7128	7000-7150	SF	230	wood	(0) (72) (28)	abundant
Drainage Basin: Heath Canyon												
H15	AA88394	KWCR17-1	189	34	180	147-191	136-225	SF	30	twig	(25) (0) (75)	abundant
	80531	KWCR18-2-2B	2230	20	2240	2185-2243	2169-2318	BS/DF	290	wood	(0) (67) (33)	abundant
	80532	KWCR18-2-3B	5905	20	6720	6700-6745	6677-6770	DF	350	seed pod	(33) (0) (67)	abundant
	80533	KWCR18-2-3C	6230	25	7170	7170-7197	7148-7029	DF	420	wood	(92) (0) (8)	abundant
	AA88393	KWCR12-4B	8862	59	9970	9910-10,121	9896-10,135	DF	500	wood	(92) (0) (8)	abundant
	AA88395	KWCR18-3	10034	56	11540	11395-11643	11278-11770	DF	560	twig	(71) (12) (18)	abundant

[1] Deposit type abbreviations: SF = sheetflood, DF = debris flow, OB = overbank and CF = channel flood.

[2] Burned vegetation type abbreviations: J = juniper, SB = sagebrush and P = pine.

[3] Charcoal abundance: abundant indicates fire-related deposit, present = likely a fire-related deposit, and scarce = probably a fire-related deposit.

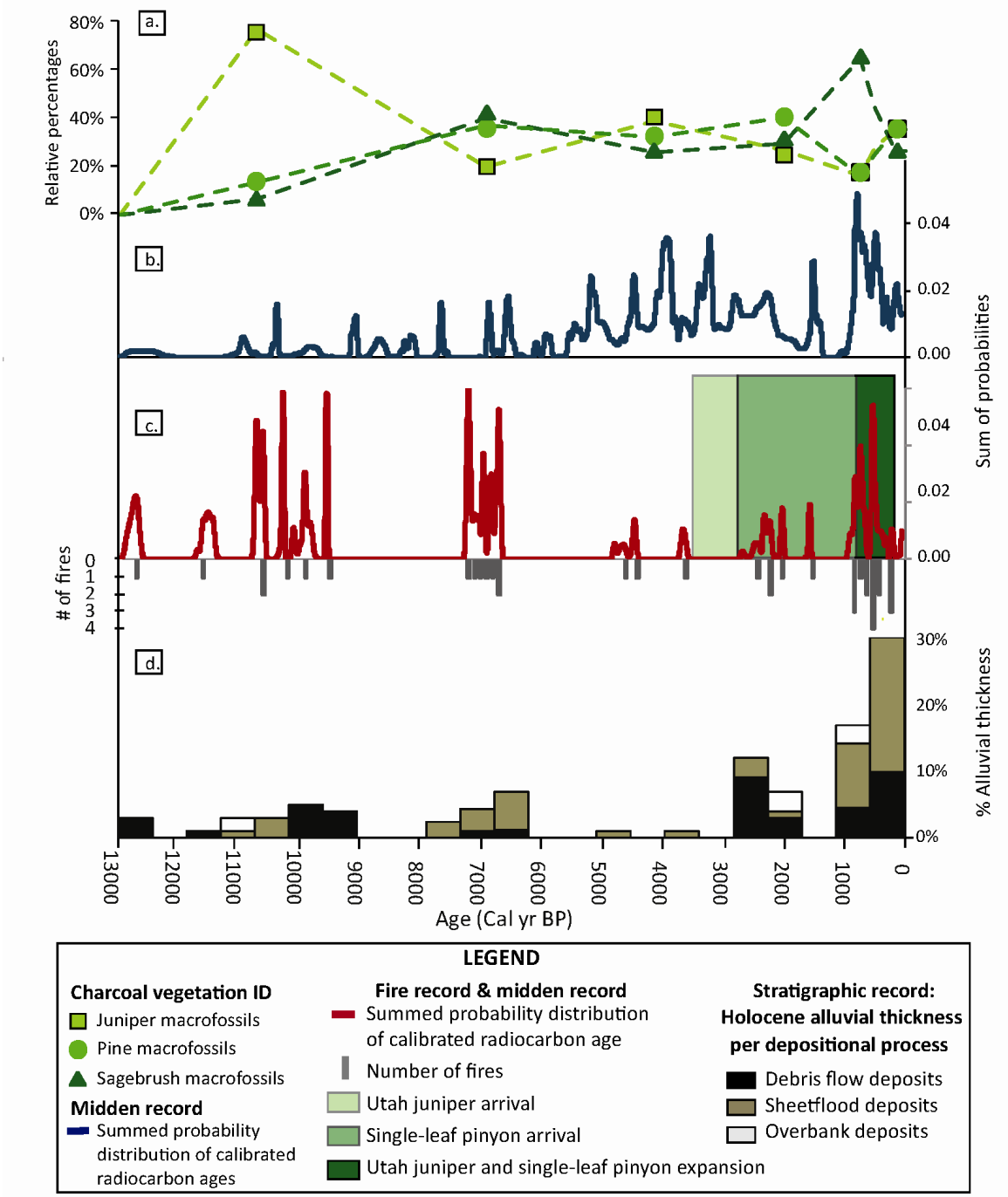

Figure 10: Summary of results from fire, vegetation and depositional processes data plotted against time. a. Relative percent of vegetation type per charcoal sample, plotted as discrete points and binned per mean age of fire interval (dashed lines simply connect points), b. calibrated radiocarbon ages for middens as an indicator of ecosystem productivity, c. calibrated radiocarbon ages for alluvial charcoal (>5000 cal yr BP ages corrected according to Surovell et al., 2009), arrival timing of juniper and pinyon and number of fires, and d. stratigraphic record of percent alluvial thickness per depositional process.

fire-related sedimentation event. At site C11, a wood macrofossil with a radiocarbon age of ~2290 cal yr BP preserved in a debris flow deposit stratigraphically overlies a channel flood deposit with a wood macrofossil dated ~2010 cal yr BP. Errors (1σ and 2σ) for both radiocarbon ages at C11 do not overlap (Table 2), therefore we interpret that these radiocarbon ages represent the timing of separate fire events. The younger (yet stratigraphically lower) sample, records a fire and the geomorphic response to the fire event, while the older sample only records the previous fire event.

Charcoal macrofossil identification indicates that during early Holocene fires (11,500-9900 cal yr BP), juniper accounted for 79% of sampled charcoal. Pine and sagebrush made up 14% and 7% of sampled charcoal, respectively. The type of vegetation burned shifted to roughly 1/3 juniper, 1/3 sagebrush, and 1/3 pine per charcoal sample, during middle to late Holocene fires (7200-6000, 4700-2600, 2500-1500 and 550 cal yr BP). However, between 850-700 cal yr BP, sagebrush made up 67% of sampled charcoal (Figure 10a).

Holocene Erosion, Fire-Related Sedimentation and Soil Development

Field observation of frequent, small-scale sheetflood deposition on moderate to gentle-slopes (<18°) and material eroded from upstream channels and arroyos is regularly transported in sheetflood events (Figure 11). Active incision in arroyos is evident, for example, following a two week storm characterized by intermittent rain that totaled 2 cm of precipitation during July-August 2010 (Western Regional Climate Center), 30 cm of material was removed from the base of arroyo site C12, and fresh incision occurred at arroyo sites C8 and H15. The same storm deposited sheetfloods at other sites.

Figure 11: Example of modern sheetflood deposit burying grass.

During the Holocene, debris flows appear to be predominantly fire-related, and debris flow activity is rare in the modern record. We observed evidence for only one recent debris flow event on an alluvial fan, where a thin, discontinuous debris flow buried trunks of ~50 year old sagebrush. Throughout the Holocene, as in the modern record, sediments are primarily transported via sheetflooding events. Sheetflood deposits account for the majority (57%) of total measured alluvial thickness, while debris flow deposits and overbank deposits make up 37% and 6% of total Holocene alluvial thickness, respectively (Figure 10d).

A period of minimal deposition is observed in the record between ~6500-2500 cal yr BP, when only 4% of the total measured alluvial thickness was deposited. During this time, debris flow activity was at a minimum and overbank deposition is absent from the record (Figure 10d). Although four debris flow deposits were identified during this timeframe, they are all thin (<10 cm), muddy units with fine-grained clasts. These

deposits are strikingly different from debris flows deposited during the early and late Holocene, which are much thicker (>40 cm), and contain coarser clasts. Four debris flow deposits were dated older than ~9500 cal yr BP, and one more was stratigraphically inferred as older than ~7000 cal yr BP. After ~2200 cal yr BP, we identified fourteen fire-related debris flow deposits: nine were radiocarbon dated, and five more were stratigraphically inferred ages (Figure 6; Figure 10d). At site C12, there is a gap in deposit ages between ~700 cal yr BP and ~7000 cal yr BP with ~100 cm of undated charcoal-poor sheetfloods filling in the age gap, and at site H15 there is a gap in deposit ages between ~2200 cal yr BP and 6800 cal yr BP. However, there is no stratigraphic evidence of erosion (e.g., cut-and fill or unconformable contacts between deposits) and dated units are laterally continuous within the exposures at these sites (Figure 6).

Active hillslope erosion in coarse-grained, grussy parent material with low vegetation density has inhibited modern soil development on hillslopes at CIRO. In some locations, disturbed and platy upper horizons, overlying plow pans are observed, and are likely a result of turn of the century agricultural practices (Morris, 2006). Modern soils in granitic parent material at CIRO are poorly developed, with absent to weakly developed B-horizons (USDA, NRCS, 2011). However, we did observe well-developed soils at CIRO: two are buried soils and two are unburied soils. At site S3, one ~12,700 cal yr BP soil developed on a debris flow deposit that was subsequently buried by sheetfloods exposed in a recently incised alluvial fan. These units are capped by another debris flow deposit that exhibits extensive soil development. At arroyo site A15, soil developed on a ~2230 cal yr BP debris flow deposit and was later buried by 170 cm of <300 year old sheetflood deposits. Another well-developed soil formed on a ~2290 cal yr BP fire-

related debris flow deposit exposed in the incised streambank site C10 (Figure 6; Table 2; Appendix).

Fire-Related Geomorphic Response Recorded in Arroyo Stratigraphy

The combined stratigraphic records from four arroyo sites (C8, C9, C12, and H15) tell a relatively complete story of Holocene fire and fire-related erosion. The complete arroyo site descriptions, details, and ages are summarized in the appendix. Arroyo site H15 drains west to east, and is situated in a saddle below a northern summit composed of Almo granite and a southern granitic knob capped with Miocene rhyolite tuff (Miller et al., 2008; Pogue and Katz, 2008; Figure 2; Figure 3; Figure 7). H15 originates 0.5 km north of the saddle from the northern summit (<1 m depth) exposing sheetflood deposits. At the saddle, the arroyo drops abruptly over a bedrock knickpoint and at its deepest point, exposes ~575 cm of fire-related stratigraphy (Figure 12). Incision disappears at a bedrock bench 0.25 km downslope from the saddle. The four oldest debris flow deposits exposed in the H15 arroyo contain a combination of rhyolitic and granitic clasts, suggesting that earlier Holocene debris flow deposition initiated from the southerly knob (H15 South; Figure 7). More recent sheetflood and debris flow events likely originated from the northern summit because deposits are granitic composition and upslope incision exhibits a northerly trend (Figure 3; H15 North; Figure 7).

The uppermost ~160 cm of stratigraphy exposed at H15 consists of ~180+ cal yr BP charcoal-rich sheetflood deposits. The dated sample was collected from the top 40 cm of this unit, so underlying sheetfloods are possibly older. Based on comparison with radiocarbon ages and stratigraphic characteristics of other arroyo exposures, these

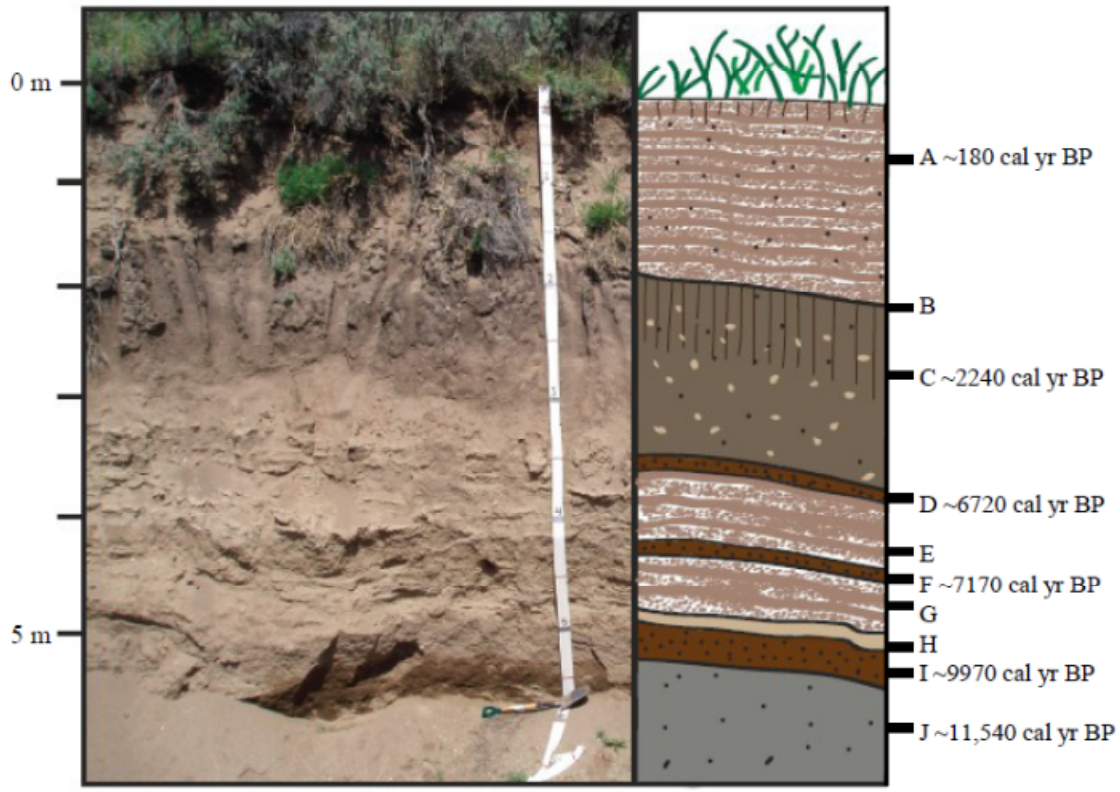

Figure 12: Site H15 exposure of arroyo fire-related stratigraphy with black dots representing charcoal: A) charcoal rich sheetflood deposits, B) abrupt boundary between units, C) buried soil developed on thick fire-related debris flow deposit, D) continuous, thin, fine-grained (muddy) fire-related debris flow deposit with abrupt upper boundary, E) sheetflood deposits, F) continuous, thin, fine-grained (muddy) fire-related debris flow deposit with abrupt upper boundary, G) sheetflood deposits, H) light-colored, fine-grained unit, Mazama Ash ~7700 cal yr BP (Zdanowicz et al., 1999), I) continuous, fine-grained (muddy) fire-related debris flow deposit and, J) medium-sand with charcoal, overbank deposit or debris flow deposit.

sediments may correspond with deposition ~400 to 600 cal yr BP. Farther down in the profile, a buried soil that developed on the ~2240 cal yr BP debris flow deposit (discussed above) is exposed at 160-350 cm depth. The buried soil surface and the underlying units exhibit a moderately steeper slope than the modern surface, suggesting that sheetflood deposits have filled in a surface concavity over the last ~400-600 years. At a depth of 350 cm, an abrupt boundary is formed between the overlying debris flow deposit, and a thin (10 cm), fine-grained, fire-related ~6720 cal yr BP debris flow deposit. Another thin, fine-grained ~7170 cal yr BP fire-related debris flow deposit is exposed at

420 cm depth, and is sandwiched by ~120 cm of undated, charcoal-poor sheetflood deposits. At a depth of 497 cm, a thin, lighter-colored, fine-grained unidentified tephra unit overlies a 50 cm thick 9970 cal yr BP fire-related debris flow deposit. While geochemical analysis of the tephra unit did not identify the unit as Mazama ash (~7700 cal yr BP; Zdanowicz et al., 1999), extensive mixing may have contaminated the sample, and we infer that this glass-rich unit constrained by 7170-9970 cal yr BP charcoal ages is likely Mazama ash. At the base of the exposure, ~75 cm of an ~11,540 cal yr BP debris flow deposit is exposed.

Arroyo sites C12 (Figure 13) and C8 drain southward into South Fork of Circle Creek, and have small upslope contributing areas of 0.04 km^2 and 0.03 km^2, respectively (Figure 3; Figure 7). Located only 0.5 km apart, and separated by a sharp granitic fin, these sites record fires from ~10,600 to 400 cal yr BP. Radiocarbon ages and stratigraphic characteristics of sites C8 and C12 corroborate, and when combined, provide a more complete fire and depositional history (Figure 6).

Incision at site C12 exposes ~500 cm of stratigraphy (Figure 13; Table 2; Appendix). The top of the profile consists of 115 cm of charcoal-rich sheetfloods that are dated ~450 cal yr BP at 60 cm depth, and~ 610 cal yr BP at 115 cm depth. These upper sheetfloods form an abrupt boundary with an underlying ~50 cm thick ~690 cal yr BP fire-related debris flow deposit. Stratigraphy exposed between 150-250 cm depth consists of undated sheetfloods interbedded with two undated thin (<5 cm), fine-grained, charcoal-rich debris flow deposits, or these are possibly fine-grained portions of sheetflood couplets. These deposits overlie a sequence made up of three thin (~10 cm), fine-grained, fire-related debris flow deposits dated downward in the profile ~6830, 6950,

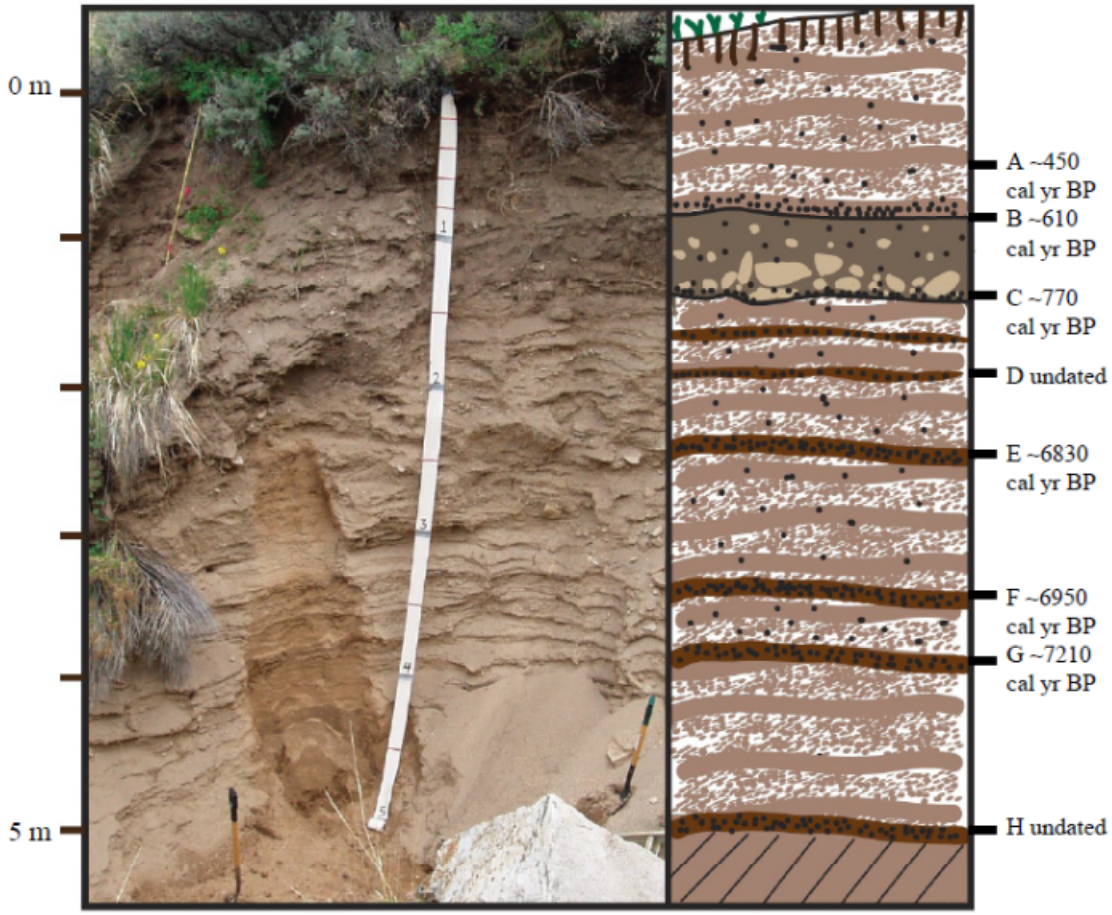

Figure 13: Site C12 exposure of arroyo fire-related stratigraphy where black circles represent charcoal: A) charcoal-rich sheetflood deposits, B) charcoal-rich sheetflood deposits, C) charcoal -rich debris flow deposit (charcoal is more concentrated within unit compared to unit B with abrupt lower boundary, D) undated sheetfloods interbedded with very thin (<5 cm) muddy debris flow deposits, that may correspond to ~2500-2000 cal yr BP fire interval or to 4490 cal yr BP sheetflood deposits at site C8, E) thin debris flow deposit (~10 cm) interbedded within sheetfloods, F) thin debris flow deposit (~10 cm) interbedded within sheetfloods, G) thin debris flow deposit (~10 cm) interbedded within sheetfloods and, H) debris flow deposit.

and 7210 cal yr BP, respectively, interbedded with ~130 cm of charcoal-rich sheetfloods exposed between ~250 and 380 cm depth. Below 380 cm depth, a ~100 cm thick package of sheetfloods overlies an undated thin (~10 cm) debris flow deposit exposed at the base of the profile.

Site C8 exposes ~650 cm of stratigraphy and was measured and described from two sections that consist of a ~285 cm thick upper section and a ~375 cm thick lower section, on opposite sides of the arroyo (Figure 6). At the top of the upper section, ~50 cm of undated sheetfloods overlie a ~75 cm thick ~710 cal yr BP debris flow deposit, which may have deposited during the same fire interval as the ~690 cal yr BP debris flow at C12. This unit overlies ~160 cm of sheetfloods dated ~4490 cal yr BP. Across the drainage at C8, and stratigraphically below the ~4490 cal yr BP unit, is a 175 cm thick debris flow deposit dated ~9550 cal yr BP. This unit likely corresponds to the undated debris flow deposit at the base of C12 based on stratigraphic characteristics and location within the profile (Figure 6; Figure 13; Table 2; Appendix). The debris flow deposit overlies ~200 cm of sheetfloods dated ~10,390 and ~10,620 cal yr BP, respectively.

The nearby arroyo site C9 records fires and fire-related deposition in 150 cm of successive sheetflood deposits and one debris flow deposit dated between 390-490 cal yr BP (Figure 6; Table 2; Appendix). Sheetfloods at site C9 correspond to sheetfloods exposed in sites A1, H15, C12, and C8, and indicate active and widespread fire-related sheetflooding during the last ~700 years (Figure 6).

Fire-Related Geomorphic Response Recorded in Streambank Stratigraphy

In this section, we provide a detailed description of one streambank site (Site C10) because it is the deepest streambank exposure and exposes the oldest streambank stratigraphy in the study area. The rest of CIRO streambank stratigraphy is summarized in the appendix. Site C10 exposes ~350 cm of fire-related stratigraphy (Figure 14) in the active channel of South Fork of Circle Creek (Figure 3; Figure 6; Table 2; Appendix).

During the last ~10 years, this site has experienced meander cutbank erosion that

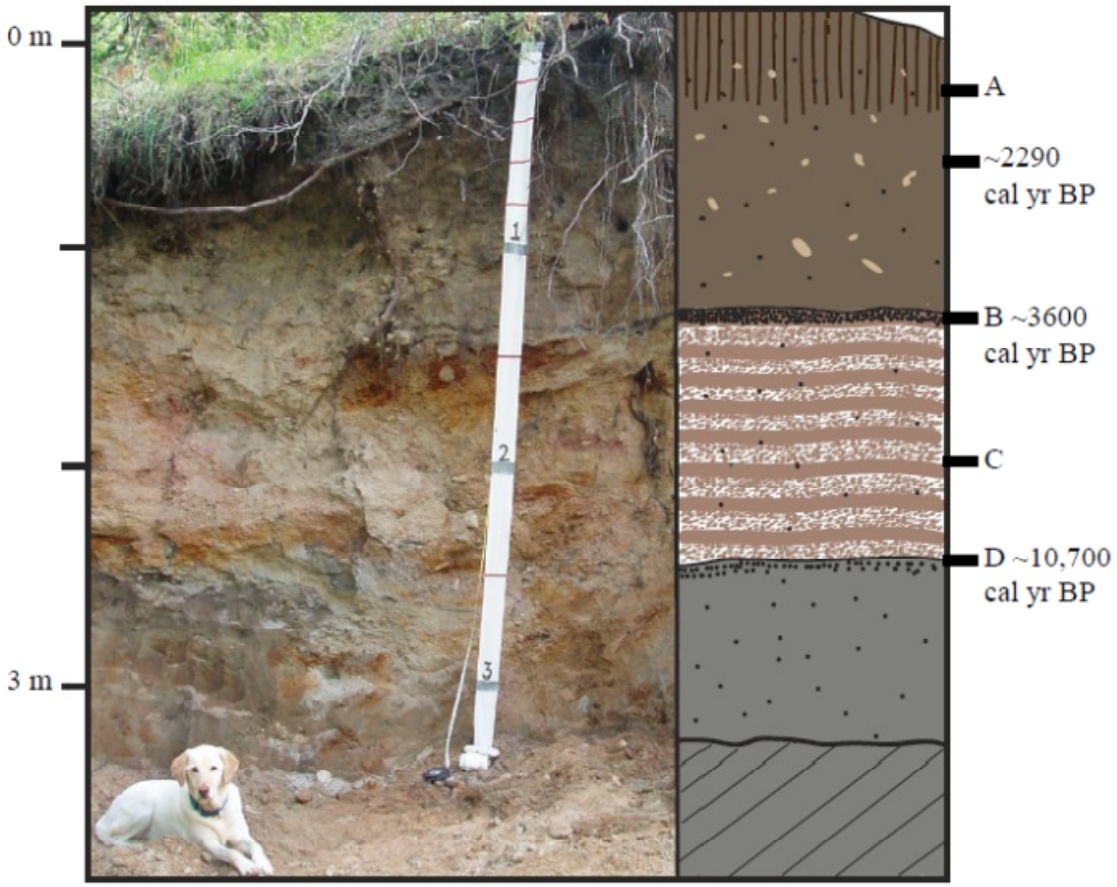

Figure 14: Site C10 streambank exposure: A) extensive soil developed on thick continuous debris flow deposit, B) continuous charcoal-rich debris flow deposit, C) undated oxidized sheetflood deposits containing sparse charcoal and, E) overbank deposit with upper charcoal-rich layer.

removed part of a hiking trail and caused park staff to re-route the trail near the creek. Between the 2010 and 2011 summer field seasons, a thin tongue of land that existed between two meanders (one that exposed C10 stratigraphy) was breeched and a tree fell into the channel, burying much of the C10 exposure (Figure 15; Figure 16).

The top ~150 cm of C10 consists of a thick debris flow deposit dated 2290 cal yr BP that was sampled from site C11, an upstream exposure in an ephemeral channel (Figure 6; Figure 7; Table 2; Appendix). The age of this debris flow deposit and subsequent period of stability (indicated by soil development) corresponded with a ~2300 cal yr BP fire-related debris flow deposit and soil at site H15. Lower in the profile, a

Figure 15: Site C10. The upper photo was taken in 2010. The lower photo was taken in 2011 after streambank collapse. Tree roots shown in the upper corner of the 2010 photo are from the same tree that fell into the stream shown in the lower left corner of the 2011 photo.

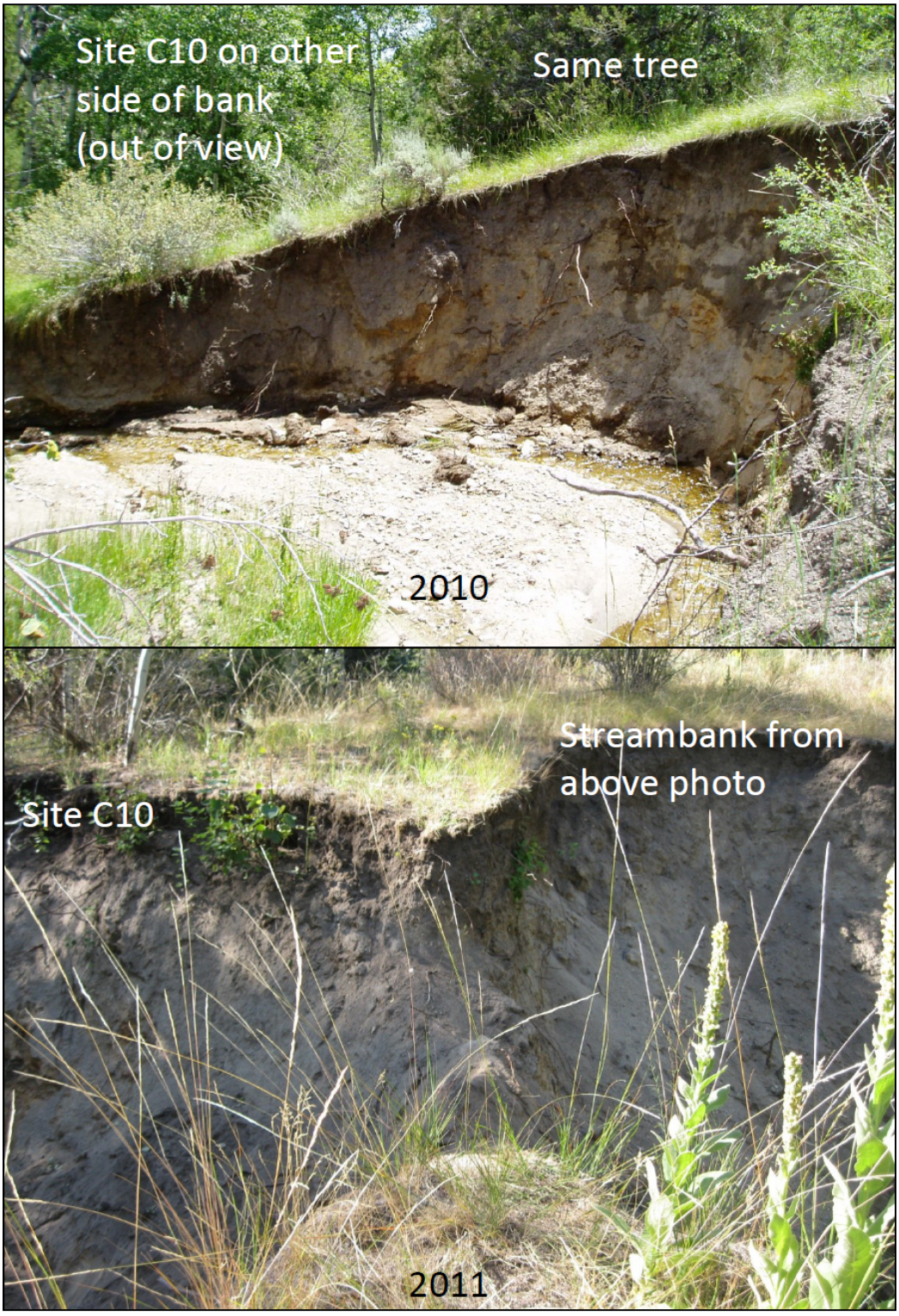

Figure 16: Site C10. The upper photo showing 2010 site conditions and lower photo showing 2011 site conditions following channel erosion. Note the same tree is shown in upper photo as indicated in Figure 15.

charcoal-rich sheetflood deposit dated ~3640 cal yr BP is exposed at 150 cm depth. This fire-related deposit tops a ~100 cm thick package of sheetfloods that contain sparse charcoal. These lower, undated sheetfloods may correspond to active charcoal-poor sheetflooding during the 7200-6700 cal yr BP fire interval also observed at sites C12 and H15. A ~75 cm thick charcoal-rich overbank deposit dated 10,700 cal yr BP is exposed at the base of the profile.

Climate and Vegetation Reconstructions from Woodrat Middens

The CIRO midden record shows that Rocky Mountain juniper, limber pine, and big sagebrush have been present on the landscape since ~50,000 cal yr BP (Table 3). Utah juniper migrated to CIRO at ~3800 cal yr BP and was followed by single-leaf pinyon at ~2800 cal yr BP. Single-leaf pinyon is abundant in middens from ~2800-2400 cal yr BP; however, it is absent in middens dated ~2400-700 cal yr BP, suggesting either slow expansion or colonization occurred as two events. The first was a failed invasion, while the post-700 cal yr BP event successfully established single-leaf pinyon as a dominant species (Betancourt, unpublished data).

Periods of frequent midden radiocarbon ages are indicative of flourishing packrat midden populations and can be used as a measure for ecosystem productivity (Webb and Betancourt, 1990). Summed calibrated radiocarbon ages of middens from CIRO, Oneida Narrows, and the Lost River Range are compared to the CIRO fire record in Figure 10b. We do not apply the correction for taphonomic bias to the summed probability distribution of midden ages, since midden preservation would not be subject to taphonomic bias caused by erosion and weathering because middens are typically

Table 3: Summary of midden data collected at CIRO.

Lab ID	Sample ID	^{14}C Age BP	Ana-lytical error ±	Median calibrated age (cal yr BP)	Error (1 σ)	Error (2 σ)	Vegetation ID
81158	526-Pinnacle Pass Cave	115	15	162	66-258	58-264	Single-leaf pinyon
81146	211C-PIMO-Twin Sisters	120	20	165	67-262	55-268	Single-leaf pinyon
81143	564-PIMO-Twin Sisters	330	15	373	350-396	347-460	Single-leaf pinyon
81300	209A-Flaming Rock Trail	315	15	402	376-427	349-437	Single-leaf pinyon
81301	209B(2)-Flaming Rock Trail	315	15	402	376-427	349-437	Single-leaf pinyon
81165	504-Flaming Rock Trail	345	15	444	428-459	317-478	Single-leaf pinyon
81308	208-Window Arch	575	15	615	604-626	594-634	Single-leaf pinyon
81306	568-South Fork Circle Creek	720	15	671	666-676	661-682	Single-leaf pinyon
81309	207-Window Arch	1280	15	1249	1234-1264	1220-1275	Rocky Mtn juniper
81147	211C-JUOS-Twin Sisters	1380	15	1297	1291-1302	1283-1310	Utah juniper
81310	507-Window Arch	2410	15	2431	2406-2456	2352-2474	Single-leaf pinyon
81144	564-JUOS-Twin Sisters	2685	15	2771	2759-2783	2752-2797	Utah juniper
81304	541-Bath Rock	2740	15	2810	2792-2828	2783-2863	Single-leaf pinyon
81297	511A-Flaming Rock Trail	2835	15	2942	2923-2960	2916-2991	Limber pine
81157	525-Pinnacle Pass Cave	2970	15	3174	3140-3207	3077-3211	Utah juniper
81156	524-Pinnacle Pass Cave	3105	15	3349	3334-3364	3320-3377	Utah juniper
81166	510-Flaming Rock Trail	3180	20	3393	3378-3407	3367-3445	Limber pine
81161	529-Pinnacle Pass Cave	3260	20	3465	3446-3483	3442-3558	Utah juniper
81303	567-Bath Rock Trail	3585	15	3877	3853-3901	3838-3925	Rocky Mtn juniper
81298	511B-Flaming Rock Trail	4000	15	4497	4480-4513	4463-4518	Limber pine
81162	576A-Staircase Trail	4170	15	4723	4702-4743	4685-4762	Rocky Mtn juniper
81299	503-Flaming Rock Trail	4525	15	5148	5132-5164	5054-5186	Rocky Mtn juniper
81163	576B-Staircase Trail	4975	15	5677	5661-5693	5656-5733	Rocky Mtn juniper
81307	210-Window Arch	5225	15	5946	5938-5953	5929-5993	Rocky Mtn juniper
81305	570-Bath Rock Trail	5830	15	6652	6638-6666	6603-6373	Limber pine
81164	531-Flaming Rock Trail	6215	20	7090	7066-7113	7015-7125	Limber pine
81302	542-Bath Rock Trail	7070	15	7883	7870-7895	7856-7903	Limber pine
81148	211D-Twin Sisters	8100	20	9017	9005-9028	8996-9033	Rocky Mtn juniper
81150	211F-Twin Sisters	28460	140	32886	32599-33172	32139-33312	Limber pine
81149	211E-Twin Sisters	28890	140	33364	33061-33667	32940-34232	Limber pine
81155	523-Pinnacle Pass Cave	29720	160	34582	34439-34725	33866-34808	Limber pine
81145	211A-Twin Sisters	31760	190	36432	36263-36600	36152-36723	Limber pine
81153	509A-Pinnacle Pass Cave	42540	690	45706	45172-46239	44631-46974	Limber pine
81152	506B-Pinnacle Pass Cave	44930	910	48116	47027-49204	46342-49950	Limber pine
81159	527-Pinnacle Pass Cave	45140	930	48346	47267-49425	46499-50000	Limber pine
81154	502-Pinnacle Pass Cave	45600	1300	48973	47969-49976	46695-50000	Limber pine
81151	502-Pinnacle Pass Cave	47500	1300	50000	50000	50000	Limber pine
81160	528-Pinnacle Pass Cave	47800	1300	50000	50000	50000	Limber pine

preserved in rock shelters and caves (Surovell et al., 2009). The midden record began around 12000 cal yr BP, however radiocarbon ages do not form high frequency clusters until ~4500 to 2000 cal yr BP (Smith and Betancourt, 2003; Betancourt, unpublished

data). Between 2000 to 700 cal yr BP (the interval in which pinyon expanded slowly or failed in an initial expansion), midden ^{14}C ages drop off significantly. Midden frequencies increase again between 700 to 300 cal yr BP (Smith and Betancourt, 2003; Betancourt, unpublished data).

Geomorphic and Lithologic Controls on Fire-Related Erosion

Deeply incised arroyos that contain abundant fire-related deposits are common in granitic and gneissic lithologies of Circle Creek, upper Heath Canyon, Graham Creek, Stines Creek, and Almo Creek (Figure 3). However, fire-related deposits are limited and/or absent in the deep arroyos formed in quartzite basins of Emigrant Canyon and in lower reaches of Heath Canyon. This suggests that hillslopes formed in resistant quartzite are less susceptible to fire-related erosional events. For example in 2000, a mixed-severity, crown fire burned ~8.5 km^2 in quartzite terrain of southern CIRO (Monitoring Trends in Burn Severity, 2011). Local residents observed increased fire-related surface erosion during a storm event a few days following the fire (Morris, 2006), which was likely surface rilling (Shakesby and Doerr, 2006). However, field observation found no evidence for large-scale post-fire erosional events, such as sheetflood or debris flow deposition. The landscape, now characterized by standing dead pinyon and juniper, has since been invaded by cheatgrass.

One definition for surface ruggedness is variability in slope and standard deviation of slope can be used as a proxy for basin ruggedness (Grohmann et al., 2011). Standard deviation of slope calculated by ArcGIS tools indicates that Circle Creek Basin exhibits the highest degree of basin ruggedness (Figure 17). Standard deviation of slope accurately identified the local terrain variability of the Almo granitic pluton that

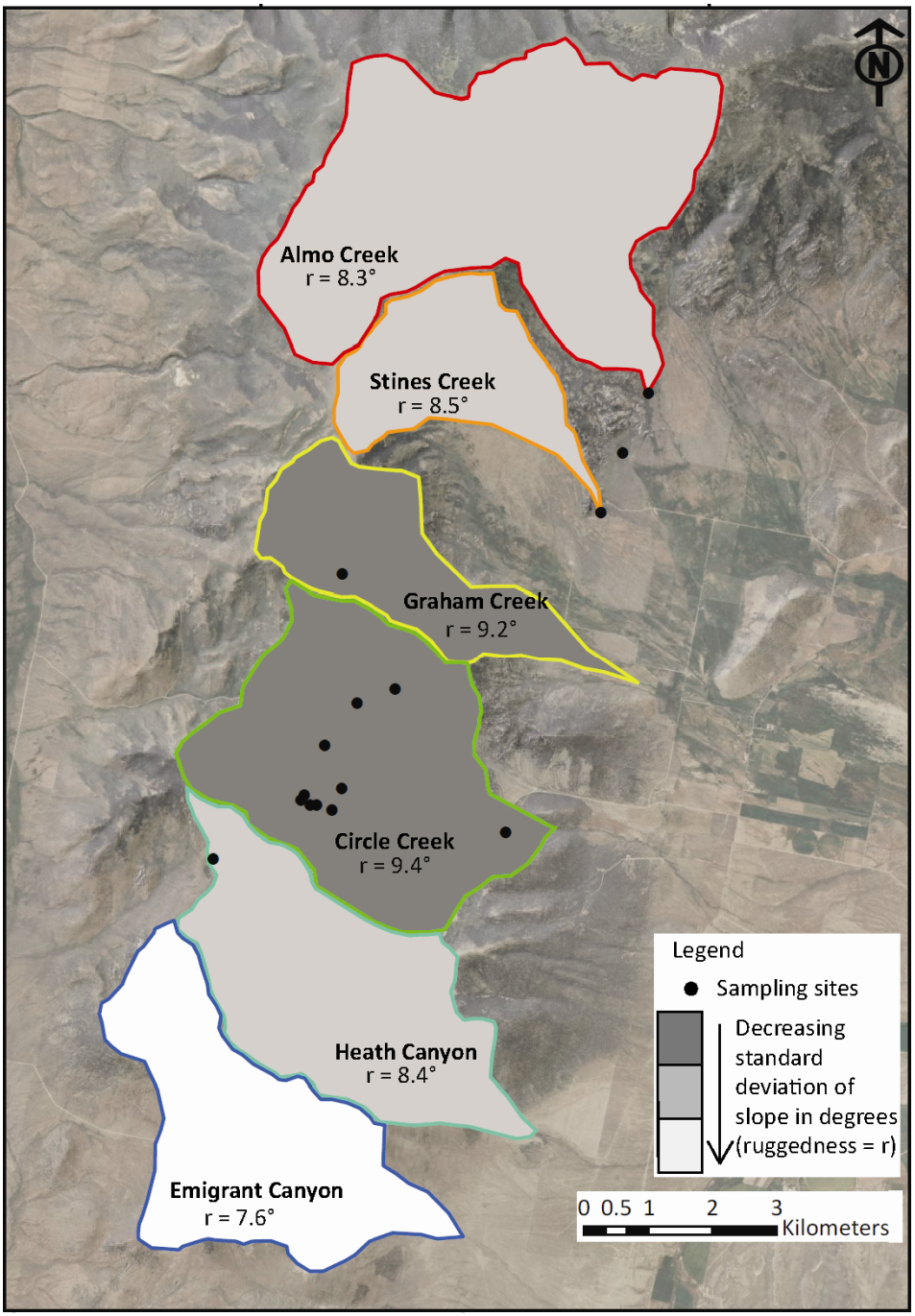

Figure 17: Map showing standard deviation of slope (ruggedness) in degrees for CIRO study basins.

comprises the majority of Circle Creek Basin, and is rapidly eroding to form fins, domes and spires. Consistent with the findings from Cannon and Reneau (2000) of characteristics of debris flow producing basins, the majority (>75%) of debris flows

occurred in the basin with the highest ruggedness value. In addition, Circle Creek Basin also contains the greatest number of fire-related deposits with 11 of 16 sampling sites located in streambanks on Circle Creek or in grussy arroyos that drain into Circle Creek, indicating that this granitic basin is altogether more susceptible to fire-related erosional processes.

Skew of slope frequency histograms are used to identify dominant diffusive processes within a basin. When a majority of gentle slopes (<16°) are plotted in a histogram, the histogram will exhibit positive skewness, while negatively skewed histograms are made up of predominantly steeper slopes (>16°). Positively skewed slope frequency histograms are indicative of basins susceptible to creep and slope-wash processes, and negatively skewed slope frequency histograms corresponds to basins that experience mass-wasting processes, such as debris flows and landslides (Wolinsky and Pratson, 2005). All basins at CIRO exhibit ≥0 (positive) skewed slope frequency histograms.

Although DEM-generated slope frequency histograms (Figure 18) do not support debris flow generation in any basins at CIRO, stratigraphic analysis shows that debris flows did occur and were common during the early and late Holocene in all basins with the exception of Emigrant Canyon. Slope frequency plots indicate a higher frequency of shallow slopes in quartzite dominated basins (Emigrant and Heath Canyon), while gneissic and granitic basins (Almo, Stines, Graham) and granitic Circle Creek exhibit moderately higher frequency of steeper slopes (Figure 2; Figure 18). Emigrant and Heath Canyon exhibit more positively skewed histograms (+2) than Circle Creek and Graham Creek (+1), while slope histograms for Stines and Almo Creek have 0 skew value. Almo,

Graham, and Stines basins exhibit bimodal slope frequency histograms, and areas of steeper slope are likely initiation points for mass wasting processes within each basin.

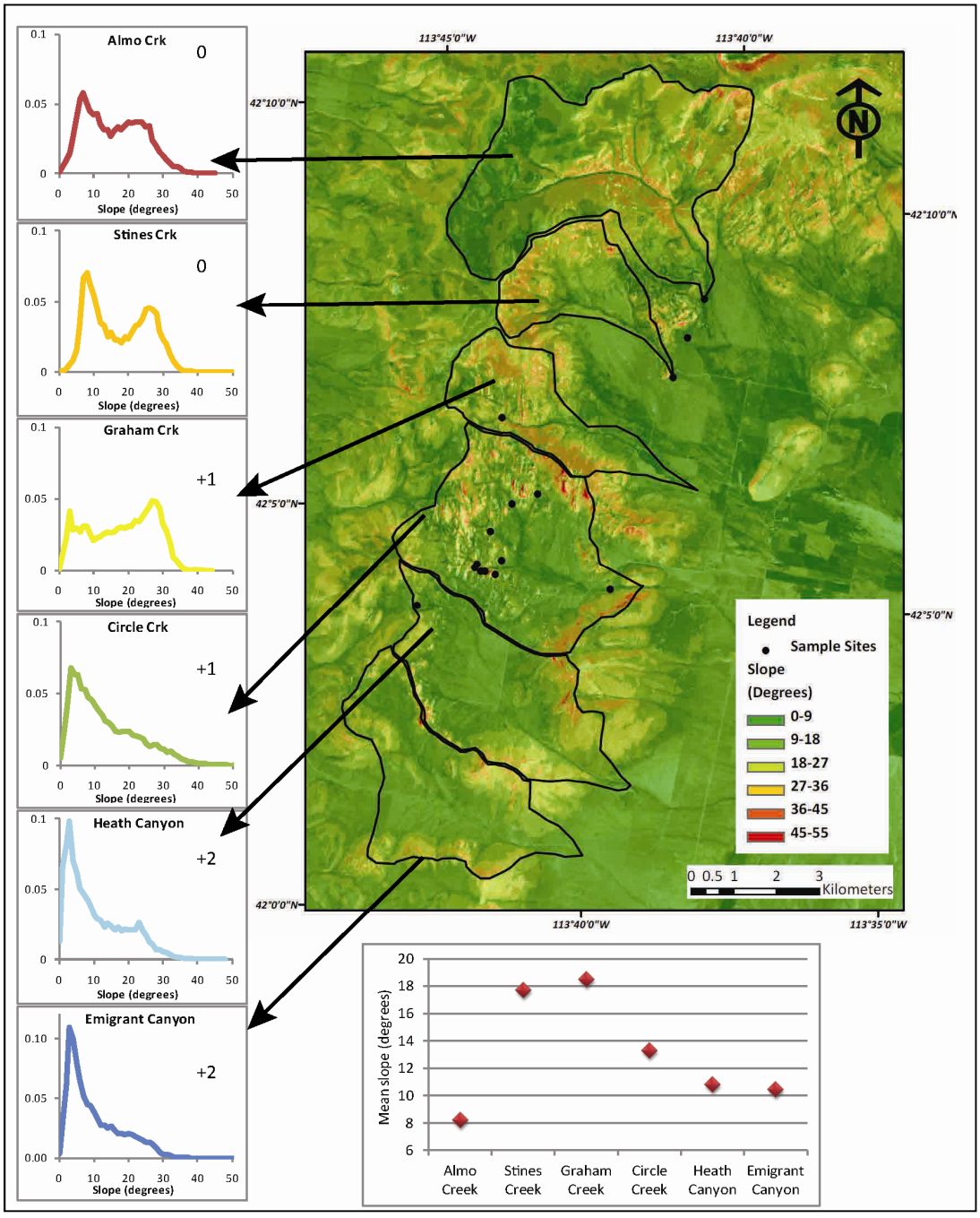

Figure 18: Slope raster map illustrating the generally gently-sloping terrain of CIRO. Slope frequency histograms and skewness values (left side) showing that all basins have positively skewed slope histograms. Bottom graph plots mean slope per basin.

DISCUSSION

The CIRO record indicates that Holocene changes in climate drove shifts in vegetation, associated fire regime, and fire-related erosional response over the course of the last ~13,000 years. During the early Holocene, fires were likely moisture-limited when long term wet intervals suppressed fire. However, a switch to a fuel-limited system likely occurred sometime during the middle Holocene when long-term dry and generally stable climate conditions decreased fire activity. Late Holocene arrivals of Utah juniper and single-leaf pinyon correspond to increased fire activity and changes in fire-related geomorphic response. As pinyon-juniper densities increased, we infer that fires likely became limited more by probability of ignition than fuel availability. These denser forests supplied abundant fuels that were often dried during decadal droughts; however, ignition occurrences, such as convective storms, were necessary.

Comparison of this record with other regional alluvial charcoal records from a range of ecosystems (Meyer et al., 1995; Pierce et al., 2004; Svenson, 2010; Nelson and Pierce, 2010) shows periods of regionally widespread fires and analogous erosional trends, indicating that region-wide climate controlled fire and geomorphic response. Below we discuss major trends in regional climate, vegetation change, and fire regimes within six time frames during the Holocene. We follow these climate sections with a discussion of Holocene patterns of fire-related erosion at CIRO and conclude with a discussion of land management implications.

Late Pleistocene to Early Holocene (13,000 to 9500 cal yr BP)

Most alluvial charcoal records do not exceed ~8000 years (e.g., Pierce et al., 2004; Nelson and Pierce, 2010); however, our record documents seven fires older than 9500 cal yr BP. Two fires burned between 12,700-11,500 cal yr BP, shortly after final glacial retreat from Mt. Harrison in the Albion Range (Bovet et al., 2002). These fires correspond to the Younger-Dryas Cool Interval (12.8-11.5 ka; Berger, 1990) and to cooler, wetter conditions in the Bonneville Basin and Great Basin (Davis et al., 1986; Murchison, 1989; Oviatt, 1997; Broughton et al., 2000; Grayson, 2000; Madsen et al., 2001; Oviatt et al., 2003; Louderback and Rhode, 2009; Doner, 2009). Ignition likely occurred during fire season drought, as indicated by diatom records from Bear Lake that show moderate lake levels between 12,000-10,800 cal yr BP. Although fluvial inputs to the lake were high, increased summer evaporation likely maintained moderate lake levels, suggesting wet winters and warm, dry summers (Moser and Kimball, 2009).

Warming and drying began ~10,800 cal yr BP, as indicated by rapid recession and possible desiccation of Lake Bonneville between 10,800-9900 cal yr BP (Murchison, 1989; Figure 19a). This prolonged dry interval is further supported by Bonneville Basin faunal, midden, and pollen records (summarized by Madsen et al., 2001), when 5 fires burned at CIRO during a 700 year period (10,700-9500 cal yr BP), indicating a minimum recorded fire frequency of one fire per ~140 years (Figure 10c). These fires were likely fueled by dense vegetation developed during the late Pleistocene.

Fire activity may have been greater than indicated by our record between 12,700-9500 cal yr BP when numerous North American lake charcoal records show increased fire activity during rapidly warming climate at ~11,700 cal yr BP (Marlon et al., 2009).

However, poor preservation of deposited alluvial charcoal likely diminishes the recorded fire frequency during this interval. If so, having seven fires older than ~9500 cal yr BP suggests that CIRO likely experienced frequent and severe fires during dramatically changing climate. Furthermore, juniper accounts for the majority of sampled macrofossils at CIRO before ~9900 cal yr BP, indicating high-severity, stand-replacing fires (Figure

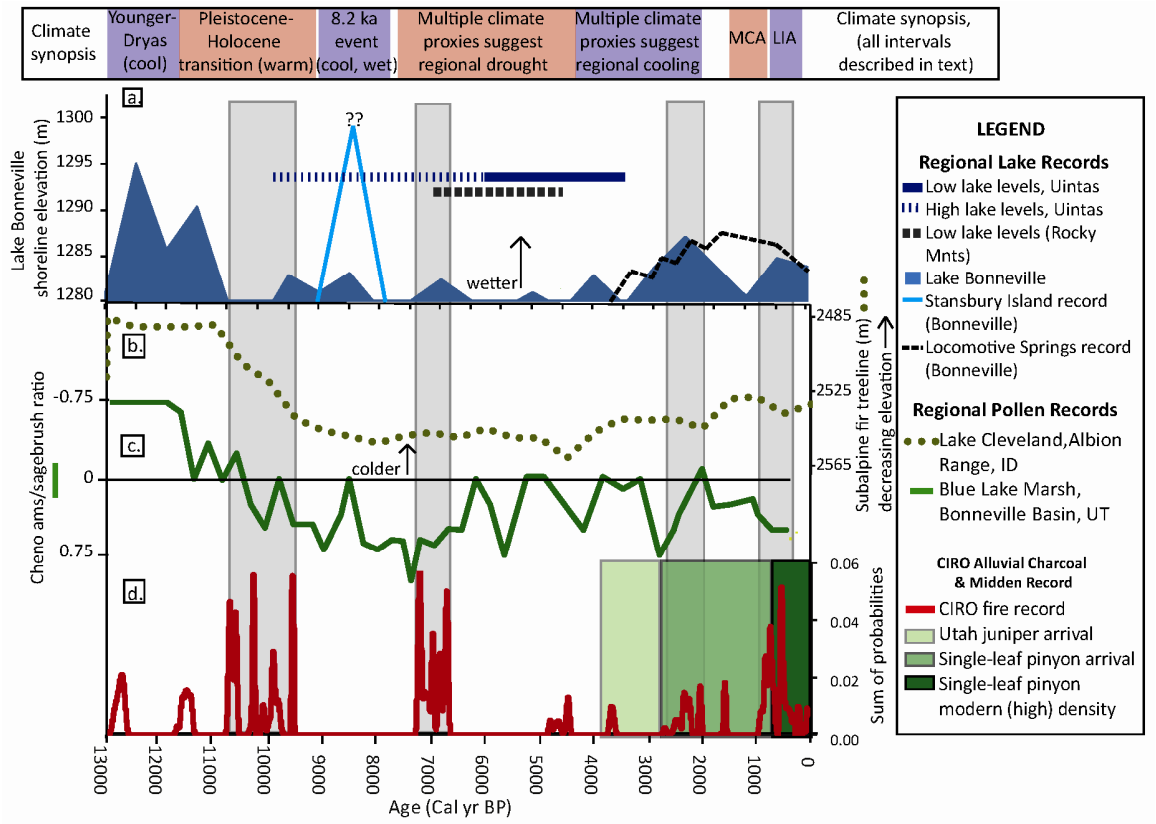

Figure 19: The CIRO fire record (>5000 cal yr BP ages corrected according to Surovell et al., 2009) compared to regional paleoclimate records, with gray bars highlighting periods of increased fire activity. a. Summary of regional lake shoreline elevations from Murchison (1989; solid blue), Patrickson et al. (2010; light blue) and Miller et al. (2005; dashed black line). Dashed and solid straight blue lines show periods of high and low lake level in the Uinta Range (Corbett and Munroe, 2010) and the dashed black line represents an interval of low lake levels in the Rocky Mountains (Shuman et al., 2009). b. Dotted green line shows a pollen reconstruction of subalpine fire elevation (lowest elevation is up) from nearby Lake Cleveland in the Albion Range (Davis et al., 1986). c. Solid green line shows pollen reconstruction of climate from the Blue Lake Marsh of the western Bonneville Basin (Louderback and Rhode, 2009), d. The CIRO fire record is shown in red with the midden vegetation reconstruction (Betancourt, unpublished data) shown in green blocks.

10a). Using modern fire severity-vegetation relationships (Miller and Rose, 1999; Baker and Shinneman, 2004; Romme et al., 2009), fires burning through this juniper-dominated landscape were likely high-severity, stand-replacing fires (Figure 10a).

A similar early Holocene fire interval was observed in the Cygnet Lake record of central Yellowstone National Park, when tundra and grasslands were colonized by lodgepole pine (Millspaugh et al., 2000). In the Blue Lake Marsh region, warmer taxa replaced colder taxa (Louderback and Rhode, 2009), and at Bear Lake, cold tolerant plants and trees shifted to sagebrush steppe vegetation (Doner, 2009). Midden records from Dutch John Mountain in the Uinta Range of northeastern Utah record a shift from mesic conifer forests to more xeric juniper woodlands (Jackson et al., 2005), and at nearby Lake Cleveland, Douglas fir was migrating upward in elevation (Davis et al., 1986; Figure 19b). We infer that CIRO was likely experiencing similar vegetation shifts, as July insolation reached its maximum in North America (Berger, 1978) and the Younger-Dryas came to an end. Warmer temperatures and increased aridity that dried fuels accumulated during the late Pleistocene likely caused one of the most fire-prone intervals on record between 10,700-9500 cal yr BP.

Early to Middle Holocene (9500 to 6500 cal yr BP)

No fires were recorded between ~9500 to 7200 cal yr BP, however fire activity increased again ~7200-6700 cal yr BP, when a 500-year fire period was recorded by seven fires, indicating a minimum recorded fire frequency of 1 fire per ~70 years. These fires are corroborated by the Lake Cleveland record, ~20 km to north, that showed a post-Mazama ash (~7700 cal yr BP) increase in lake sediment charcoal (Davis et al., 1986), suggesting widespread and possibly larger fires.

During the fire-free interval between 9500-7200 cal yr BP, fires were likely inhibited by wetter and cooler conditions. At Stansbury Island in the Great Salt Lake, radiocarbon dating of lake sediment charcoal recorded a ~8300 cal yr BP Lake Bonneville highstand (Patrickson et al., 2010), possibly 60 meters higher than the Gilbert shoreline (Oviatt, 1997; Figure 19a). Patrickson et al. (2010) attributed this highstand to the "8.2 ka cool interval," a widely recognized Heinrich event (Alley et al., 1997) that increased snowpack to the neighboring mountains (Dean et al., 2002). The highstand is corroborated by at least one record: a radiocarbon age from an organic layer presumed to have been deposited on a lagoon floor from Antelope Island in the Great Salt Lake (Murchison, 1989, Murchison and Mulvey, 2000; Figure 19a). Diatom and oxygen isotope records from Bear Lake support wetter and cooler conditions from 9.2-8.2 ka (Moser and Kimball, 2009), and lake sediments from the Uinta Range record a prolonged wet period from 10-6 ka (Corbett and Munroe, 2010; Figure 19a).

Climate began to warm again ~8200-6500 cal yr BP (Grayson, 2000; Schmitt et al., 2002; Louderback and Rhode, 2009) when regional midden radiocarbon ages indicate low ecosystem productivity (Figure 10b; Table 3; Smith and Betancourt, 2003; Betancourt, unpublished data). During this interval, Blue Lake Marsh was desiccated (Louderback and Rhode, 2009; Figure 19c), Lake Bonneville was periodically low (Murchison, 1989; Figure 19a), and in the Great Basin (8000-4000 cal yr BP), pinyon-juniper woodlands occupied elevations 500 m higher than today (Miller and Tausch, 2001).

However, several records provide evidence for a brief period of moderately cooler and wetter conditions beginning ~7500 cal yr BP that likely supplied fuel for the 7200-

6700 cal yr BP fire interval. At Bear Lake (7500-6700 cal yr BP), pollen from cold tolerant trees, shrubs, and plants were present in greater abundances than sagebrush steppe plants (Doner, 2009), and at Blue Lake Marsh beginning ~7200 cal yr BP, pollen records indicate moderate cooling (Louderback and Rhode, 2009; Figure 19a). Lake levels were moderately elevated at Lake Bonneville from 7500-6500 cal yr BP (Figure 19a; Murchison, 1989) and at Bear Lake between 7000-6500 yr BP (Smoot and Rosenbaum, 2009). Farther away in Yellowstone National Park, terrace aggradation was occurring ~7400-6700 cal yr BP (Meyer et al., 1995).

The ~7200-6700 cal yr BP fire interval may mark an ecosystem transition from a previously moisture-limited system to a fuel-limited system. The type of charcoal sampled also changed from early Holocene juniper to a three-way split of juniper, sagebrush, and limber pine (Table 2; Figure 10a), suggesting that these fires were likely stand-replacing based on studies from sagebrush and pinyon-juniper ecosystems (Kauffman and Sapsis, 1989; Baker and Shinneman, 2004). Accordingly, the type of fire-related geomorphic response shifted from early Holocene larger debris flows and thick overbank deposition to predominantly sheetflood deposition with occasional thin, fire-related debris flow deposits.

Not all middle Holocene sheetfloods were fire-related, many thick sheetflood deposits containing sparse or absent charcoal are bracketed by dated units during this time (Figure 6). Evidence for frequent charcoal-poor sheetflood deposition suggests hillslope erosion occurred when vegetation densities were low, and sparsely vegetated hillslopes also likely limited fuel. However, prior to the 7200-6700 cal yr BP fire interval, brief annual to decadal moisture must have sufficiently increased fine fuel accumulation

for fuel connectivity and fire-spread across CIRO and into higher elevation areas at nearby Lake Cleveland (Davis et al., 1986).

Interestingly, other alluvial charcoal records report fire activity between ~7500-6200 cal yr BP (Figure 20). Fires were recorded ~6300 cal yr BP in Yellowstone (Meyer et al., 1995), and at ~6500 cal yr BP in Wood Creek (Nelson and Pierce, 2010). Increased fire activity was recorded by sheetflood deposits in the South Fork of the Payette, Idaho (SFP) between ~7400-6600 cal yr BP (Pierce et al., 2004). Unlike CIRO, the SFP is characterized by significantly steeper, granitic hillslopes prone to post-wildfire debris flows; however, during this fire interval, SFP experienced analogous sheetflood deposition and limited debris flow activity from currently debris-flow prone north-facing slopes (Meyer et al., 2001; Pierce et al., 2004).

Although 7200-6700 cal yr BP fires at CIRO were likely fueled during a brief local cooling (Davis et al., 1986; Murchison, 1989; Louderback and Rhode, 2009; Doner, 2009), regionally this period marked the beginning of extended drought recorded by low lake levels in the Rocky Mountains (Shuman et al., 2009) and in the Uinta Range, Utah (Corbett and Monroe, 2010), suggesting that region wide drought was the driver of these regionally widespread fires (Figure 19a, b and c).

Middle to Late Holocene (6500 to 2500 cal yr BP)

Fires were infrequent at CIRO and fire-related erosion was at a minimum between 6500-2500 cal yr BP. Only two fires were recorded between ~4700-4500 cal yr BP and only one fire was recorded at ~3600 cal yr BP, indicating a minimum recorded fire frequency of 1 fire per ~700 years (Figure 10d).

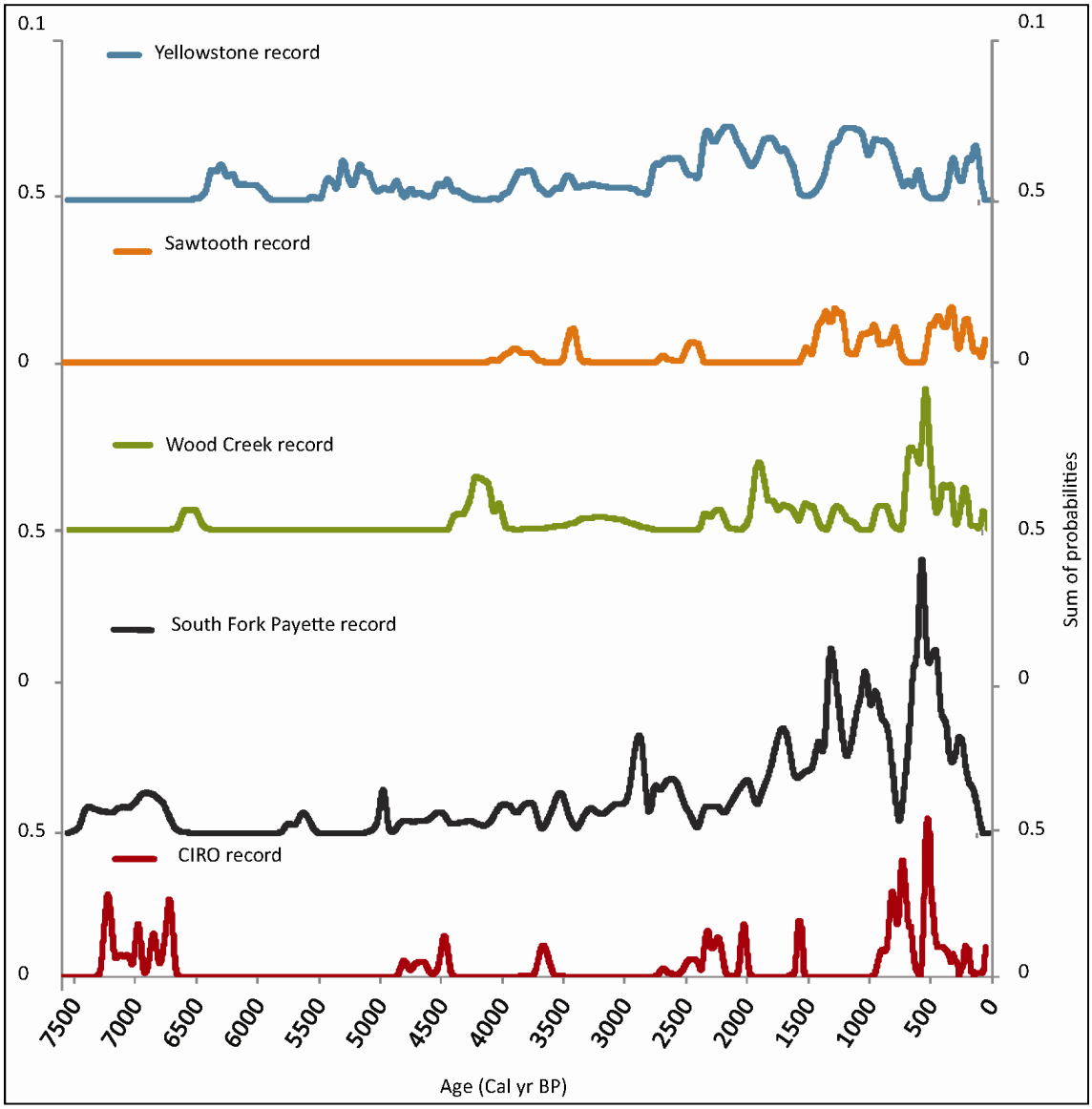

Figure 20: Comparison of the CIRO fire record (red) to other regional alluvial charcoal records (Meyer et al., 1995; Pierce et al., 2004; Svenson, 2010; Nelson and Pierce, 2010). The CIRO record is not corrected for "taphonomic bias" (Surovell et al., 2009) because the other alluvial charcoal records have not been corrected.

The period of no recorded fires from 6700-4700 cal yr BP at CIRO corresponds to extended regional drought between ~7000 to ~4000 yr BP (Murchinson, 1989; Louderback and Rhode, 2009; Shuman et al. 2009; Corbett and Munroe, 2010) that drove nearby Lake Cleveland subalpine fir forests up to a maximum elevation at ~4500 cal yr BP (Davis et al., 1986; Figure 19). At CIRO, low vegetation densities from previous fire-

removal, sustained by persistent drought, likely inhibited fuel accumulation on hillslopes. Similar no-fire periods are observed in other alluvial charcoal records, suggesting that analogous low vegetation densities were regionally persistent (Figure 20; Pierce et al., 2004; Svenson, 2010; Nelson and Pierce, 2010). While Yellowstone was burning during this interval, past fires in this moist, densely vegetated ecosystem have been correlated with severe drought (Figure 20; Meyer et al., 1995).

Beginning ~4000 cal yr BP, Lake Bonneville shorelines begin to rise (Murchison, 1989; Figure 19a) and subalpine fir elevations were descending at Lake Cleveland (Davis et al., 1986; Figure 19b). Midden records from the Oneida Narrows and Lost River Range (Figure 10b; Smith and Betancourt, 2003; Betancourt, unpublished data), and northern Wyoming (Lyford et al., 2003) suggest a return to cooler, wetter climate between ~4500-2000 cal yr BP. Regionally cooler climate is supported by faunal, midden, and pollen records in the Bonneville Basin and the Great Basin (Broughton et al., 2000; Madsen et al., 2001; Mensing et al., 2008; Louderback and Rhode, 2009). During this time, Utah juniper migrated to CIRO ~3800 cal yr BP, followed by single-leaf pinyon at ~2800 cal yr BP (Table 3; Figure 19d; Betancourt, unpublished data).

High-frequency fires that burned between ~7200-6700 cal yr BP followed by no recorded fire activity until ~4700 cal yr BP may indicate climate-forced fire removal of fuel, and subsequent drought suppression of fuels. The climate-fire model put forth by Westerling et al. (2011) predicts that as climate warms, fire rotation times will progressively decrease until there is insufficient time for forest regeneration between fire events. Eventually, fire strips the landscape of vegetation and can trigger transformative ecosystem change. According to the midden record, prior to the 7200-6700 cal yr BP fire

interval, CIRO was vegetated by limber pine, Rocky Mountain juniper, and sagebrush (Table 3). Limber pine forest regeneration can take more than ~500 years (Rebertus et al., 1991). Although pinyon was not yet present at CIRO during this time, estimates for post-fire regeneration in pinyon-juniper forests is ~150-200 years (Goodrich and Barber, 1999). However, juniper recovery can occur faster than pinyon during periods of drought (Shinneman and Baker, 2009). Recovery in sagebrush vegetation following fire can take 35-100 years (Baker, 2006). During the 7200-6700 cal yr BP fire interval, recorded fires indicate that CIRO burned a minimum of 1 fire per ~70 years. While this frequency is for the entire study area (not individual basins), synchronous fire activity at nearby Lake Cleveland (Davis et al., 1986) suggests these fires were large and widespread, so the fire frequency may have exceeded the time interval needed for regeneration of limber pine and Rocky Mountain juniper. Afterwards, persistent warm and dry conditions likely sustained low vegetation densities and suppressed fire.

The absence of fire at CIRO between 6500-4800 cal yr BP, during a period of regionally drier conditions and low ecosystem productivity (Figure 10b; Smith and Betancourt, 2003; Betancourt, unpublished data), suggests that drought suppressed fuel loads and inhibited fire (Figure 19). However, moderate burning between 4700-3600 cal yr BP corresponds to higher ecosystem productivity (Figure 10b; Table 3; Smith and Betancourt, 2003; Betancourt, unpublished data). These fires also correspond to a peak in fire in the Wood Creek record (Figure 20; Nelson and Pierce, 2010) and to increased fire frequency in a sagebrush ecosystem at Newark pond, Nevada ~290 km southwest of CIRO (Mensing et al., 2006). All three ecosystems likely experienced increased fire activity, as fuel loads increased under wetter climate beginning ~4500 cal yr BP.

Late Holocene (2500 to 200 cal yr BP)

There are two apparent trends during the late Holocene among climate, vegetation, and fire. First, Figure 10b shows a strong relationship between periods of increased fire activity (specifically at ~1600, ~850, and ~500 cal yr BP) and increased ecosystem productivity (Smith and Betancourt, 2003; Betancourt, unpublished data). Secondly, fires recorded at ~1600, ~850, and ~500 cal yr BP burned during documented droughts (discussed below) subsequent to above average moisture conditions (Figure 21).

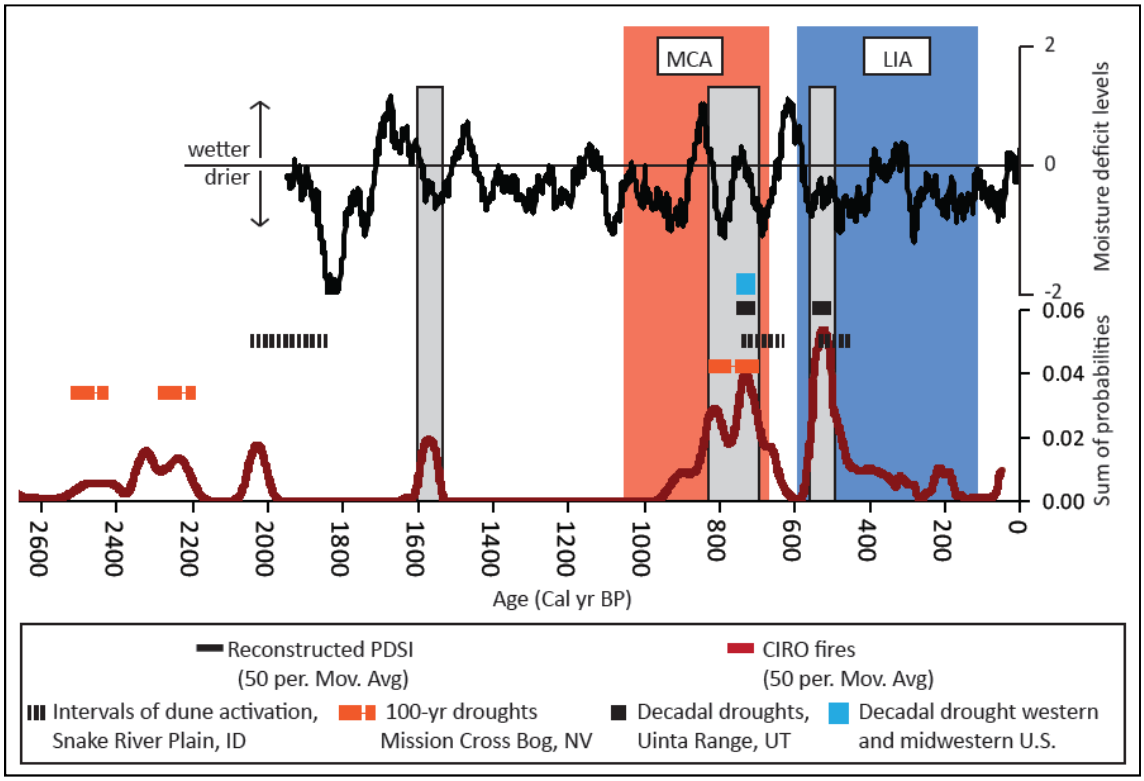

Figure 21: A 2600-yr comparison of the CIRO fire record (red) to Palmer Drought Severity Index reconstructed from tree rings (upper black line; Cook et al., 2004), and to record of drought from the Snake River Plain, Idaho (Rittenour and Pearce, 2011), Mission Cross Bog, Nevada (Mensing et al., 2008), Uinta Range, Utah (Gray et al., 2004) and the Midwestern U.S. (Stahle et al., 2007). Red and blue shading show timing of the MCA and LIA. Gray shading highlights fire intervals.

These trends suggest a strong link between variable climate and increased fire activity because CIRO fires burned fuels accumulated during wetter intervals that were dried

during ensuing drought (Figure 21). The greatest fire frequencies were recorded during pinyon-juniper expansion (discussed below), indicating that fuel availability was no longer a limiting factor and that the ecosystem likely shifted from a fuel-limited system to an ignition-limited system, where fire occurrence is limited by probability of ignition (i.e., occurrence of convective storms; Romme et al., 2009; Gedalof, 2011).

The arrival of single-leaf pinyon was followed by a period of moderate fire activity between 2400-2000 cal yr BP, when alluvial sediments recorded a minimum frequency of 1 fire per ~100 years (Figure 10c). These fires burned during the tail end of ~2000 years of cooler and wetter climate (~4000-2000 cal yr BP) as suggested by midden radiocarbon ages (Figure 10b), when lake levels were elevated in the Bonneville Basin (Figure 19a; Murchison, 1989; Miller et al., 2005) and mark the return of fire-related debris flows in the stratigraphic record (Figure 10d).

Optically Stimulated Luminescence (OSL) dating indicates a period of dune activity (as a proxy for drought) occurred ~2 ka in the Idaho Falls dune field of the Eastern Snake River Plain (Figure 21; Rittenour and Pearce, 2011). At Mission Cross Bog in northeastern Nevada, two droughts lasting at least 100 years were observed ~2500 and ~2200 cal yr BP (Figure 21; Mensing et al., 2008). Both drought records correspond well with fires dated between 2400-2000 cal yr BP at CIRO.

After ~1600 cal yr BP, fires at CIRO match up well with drought intervals from tree ring reconstruction of PDSI (Cook et al., 2004), pollen-inferred droughts from the Mission Cross Bog (Mensing et al., 2008), and globally widespread climatic intervals such as the MCA and LIA (Figure 21). Interestingly, no fires were recorded at CIRO between 1500-1000 cal yr BP, when PDSI reconstruction indicates relatively warmer but

comparatively less variable climate (Cook et al., 2004; Figure 21). The ~850-700 cal yr BP fire interval that burned towards the end of the MCA at a minimum recorded frequency of 1 fire per ~30 years, may correspond to a severe drought dated 1250-1288 A.D. (760-700 cal yr BP; Gray et al., 2004) and matches well with ~760 yr BP dune activation in the Eastern Snake River Plain (Rittenour and Pearce, 2011; Figure 21).

During the LIA, fire frequency increased to a minimum recorded frequency of 1 fire per ~20 years between ~ 550-400 cal yr BP (Figure 10c). The fire peak corresponds to a persistent drought dated 1444-81 A.D. (510-470 cal yr BP) that impacted the western and Midwestern U.S. (Stahle et al., 2007), and another drought dated 1437-1477 A.D. (510-470 cal yr BP) measured from tree rings in the Uinta range of northeastern Utah (Figure 21; Gray et al., 2004).

Following its arrival, single-leaf pinyon expanded slowly and did not establish dominance until ~700 cal yr BP (Figure 10c; Table 3). This expansion coincides with colonization by two-needle pinyon *(Pinus edulis)* to Dutch John Mountain in the Uinta Range between 1000-800 cal yr BP (Jackson et al., 2005). Expansion of two-needle pinyon was episodic and largely controlled by variable climate; in addition drought-driven removal of Utah juniper may have allowed two-needle pinyon to successfully populate the area during subsequently wetter decades (Gray et al., 2006). Perhaps at CIRO, single-leaf pinyon expansion was inhibited by fires dated between 2400-2000 cal yr BP and 1600 cal yr BP. Or perhaps, fires dated 850-700 cal yr BP stripped the landscape of other vegetation, such as sagebrush, which accounted for ~67% of sampled charcoal during this interval (Figure 10a), and primed the landscape for single-leaf pinyon to take hold as dominant species.

High stand densities of pinyon by ~700 cal yr BP likely fueled the greatest fire peak on record 550-400 cal yr BP. This fire peak was observed in other alluvial charcoal records across a range of ecosystems that include lower elevation and middle elevation forests from the Payette record (Pierce et al., 2004), more xeric Wood Creek (Nelson and Pierce, 2010), and Newark Pond records (Mensing et al., 2006), as well as, cooler high elevation forests of Yellowstone (Meyer et al., 1995) and the Sawtooth range (Svenson, 2010; Figure 20). These separate ecosystems likely burned differently, for example, in the Payette region low-severity fires typical of Ponderosa pine and Douglas fir forests were prevalent. At CIRO, a new fire regime likely took hold, and high-severity fires typical of pinyon-juniper woodlands (Baker and Shinneman, 2004; Romme et al., 2009), and sagebrush steppe (Kauffman and Sapsis, 1989) burned through the area. High-severity fires, which have been correlated to debris flow activity in the SFP record (Pierce et al., 2004) likely increased fire-related debris flow erosion at CIRO (Figure 10d).

Historical Fires (200 cal yr BP to Present)

Repeat photographs of CIRO document increases in pinyon-juniper density and downslope infilling during the last ~150 years (Morris, 2006), which is consistent with other historical observations of recent pinyon-juniper expansion in the western U.S. (Romme et al., 2009). The California trail passes through the southern portion of CIRO and many emigrants kept diaries that documented climate, fire, and vegetation at CIRO from 1846-1871 A.D. Emigrant accounts suggest cooler and wetter conditions than today with descriptions of snow-capped peaks from May through September (Morris, 2006).

This timing of active emigration through CIRO corresponds to the close of the LIA, which ended ~100 years ago (Grove, 2001).

One repeat photograph dated 1868 A.D. captures an image of a fire-scarred hillslope (Morris, 2006), located directly upslope of site C5 which exposes a fire-related debris flow deposit dated ~180 cal yr BP (~1770 A.D.). A 50 cm thick layer of charcoal-rich sheetfloods overlie this ~180 cal yr BP debris flow deposit suggesting that the 1868 A.D. fire produced these fire-related sheetfloods (Figure 6; Figure 7). Another photograph of a fire-scarred hillslope located in the southern portion of CIRO directly upslope of site C14 (Figure 6; Figure 7) has an inferred age from the early 1900's based on the clothing-style worn by the people in the foreground (Morris, 2006). Site C14 shows no evidence for fire-related deposition associated with this fire. However, the hillslope above site C14 is composed of quartzite, while the hillslope above C5 forms a contact between upper slope gneiss and lower slope granite. These varying lithologic properties between sites likely explain differences in the fire-related erosional response.

Holocene Shifts in Fire-Related Erosion and Deposition

Changes in the nature of alluvial deposits may reveal shifts in both the nature and severity of wildfire, and changes in the density of hillslope vegetation. Post-wildfire debris flows can develop on hillslopes during small to average-sized storm events a few days to a few years after fire (Meyer et al., 2001; Cannon et al., 2008) when most (but not all) of the following conditions are met. First, a fire-induced hydrophobic layer can develop within the upper few centimeters of soil (DeBano, 2000), which segregates water to the surface and increases runoff during post-wildfire storms (Shakesby and Doerr, 2006; DeBano, 2000). The thin layer of surface material above the hydrophobic layer

saturates quickly because dry soil hydrophobic properties cause rainfall to rapidly exceed infiltration rates, and small-scale slope failures (rills) entrain surface ash and burned soil (DeBano, 2000). Increased surface runoff can also occur in the absence of a hydrophobic soil layer by fire removal of vegetation, surface duff, and litter, which reduces surface roughness (Shakesby and Doerr, 2006). In this scenario, small-scale rilling can develop when surface runoff entrains ash and burned soil. Extensive rill networks can develop and have been observed on hillslopes following fire. A debris flow may develop from rills through progressive downslope entrainment of surface ash and burned soil during post-fire storm events (Meyer and Wells, 1997; Cannon et al., 2001).

Burned hillslopes have been shown to experience exponential increases in erosion as slope increases above 5.7° (Wilcox et al., 2011), and Cannon et al. (2010) identified a 16.7° slope threshold for debris flow formation. However, mean slopes at CIRO are ~15.6°, which is steeper than the 5.7° erosional threshold and shallower than the 16.7° debris flow threshold (Figure 18), indicating that burned hillslopes will likely experience post-fire erosion but may not necessarily develop into debris flows. At CIRO, basins with positively skewed slope frequency histograms (Figure 18; Wolinsky and Pratson, 2005) and hillslopes composed of grussy colluvium that lack fine silts and clays necessary for debris flow development further support modern observations that indicate landform and lithologic limitations on debris flow activity. Yet, our record indicates that fire-related debris flows were an important erosional process before ~7000 cal yr BP and after ~2500 cal yr BP (Figure 10d). This suggests that severe fires tipped this landscape past an erosional threshold, where debris flows become a dominant process.

The notable absence of fire-related debris flow deposition during the warmer and drier period between ~7000-2500 cal yr BP (Figure 10d) suggests several scenarios that are not mutually exclusive (Figure 22):

1. Sufficient colluvial storage and pedogenically-produced silt and clay-sized particles needed for debris flow formation were limited by paucity in hillslope vegetation.
2. A discontinuous fuel source restricted fire size, severity, and frequency.
3. Limited precipitation during the warmer, drier mid-Holocene restricted storm events needed to produce debris flows.

The period between ~7000-2500 cal yr BP was marked by the July insolation maximum (Berger, 1978), manifested by increased temperatures and aridity in the Bonneville Basin (Figure 19a, b and c; e.g., Murchison, 1989; Louderback and Rhode, 2009) that likely limited vegetation on hillslopes. Such drought-induced vegetation removal has been linked to enhanced erosion rates (Allen and Breshears, 1998; Yetemen et al., 2010), particularly in arid and semiarid zones (Collins and Bras, 2008). At CIRO, charcoal-poor sheetfloods constrained by dated fire-related deposits between ~7000-3600 cal yr BP indicate that frequent sheetflooding occurred under droughty climate in the absence of fire (Figure 6).

Paleo-fire records, and modern observation, have shown that low-severity fires typically produce sheetfloods, while high-severity fires produce debris flow deposits (Meyer et al., 1995; 2001; Pierce et al., 2004). During the mid-Holocene, sagebrush, juniper, and limber pine were present on the landscape. Sagebrush and juniper woodlands do not typically sustain low-severity fires during drier climate when ground fuels are

discontinuous. Rather, these ecosystems are prone to high-severity fires that occur under more mesic conditions (Baker and Shinneman, 2004; Mensing et al., 2006; Romme et al., 2009; Bauer and Weisberg, 2009). Such ecosystem conditions may explain periods of low fire activity during the bulk of this timeframe. However, frequent fires dated 7200-6700 cal yr BP that produced thin, muddy debris flows and sheetfloods, likely burned as more severe fires. Ignition occurred during drought following a brief moist snap when

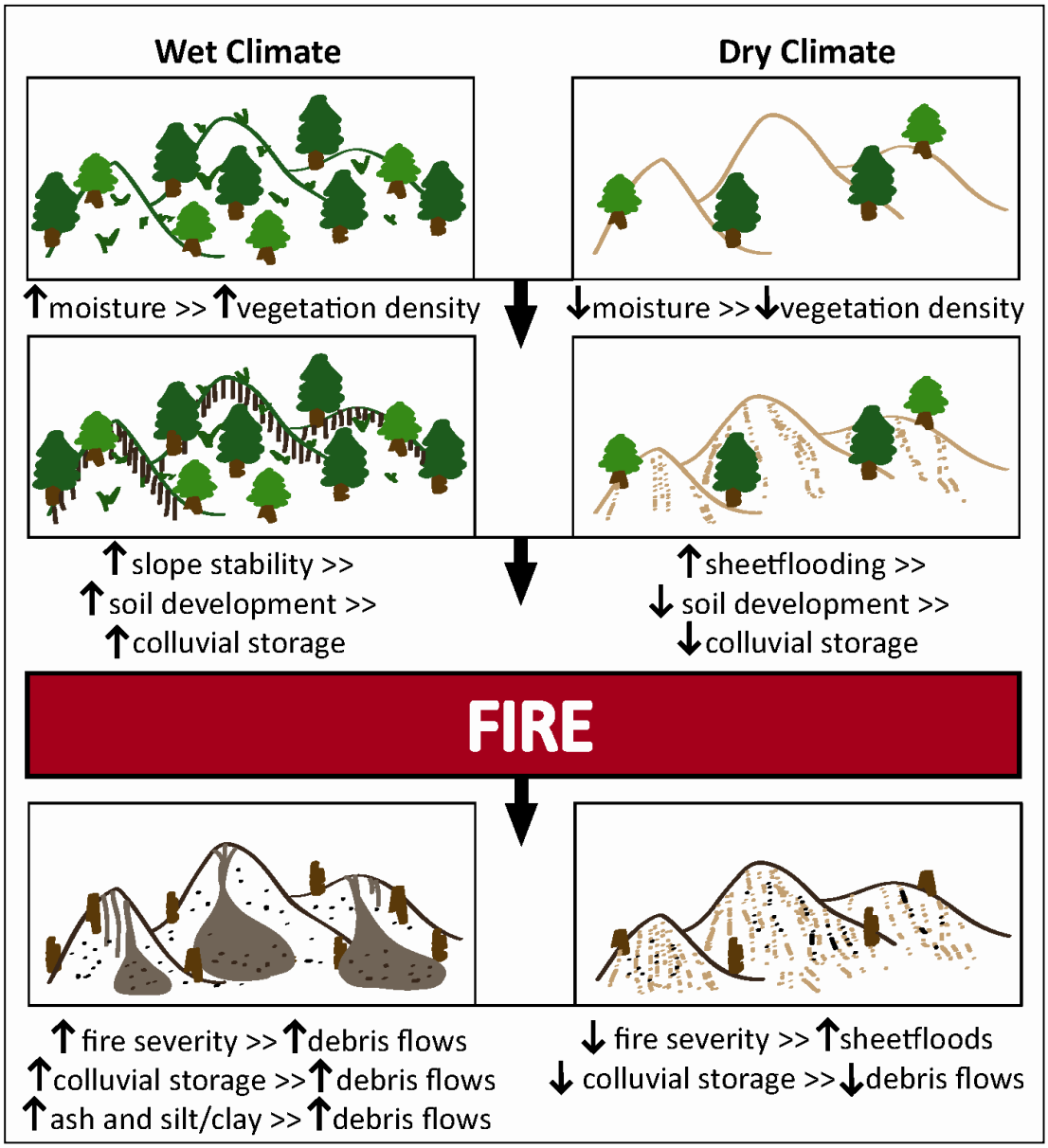

Figure 22: Conceptual model of wet climate vs. dry climate and resulting fire-related erosional response.

accumulated fine fuels increased fuel connectivity for fire to spread on an otherwise sparsely-vegetated landscape. However, suppressed colluvial storage likely inhibited debris flow development during this time.

After ~2200 cal yr BP, at the end of ~2000 years of cooler and wetter climate (Murchison, 1989; Madsen et al., 2001; Miller and Tausch, 2001; Miller et al., 2005; Louderback and Rhode, 2009; Betancourt, unpublished data), when vegetation densities were increasing, and Utah juniper and single-leaf pinyon were expanding (Table 3), fire frequency increased and erosion shifted from predominantly sheetflooding to episodic debris flow activity combined with sheetflooding. This erosional shift may be entirely attributable to a fuel-driven switch from low-severity to high-severity fires combined with increased ash production that provided the fine-textural component necessary for debris flow development. However, evidence for soil development suggests that increased colluvial storage and increased silt and clay production from soil formation may have also played a role.

In general, well-developed surface soil horizons and buried soils are limited at CIRO. In semiarid environments, soil development can be inhibited by lower precipitation rates, which decrease vegetation and organic input to soil. Drier climate reduces leaching processes responsible for translocation of clays and other minerals into stratified soil horizons (Jenny, 1941). Soil development is not only climate-dependent but occurs on slopes stabilized by dense vegetation, where erosion rates are low (Jenny, 1941) and colluvial storage is increased. Two buried soils and one unburied soil identified in the CIRO alluvial record were developed on debris flow deposits dated ~12,740, 2290, and 2240 cal yr BP, when climate was wetter/cooler relative to the middle

Holocene (Figure 6). Post ~2200 cal yr BP soils correspond to documented increases in vegetation densities after the arrival and during the expansion of Utah juniper and single-leaf pinyon (Table 3). The reemergence of debris flow activity during the late Holocene, coupled with soil formation and increased vegetation densities, suggests that the landscape was not only experiencing a modification in fire regime but also an erosional and geomorphic shift.

Land Management Implications

The CIRO fire and vegetation record indicates fire has been a natural and common component of pinyon-juniper woodlands since colonization, and fires were most frequent when pinyon-juniper populations thrived and woodlands expanded. Along with increased fire frequency, the fire-related erosional response also changed. High-severity fires that burned dense pinyon-juniper stands shifted erosional processes from sheetflooding to more catastrophic debris flows. Recent woodland infilling and density increases at CIRO (Morris, 2006) suggest increased risk of large and high-severity fires in the event of ignition. Along with fire damage, fire-related debris flows would likely extend beyond burned area boundaries, and further threaten park structures and infrastructure.

Documented pinyon-juniper invasion into sagebrush ecosystems during the last ~150 years has been attributed to land management practices that include fire exclusion and livestock grazing. However, the CIRO record indicates Utah juniper and single-leaf pinyon colonized the area much earlier (~3800 cal yr BP and 2800 cal yr BP, respectively) and woodlands have been expanding ever since. Expansion and infilling of pinyon-juniper woodlands that began long before historically documented expansion

suggests that recent pinyon-juniper dynamics fall within the natural range and variability of this system; however, livestock grazing may be enhancing contemporary tree densities (Shinneman and Baker, 2009).

Future fires combined with an overall drier and warmer climate may be detrimental to the limber pine and Rocky Mountain juniper populations at CIRO, which likely exist as relict species from a colder and wetter Pleistocene climate (Figure 4). In the event of pinyon-juniper woodland ignition, high-severity fires could remove these holdover tree species because regeneration may be difficult under modern warmer, drier conditions (Figure 4). Fires would likely spread into already threatened sagebrush steppe that forms the ecotone boundary at CIRO, and post-fire invasion by cheatgrass, as observed in the southern portion of CIRO following the 2000 fire, would further alter fire regimes.

CONCLUSIONS

Changes in climate produced shifts in vegetation populations, fire regimes, and geomorphic processes during the last 13,000 years at CIRO. This study documents these changes and may provide a useful analog for modern climate-driven relationships among fire, vegetation, and erosion.

Frequent fires burned between 10,700-9500 cal yr BP, during abruptly warming and drying climate of the Pleistocene-Holocene transition. These fires produced debris flows, suggesting high-severity, stand-replacing fires (Meyer et al., 2001; Pierce et al., 2004) that burned dense forests developed during the late Pleistocene. Wetter climate followed, when no fires were recorded between 9500-7200 cal yr BP, indicating that fires were suppressed by moist conditions (i.e., moisture-limited fires).

During the middle Holocene, frequent fires burned between 7200-6700 cal yr BP. Climate during this time was characterized by extended warmer, drier conditions (Murchison, 1989; Louderback and Rhode, 2009; Shuman et al., 2009; Corbett and Monroe, 2010), however fires were preceded by briefly wetter climate that supplied fine fuels and increased fuel connectivity. Mid-Holocene fires produced sheetfloods instead of debris flows, suggesting lower severity fires on sparsely vegetated hillslopes (Meyer et al., 2001; Pierce et al., 2004). No fires were recorded between 6700-4700 cal yr BP when prolonged drought limited fuels, suggesting a fire regime shift from a moisture-limited system to a fuel-limited system.

Following the arrivals of Utah juniper and single-leaf pinyon (~3800 and ~2800 cal yr BP, respectively), clusters of high-frequency fires were recorded at 2400-2000, 850-700, and 550-400 cal yr BP. These fires produced debris flows and burned during longer-term (10^2-10^3 years) wet, cool periods when ecosystem productivity was high (Betancourt, unpublished data), however ignition occurred during annual and decadal droughts (e.g., Cook et al., 2004; Gray et al., 2004; Stahle et al., 2007; Mensing et al., 2008; Nelson and Pierce, 2010; Rittenour and Pearce, 2011). Higher severity fires in expanding pinyon-juniper woodlands were likely no longer limited by fuel availability but rather by climate control on ignition (i.e., ignition-limited system).

We propose a conceptual model of Holocene climate control on vegetation and fire, and the resulting geomorphic processes (i.e., debris flows vs. sheetfloods). During the early and late Holocene, wetter climate increased forest densities, which in turn stabilized hillslopes and increased colluvial storage. Larger, high-severity fires fueled by abundant vegetation produced fire-related debris flows (Meyer et al., 2001; Pierce et al., 2004). At the same time, increased colluvial storage on more stable, densely vegetated hillslopes supplied material for debris flow development. During the middle Holocene, prolonged drought decreased vegetation densities and limited fire activity. Grussy, sparsely vegetated hillslopes produced frequent sheetflooding in the absence of fire, therefore limiting colluvial storage. Low-severity fires that burned less densely vegetated hillslopes with limited colluvial material produced fire-related sheetflooding instead of episodic debris flows. Although the gently-sloping, granitic terrain at CIRO is not conducive to debris flow formation, debris flows deposited during the early and late Holocene suggest that fire has pushed erosional responses past geomorphic thresholds.

The fire intervals dated 7200-6700 and ~550 cal yr BP are corroborated by multiple alluvial charcoal records that span a range of ecosystems from Idaho and Yellowstone National Park (Meyer et al., 1995; Pierce et al., 2004; Svenson, 2010; Nelson and Pierce, 2010). Such widespread fire implies significant regional climate forcings. During the middle Holocene, regional drought likely drove regionally widespread fires, while during the LIA regional fires burned during globally cooler and wetter conditions. Although these fires burned at roughly the same time in response to similar climate conditions, the nature of fires (i.e., high-severity vs. low-severity fires) likely varied according to ecosystem and pre-fire fuel conditions.

Since pinyon-juniper colonization of CIRO, high-severity wildfires have burned dense fuel loads that were accumulated and subsequently dried during periods of variable climate (Cook et al., 2004). Recently, pinyon-juniper woodlands have increased in density and expanded into neighboring vegetation committees at CIRO (Morris, 2006) and throughout the western U.S. (Romme et al., 2009). Dense woodland conditions combined with increased potential for climate extremes in both precipitation and temperatures caused by amplified levels of atmospheric greenhouse gases (e.g., Groisman et al., 2005; Duffy and Tebaldi, 2012) suggest elevated risks of catastrophic fires and fire-related debris flows.

REFERENCES

Abatzoglou, J. T., Redmond K.T., 2007. Asymmetry between trends in spring and autumn temperature and circulation regimes over western North America, Geophysical Research Letters, 34, L18808.

Adams, K.D., 2003. Age and paleoclimatic significance of late Holocene lakes in the Carson Sink, Nevada: Quaternary Research 60, 294-306.

Adams, K.R., Murray, S.S., 2011. Identification Criteria for Plant Remains Recovered from Archaeological Sites in the Central Mesa Verde Region [HTML Title]. Available: http://www.crowcanyon.org/plantID. Date of use: 2011.

Allen, C.D., Breashears, D.D., 1998. Drought-induced shift in a forest-woodland ecotone: Rapid landscape response to climate variation. Proceedings of the National Academy of Sciences 95, 14839-14842.

Alley, R.B., Mayewski, P.A., Sowers, T., Stuiver, M., Taylor, K.C., and Clark, P.U., 1997. Holocene climatic instability: A prominent, widespread event 8,200 years ago. Geology 25, 483-486.

Automated Georeference Center, 2001. HistoricLakeBonneville (SGID93 Water), State of Utah SGID. AGRC, Salt Lake City, UT. ftp://ftp.agrc.utah.gov/SGID93_Vector/NAD83/MetadataHTML/SGID93_WATER_HistoricLakeBonneville.html

Baker, W.L., Shinneman, D.J., 2004. Fire and restoration of piñon–juniper woodlands in the western United States: a review, Forest Ecology and Management 189, 1–21.

Baker, W.L., 2006. Fire and Restoration of Sagebrush Ecosystems. Wildlife Society Bulletin 34, 177–185.

Baker, W.L., 2009. Fire ecology in Rocky Mountain landscapes. Island Press, Washington D.C.

Bauer, J.M., Weisberg. P.J. 2009. Fire history of a central Nevada pinyon–juniper woodland. Canadian Journal of Forest Research 39, 1589-1599.

Benson, L.V., Lund, S.P., Smoot, J.P., Rhode, D.E., Spencer, R.J., Verosub, K.L., Louderback, L.A., Johnson, C.A., Rye, R.O., Negrini, R.M., 2011. The rise and fall of Lake Bonneville between 45-10.5 ka. Quaternary International 235, 57-69.

Berger, A.L., 1978. Long-term variations of caloric insolation resulting from the earth's orbital elements. Quaternary Research 9, 139-167.

Berger, W.H., 1990. The Younger Dryas cold spell — a quest for causes. Global and Planetary Change 3, 219–237.

Betancourt, J.L., Schuster, W.S., Mitton, J.B., Anderson, R.S., 1991. Fossil and genetic history of a pinyon pine *(Pinus edulis*) isolate. Ecology 72, 1685-1697.

Birkeland, P.W., Machette, M.N., Haller, K.M., 1991. Soils as a tool for applied Quaternary geology. Utah Geological and Mineral Survey Miscellaneous publication 91-3, 44 pp.

Blair, T.C., 1999. Cause of dominance by sheetflood vs. debris flow processes on two adjoining alluvial fans, Death Valley, California. Sedimentology 46, 1015-1028.

Bovet, P., Bowerman, N., Cadol, D., 2002. Glaciologic and paleoclimatic significance of cirque-lake sediments in the Albion Range, south-central Idaho. http://keckgeology.org/files/pdf/symvol/16th/idaho/bovetbowermancadol.pdf

Braconnot, P., Ott-Bliesner, B., Harrison, S., Joussaume, S., Peterchmitt, J.Y., Abe-Ouchi, A., Cruxifix, M., Driesschaert, E., Fichefet, Th., Hewitt, C.D., Kageyama, M., Kitoh, A., Laine, A., Loutre, M.F., Marti, O., Merkel, U., Ramstein, G., Valdes, P., Weber, S.L., Yu, Y., Zhao, Y., 2007. Results of PMIP2 coupled simulations of the Mid-Holocene and Last Glacial Maximum-Part 1: experiments and large-scale features. Climates of the Past 3, 261-277.

Broughton, J.M., Madsen, D.B., Quade, J., 2000. Fish remains from Homestead Cave and lake levels of the past 13,000 years in the Bonneville Basin, Quaternary Research 53, 392-401.

Brown, D.P., Comrie, A.C., 2004. A winter precipitation “dipole” in Western United States associated with multidecadal ENSO variability. Geophysical Research Letters 31, 1-4.

Brown, P.M., Schoettle, A.W., 2008. Fire and stand history in two limber pine (Pinus flexilis) and Rocky Mountain bristlecone pine (*Pinus aristata*) stands in Colorado. International Journal of Wildland Fire 17, 339-347.

Cannon, S.H., Reneau, S.L., 2000. Conditions for generation of fire-related debris flows, Capulin Canyon, New Mexico. Earth Surface Processes and Landforms 25, 1103-1121.

Cannon, S.H., Kirkham, R.M., Parise, M., 2001. Wildfire-related debris-flow initiation processes, Storm King Mountain, Colorado. Geomorphology 39, 171-188.

Cannon, S.H., Gartner J.E., Wilson, R.C., Laber, J.L., 2008. Storm rainfall conditions for floods and debris flows from recently burned areas in southwestern Colorado and southern California. Geomorphology 6, 250-269.

Cannon, S.H., Gartner J.E., Rupert, M.G., Michael, J.A., Rea, A.H., Parrett, C., 2010. Predicting the probability and volume of post wildfire debris flows in the intermountain western United States. Geological Society of America Bulletin 122, 127-144.

Collins, D. B. G., Bras, R. L., 2008. Climatic control of sediment yield in dry lands following climate and land cover change. Water Resources Research 44, 0043-1397.

Cook, E.R., Woodhouse, C.A., Easkin, C.M., Meko, D.M., Stahle, D.W., 2004. Long-term aridity changes in the western United States. Science 306, 1015-1018.

Corbett, L.B., Munroe, J.S., 2010. Investigating the influence of hydrogeomorphic setting on the response of lake sedimentation to climatic changes in the Uinta Mountains, Utah, USA. Journal of Paleolimnology 44, 311-325.

Davis L.G., Muehlenbachs, K., Schweger, C.E., Rutter, N.W., 2002. Differential response of vegetation to postglacial climate in the Lower Salmon River Canyon, Idaho. Palaeogeography, Palaeoclimatology, Palaeoecology 185, 339-354.

Davis, O.K., Sheppard, J.C., Robertson, S., 1986. Contrasting climatic histories for the Snake River Plain, Idaho, resulting from multiple thermal maxima. Quaternary Research 26, 321-329.

Dean, W.E., Forester, R.M., Bradbury, J.P., 2002. Early Holocene change in atmospheric circulation in the Northern Great Plains: an upstream view of the 8.2 ka cold event. Quaternary Science Reviews 21, 1763-1775.

DeBano, L.F., 2000. The role of fire and soil heating on water repellency in wildland environments: a review. Journal of Hydrology 231-232, 195-206.

Dettinger, M.D., Cayan, D.R., Diaz, H.F., Meko, D.M., 1998. North-south precipitation patterns in western North America on interannual-to-decadal time scales. Journal of Climate 11, 3095-3111.

Doner, L.A., 2009. A 19,000-year vegetation and climate record for Bear Lake, Utah and Idaho in Paleoenvironments of Bear Lake, Utah and Idaho, and its catchment ed Rosenbaum, J.G. and Kaufman, D.S. Geological Society of America Special Paper 450: 217-227.

Duffy, P.B., Tebaldi, C., 2012. Increasing prevalence of extreme summer temperatures in the U.S. Climatic Change 111, 487-495.

Flannigan, M.D., Stocks, B.J., Wotton, B.M., 2000. Climate change and forest fires. Science of the Total Environment 262, 221-229.

Floyd, M.L., Romme, W.H., Hanna, D.D., 2000. Fire history and vegetation pattern in Mesa Verde National Park, Colorado, USA. Ecological Applications 10, 1666–1680.

Gavin, D.G., 2001. Estimation of inbuilt age in radiocarbon ages of soil charcoal for fire history studies. Radiocarbon 43, 27–44.

Gedalof, Z., 2011. Climate and spatial patterns of fire in North America. In McKenzie, D., Miller, C., Falk, Falk. 2011. The Landscape Ecology of Fire, Springer, New York, 89-115.

Gesch, D.B., 2007. The national elevation dataset in Maune, D., ed., Digital Elevation Model Technologies and Applications: The DEM Users Manual, 2nd Edition: Bethesda, Maryland, American Society for Photogrammetry and Remote Sensing, 99-118.

Gesch, D., Oimoen, M., Greenlee, S., Nelson, C., Steuck, M., and Tyler, D., 2002. The national elevation dataset: photogrammetric engineering and remove sensing 68, 5-11.

Goodrich, S., Barber, B. 1999. Return interval for pinyon-juniper following fire in the Green River corridor, near Dutch John, Utah. In Monsen, S.B., Stevens, R., editors. Proceedings: ecology and management of pinyon-juniper communities within the interior West. United States Department of Agriculture Forest Service, Proceedings, RMRS-P-9, 391-393.

Gray, S.T., Jackson, S.T., and Betancourt, J.L. 2004. Tree-ring based reconstructions of interannual to decadal-scale precipitation variability for northeastern Utah since 1226 A.D. Journal of the American Water Resources Association 40, 947-960.

Gray, S.T., Betancourt, J.L., Jackson, S.T., Eddy, R.G., 2006. Role of multidecadal climate variability in a range extension of pinyon pine. Ecology 87, 1124-1130.

Grayson, D.K., 2000. Mammalian responses to middle Holocene climatic change in the Great Basin of the Western United States. Journal of Biogeography 27, 181-192.

Grissino-Mayer, H.D., Swetnam,T.W., 2000. Century scale climate forcing of fire regimes in the American Southwest, The Holocene 10, 213-220.

Grohmann, C.H., Smith, M.J., Riccomini, C., 2011. Multiscale analysis of topographic analysis of topographic roughness in the Midland Valley, Scotland. Geoscience and Remote Sensing 49, 1200-1213.

Groisman, P.Y., Knight, R.W., Easterling, D.R., Karl, T.R., Hegerl, G.C., Razuvaev, V.N., 2005. Trends in intense precipitation in the climate record. Journal of Climate 18, 1326-1350.

Grove, J.M., 2001. The initiation of the "Little Ice Age" in regions round the North Atlantic. Climate Change 48, 53-82.

Heyerdahl, E.K., Brubaker, L.B., Agee J.K., 2002. Annual and decadal climate forcing of historical fire regimes in the interior Pacific Northwest, USA. The Holocene 12, 597-604.

Huffman, D.W., Fule, P.Z., Pearson, K.M., Crouse, J.E., 2008. Fire history of pinyon–juniper woodlands at upper ecotones with ponderosa pine forests in Arizona and New Mexico Canadian Journal of Forest Research, 38, 2097-2108.

Jackson, M., Roering J.J., 2009. Post-fire geomorphic response in steep, forested land-scapes: Oregon Coast Range, USA. Quaternary Science Reviews 28, 1131-1146.

Jackson, S.T., Betancourt, J.L., Lyford, M.E., Gray, S.T., Rylander, K.A., 2005. A 40,000 year woodrat midden record of vegetational and biogeographic dynamics in north-eastern Utah, USA. Journal of Biogeography 32, 1085–1106.

John, T., 1993. Vascular flora of City of Rocks and vicinity – a preliminary checklist. [No Publisher]. Published Report 132206.

Jenny, H., 1941. Factors of soil formation, a system of quantitative pedology. Dover Publications Inc., New York, New York.

Kauffman, J.B., Sapsis, D.B., 1989. The natural role of fire in Oregon's High Desert. In: Oregon's High Desert: The last 100 years. 1989 Range Field Day Report. June 1989. Special Report 841. Oregon State University, Corvallis, OR, 15-19.

Keane, R.E., Holsinger, L.M., Parsons, R.A., Gray, K., 2008. Climate change effects on historical range and variability of two large landscapes in western Montana, USA, Forest Ecology and Management 254, 375-389.

Kunkel, M.L., Pierce, J.L., 2010. Reconstructing snowmelt in Idaho's watershed using historic streamflow records. Climatic Change 98, 155-176.

Littell, J.S., McKenzie,D., Peterson, D.L., Westerling A.L., 2009. Climate and wildfire area burned in western U.S. ecoprovinces, 1916–2003. Ecological Applications 19, 1003-1021.

Little, E.L., Jr., 1971. Atlas of United States trees, volume 1, conifers and important hardwoods: U.S. Department of Agriculture Miscellaneous Publication 1146, 9 p., 200 maps.

Louderback, L.A., Rhode, D.E., 2009. 15,000 Years of vegetation change in the Bonneville basin: the Blue Lake pollen record. Quaternary Science Reviews 28, 308–326.

Ludington, S., Moring, B.C., Miller, R.J., Flynn, K.S., Bookstrom, A.A., 2006. Idgeol_lcc. USGS. http://pubs.usgs.gov/of/2005/1305/

Lyford, M.E., Jackson, S.T., Betancourt, J.J., and Gray, S.T., 2003. Influence of landscape structure and climate variability on a late Holocene plant migration. Ecological Monographs 73, 567-583.

Madsen, D.B., Rhode, D., Grayson, D.K., 2001. Late Quaternary environmental change in the Bonneville basin, western USA. Palaeogeography, Plaeoclimatology, Palaeoecology 167, 243–271.

Marlon, J.R., Bartlein, P.J., Walsh, M.K., Harrison, S.P., Brown, K.J., Edwards, M.E., Higuera, P.E., Power, M.J., Anderson, R.S., Briles, C., Brunelle, A., Carcaillet, C., Daniels, M., Hu, F.S., Lavoie, M., Long, C., Minckley, T., Richard, P.J.H., Scott, A.C., Shafer, D.S., Tinner W., Umbanhowar, Jr., C.E., Whitlock, C., 2009. Wildfire responses to abrupt climate change in North America. Proceedings of the National Academy of Sciences 106, 2519-2524.

Mensing, S., Livingston, S., Barker, P., 2006. Long-term fire history in Great Basin sagebrush reconstructed from macroscopic charcoal in spring sediments, Newark Valley, Nevada. Western North American Naturalist 66, 64-77.

Mensing, S., Smith, J., Norman, K.B., Allan, M., 2008. Extended drought in the Great Basin of western North America in the last two millennia reconstructed from pollen records. Quaternary International 188, 79-89.

Meyer, G.A., Wells, S.G., Jull, A.J.T., 1995. Fire and alluvial chronology in Yellowstone National Park: Climatic and intrinsic controls on Holocene geomorphic processes. Geological Society of America Bulletin 107, 1211–1230.

Meyer, G.A., Wells, S.G., 1997. Fire-related sedimentation events on alluvial fans, Yellowstone National Park, U.S.A. Journal of Sedimentary Research A67, 776-791.

Meyer, G.A., Pierce, J.L., Wood, S.H., Jull, A.J.T., 2001. Fire, storms, and erosional events in the Idaho batholith. Hydrological Processes 15, 3025-3038.

Miller, D.M., Bedford, D.R., 1999. Pluton intrusion styles, roof subsidence and stoping, and timing of extensional shear zones in the City of Rocks National Reserve, Albion Mountains, southern Idaho. Utah Geological Association Publication 27, 11-26.

Miller, D.M., Oviatt, C.G., Dudash, S.L., Mcgeehin, J.P., 2005. Late Holocene highstands of Great Salt Lake at Locomotive Springs, Utah. Geological Society of America Abstracts with Programs 37 (7), 335.

Miller, D.M., Armstrong, R.L., Bedford, D.R., Davis, M., 2008. Geologic map and digital data base of the Almo quadrangle and City of Rocks National Reserve, Cassia County, Idaho. U.S. Geological Survey Open-File Report 2008-1103, 36 p., 1 sheet, scale 1:24,000.

Miller R.F., Rose J.A., 1999. Fire history and western juniper encroachment in sagebrush steppe. Journal of Rangeland Management 52, 550-559.

Miller, R.F., Tausch, R.J., 2001. The role of fire in juniper and pinyon woodlands: a descriptive analysis. Pages 15 – 30 *in* K.E.M. Galley and T.P. Wilson (eds.). Proceedings of the Invasive Species Workshop: The Role of Fire in the Control and Spread of Invasive Species. Fire Conference 2000: the First National Congress on Fire Ecology, Prevention, and Management. Miscellaneous Publication No. 11, Tall Timbers Research Station, Tallahassee, FL.

Millspaugh, S.H., Whitlock, C., Bartlein, P.J., 2000. Variations in fire frequency and climate over the past 17000 yr in central Yellowstone National Park. Geology 28, 211–214.

Monitoring Trends in Burn Severity Data Access, 2011. Fire level geospatial data, MTBS Project (USDA Forest Service/U.S. Geological Survey).

Morris, L., 2006b. Fire history of the City of Rocks National Reserve from 1926 to 2005. National Park Service Pacific Northwest Region, Seattle, Washington.

Moser, K.A., Kimball, J.P. 2009. A 25,000 year record of hydrologic and climatic change inferred from diatoms from Bear Lake, Utah/Idaho, USA in Paleoenvironments of Bear Lake, Utah and Idaho, and its catchment ed Rosenbaum, J.G. and Kaufman, D.S. Geological Society of America Special Paper 450: 229-246.

Mote, P. W., 2006. Climate-driven variability and trends in mountain snowpack in western North America. Journal of Climate 19, 6209-6220.

Murchison, S.B., 1989. Fluctuation history of the Great Salt Lake, Utah, during the last 13,000 years. Ph.D. dissertation, University of Utah.

Murchison, S.B., Mulvey, W.E., 2000. Late Pleistocene and Holocene shoreline stratigraphy on Antelope Island. The Geology of Antelope Island, Davis County, Utah. Miscellaneous Publication 00-1, Utah Geological Survey, 77-83.

National Interagency Fire Center, www.nifc.gov

Nelson, N.A., Pierce, J.L., 2010. Late-Holocene relationships among fire, climate and vegetation in a forest-sagebrush ecotone of southwestern Idaho, USA. The Holocene 20, 1179-1194.

Oviatt, C.G., 1997. Lake Bonneville fluctuations and global climate change. Geology 25, 155-158.

Oviatt, C.G., Madsen D.B., Schmitt, D.N., 2003. Late Pleistocene and early Holocene rivers and wetlands in western Utah. Quaternary Research 60, 200–210.

Patrickson, S.J., Sack, D., Brunelle, A.R., Moser, K.A., 2010. Late Pleistocene to early Holocene lake level and paleoclimate insights from Stansbury Island, Bonneville basin, Utah, Quaternary Research 73, 237-246.

Pederson, G.T., Gray, S.T., Woodhouse, C.A., Betancourt, J.L., Fagre, D.B., Littell, J.S., Watson, E., Luckman, B.H., Graumlich, L.J., 2011. The unusual nature of recent snowpack declines in the North American Cordillera. Science 15, 332-335.

Pierce, J.L., Meyer, G.A., Jull, A.J.T., 2004. Fire-induced erosion and millennial-scale climate change in northern ponderosa pine forests. Nature 432, 87-90.

Pogue, K.R., Katz, C., 2008. Etched in Stone: The Geology of City of Rocks National Reserve and Castle Rocks State Park, Idaho. Idaho Geological Survey.

Rebertus, A.J., Burns, B.R., Veblen, T.T., 1991. Stand dynamics of *Pinus flexilis*-dominated subalpine forests in the Colorado Front Range. Journal of Vegetation Science2, 445-458.

Rittenour, T.M., Pearce, H.R, 2011. Dune activity in the Idaho Falls Dune field on the Snake River Plain, southeastern Idaho, Geological Society of America Abstracts with Programs 43, 7.

Romme, W., Allen, C.D., Bailey, J.D., Baker, W.L., Bestelmeyer, B.T., Brown, P.M., Eisenhart, K.S., Floyd, L., Huffman, D.W., Jacobs, B.F., Miller, R.F., Muldavin, E.H., Swetnam, T.W. ,Tausch, R.J., Weisberg, P.J., 2009. Historical and modern disturbance regimes, stand structures, and landscape dynamics in pinon-juniper vegetation of the western United States. Rangeland Ecology & Management 62, 203-222.

Schmitt, D.M., Madsen, D.B., Lupo, K.D., 2002. Small-mammal data on early and middle Holocene climates and biotic communities in the Bonneville Basin, USA. Quaternary Research 58, 255-260.

Schmittner, A., Urban, N.M., Shakun, J.D., Mahowald, N.M., Clark, P.U., Bartlein, P.J., Mix, A.C., Rosell-Mele, A., 2011. Climate sensitivity estimated from temperature reconstruction of the Last Glacial Maximum. Science 334, 1385-1388.

Schoettle, A.W., 2004. Ecological roles of five-needle pines in Colorado: potential consequences of their loss. In: Sniezko, R.A., Samman, S., Schlarbaum, S.E., Howard, B.E. (Eds.). Breeding and Genetic Resources of Five-needle Pines: Growth, Adaptability and Pest Resistance. USDA Forest Service Proceedings RMRS-P-32. Rocky Mountain Forest and Range Experimental Station, Fort Collins, CO, 124–135.

Shakesby, R.A., Doerr, S.H., 2006. Wildfire as a hydrological and geomorphological agent. Earth Science Reviews 74, 269-307.

Shinneman, D.J., Baker, W.L., 2009. Historical fire and multidecadal drought as context for pinyon-juniper woodland restoration in western Colorado. Ecological Applications 19, 1231-1245.

Shuman, B., Henderson, A., Coleman, S.N., Stone, J.R., Fritz, S.C., Stevens, L.R., Power, M.J., Whitlock, C., 2009. Holocene lake-level trends in the Rocky Mountains, U.S.A. Quaternary Science Reviews 28, 1961-1979.

Smith, F.A., Betancourt, J.L., 2003. The effects of Holocene temperature fluctuations on the evolution and ecology of *Neotoma* (woodrats) in Idaho and northwestern Utah. Quaternary Research 59, 160-171.

Smoot, J.P., Rosenbaum, J.G., 2009. Sedimentary constraints on late Quaternary lake-level fluctuations at Bear Lake, Utah and Idaho, *in* Rosenbaum, J.G., Kaufman, D.S., eds., Paleoenvironments of Bear Lake, Utah and Idaho, and its catchment: Geological Society of America Special Paper 450, 263-290.

Stahle, D., Fye, F., Cook, E., Griffin, R., 2007. Tree-ring reconstructed megadroughts over North America since A.D. 1300. Climatic Change 83, 133-149.

Stewart, I.T., Cayan, D.R., Dettinger, M.D., 2004. Changes in snowmelt runoff timing in Western North America under a `business as usual' climate change scenario. Climate Change 62, 217-232.

Stine, S., 1994. Extreme and persistent drought in California and Patagonia during medieval time. Nature, 369, 546-549.

Stuiver, M., Reimer, P.J., 1993. Extended ^{14}C database and revised CALIB Radiocarbon Calibration Program. Radiocarbon 35, 215–230.

Surovell, T.A., Finley, J.B., Smith, G.M., Brantingham, P.J., Kelly, R., 2009. Correcting temporal frequency distributions for taphonomic bias. Journal of Archaeological Science, 36, 1715-1724.

Svenson, L.O., 2010. Fire and climate in a lodgepole forest of central Idaho: annual, decadal, centennial and millennial perspectives. Thesis, Boise State University, Boise, Idaho.

Swetnam, T.W., Betancourt, J.L., 1998. Mesoscale disturbance and ecological response to decadal climate variability in the American Southwest. Journal of Climate 11, 3128-3147.

Thomas, P., Packham J.R., 2007. Ecology of woodlands and forests: description, dynamics and diversity, Cambridge University Press.

Thompson, R. S. 1990. Late Quaternary vegetation and climate in the Great Basin. Pp. 200-239 *in* J. L. Betancourt, T. R. Van Devender, and P. S. Martin (eds.). Packrat Middens: The Last 40,000 Years of Biotic Change. University of Arizona Press, Tucson.

Thompson, R.S., Anderson, K.H., Bartlein, P.J., 1999. Atlas of relations between climatic parameters and distributions of important trees and shrubs in North America U.S. Geological Survey Professional Paper 1650 A&B. http://pubs.usgs.gov/pp/p1650-a/datatables/index.html

United States Department of Agriculture, Natural Resources Conservation Service, and United States Department of the Interior, National Park Service. 2011. Soil survey of City of Rocks National Reserve, Idaho.

Webb, R.H., and Betancourt, J.L., 1990. The spatial distribution of radiocarbon ages from packrat middens, in Betancourt, J.L., Van Devender, T.R., and Martin, P.S., (eds), Packrat middens: The last 40,000 years of biotic change: Tucson, Arizona, University of Arizona Press, 85-102.

Westerling, A.L., Brown, T.J., Gershunov, A., Cayan D.R., Dettinger, M.D. 2003. Climate and wildfire in the western United States, Bulletin of the American Meteorological Society, 84(5) 595-604.

Westerling, A.L., Hidalgo, H.G., Cayan, D.R., Swetnam, T.W., 2006. Warming and earlier spring increase western U.S. forest wildfire activity. Science 313, 940-943.

Westerling, A.L., Turner, E.A., Smithwick, A.H., Romme, W.H., Ryan, M.G., 2011. Continued warming could transform Greater Yellowstone fire regimes by mid-21st century. PNAS: Proceedings of the National Academy of Sciences 108, 13165–13170.

Western Regional Climate Center, http://www.wrcc@dri.edu

Wilcox, B.P., Turnbull, L., Young, M.H., Williams, C.J., Ravi, S., Seyfried, M.S., Bowling, D.R., Scott, R.L., Germino, M.J., Caldwell, T.G., Wainwright, J., 2011. Invasion of shrublands by exotic grasses: ecohydrological consequences in cold versus warm deserts. Ecohydrology.

Whitlock, C., Shafer, S. L., Marlon, J., 2003. The role of climate and vegetation change in shaping past and future fire regimes in the Northwestern US and the implycations for ecosystem management. Forest Ecology and Management 178, 5–21.

Whitlock,C., Higuera, P.E., McWethy, D.M., Briles,C.E., 2010. Paleoperspectives on fire ecology: revisiting the fire regime concept. The Open Ecology Journal 3, 6-23.

Wolinsky, M.A., Pratson, L.F., 2005. Constraints on landscape evolution from slope histograms. Geology 33 (6), 477.

Yetemen, O., Istanbulluoglu, E., Vivoni, E.R., 2010. The implications of geology, soils, and vegetation on landscape morphology: Inferences from semi-arid basins with complex vegetation patterns in Central New Mexico, USA. Geomorphology 116, 246-263.

Zdanowicz, C.M., Zielinski, G.A., Germani, M.S., 1999. Mount Mazama eruption: calendrical age verified and atmospheric impact assessed. Geology 27, 621-624.

APPENDIX

Field Notes

Table A1: Summary of field notes.

Site A1: Active channel on Almo Creek				Elevation: 1858 m		Coordinates: 42° 08.502N, 113° 39.873W
Depth (cm)	Thickness (cm)	Texture (% >2 mm)	Texture (type)[1]	Process[2]	Age (cal yr BP)	Notes
0-80	0-110	30%	Si-L	DF		undated debris flow incised older sheetfloods, ~200 cm wide, 20-year old sagebrush at surface, upstream ~10 m is another incised and filled DF
80-110	20-40	10-15%	L	SF	520	sampled from fine-unit of sheetflood couplet that is charcoal rich
110-150	40-60	40%	LS	SF		
150-190	20-40	25%	SL	SF	2,470	sampled from fine-unit of sheetflood couplet that is charcoal rich
190-200				CF		active channel deposits b-max = 30 cm, base of exposure
Site A2: Arroyo near Almo Creek				Elevation: 1805 m		Coordinates: 42° 07.944N, 113° 40.057W
Depth (cm)	Thickness (cm)	Texture (% >2 mm)	Texture (type)[1]	Process[2]	Age (cal yr BP)	Notes
0-85	20-90	20%	Si-Cl-L	DF		weak soil development in upper 25 cm, weak A, B horizons thin O horizon, Munsel color: (wet) 2.5y 2.5/1, maximum clast size is 2 cm, angular clasts, matrix supported, 50 year old pinyon at surface (trunk looks buried by sheetfloods)
85-120	30-40	25%	SL	SF		no couplets evident, resembles modern arroyo channel
120-135	10-15	50%/15%	S/L	SF		6 sheetflood couplets with alternating light/dark color, texture for coarse/fine component of couplets
135-180	20-25	50%/5%	S/Si-L	SF		2 sets of thick sheetflood couplets, ~5-10 cm each, texture for coarse/fine, alternating dark fine, charcoal-rich units with coarse lighter colored units
180-200	20-25	30%	S	SF	810	no couplets evident, resembles modern arroyo channel, bottom of exposure

[1] Texture types: S = sand, Si = silt, Cl = clay, and L = loam.

[2] Process: DF = debris flow, SF = sheetflood, OB = overbank, CF = channel flood, BS = burned surface.

Table A1 continued: Summary of field notes.

Site S3: Incised alluvial fan near Stines Crk				Elevation: 1798 m		Coordinates: 42° 07.437N, 113° 40.137W
Depth (cm)	Thickness (cm)	Texture (% >2 mm)	Texture (type)[1]	Process[2]	Age (cal yr BP)	Notes
0-70	50-70	10-15%	Si-C-L	DF?		soil developed on DF? Munsel color: (wet) 10 yr 2/2, long blocky vertical peds, well-developed A and B horizons, 50-100 yr old sagebrush at surface
70-102	25-35	< 5%	LS	SF?		charcoal present, lighter color than upper and lower deposits
102-105	1-3	< 5%	Si-C-L	BS	12,740	burned soil surface, grungy charcoal present
105-140	25-40	< 5%	Si-C-L	DF?		buried soil developed on DF? Munsel color: (wet) 10 yr 4/3, base of exposure
Site G4: Active channel on Graham Creek				Elevation: 2155 m		Coordinates: 42° 06.440N, 113° 43.125W
Depth (cm)	Thickness (cm)	Texture (% >2 mm)	Texture (type)[1]	Process[2]	Age (cal yr BP)	Notes
0-50	20-60	15%	Si-Cl-L	DF		matrix supported w/ flecks of charcoal throughout, maximum clast size is 15 cm, mature 50+ year old riparian trees on surface
50-75	20-25	60%	S/LS	SF		very wavy, clast supported, maximum clast size 5 cm
75-120	30-50	5%	Si-L	DF	1,560	very charcoal rich, lenses of sheetflood deposits, base of exposure
Site C5: Arroyo site near North Fork Circle				Elevation: 1864 m		Coordinates: 42° 05.690N, 113° 41.975W
Depth (cm)	Thickness (cm)	Texture (% >2 mm)	Texture (type)[1]	Process[2]	Age (cal yr BP)	Notes
0-45	40-50	30%	LS	SF		no couplets evident, resembles modern arroyo channel, very weak soil development, no O horizon, no B horizon, charcoal present, 10-20 yr old sagebrush and bunch grass at surface
45-110	50-60	50%	Si-L/ Si-Cl-L	DF	180	abundant charcoal
110-200	50-60	20%	L/Si-L	DF		buried soil? Munsel color: wet 7.5 yr 3/2, burned root present, base of exposure (bedrock channel)

[1] Texture types: S = sand, Si = silt, Cl = clay, and L = loam.

[2] Process: DF = debris flow, SF = sheetflood, OB = overbank, CF = channel flood, BS = burned surface.

Table A1 continued: Summary of field notes.

Site C8: Arroyo near South Fork Circle				Elevation: 1848 m		Coordinates: 42° 04.595N, 113° 42.697W
Depth (cm)	Thickness (cm)	Texture (% >2 mm)	Texture (type)[1]	Process[2]	Age (cal yr BP)	Notes
0-40	30-40	30%	LS	SF		charcoal rich, surface is 25-50 yr old aspens, pinyon, juniper, weak soil development, thin O, weak B, Munsel color: (wet) 10 yr 3/1, no visible couplets
40-140	90-100	25%	Si-L	DF	710	thick unit, with clasts slightly larger than matrix material (maximum clast size = 5 cm)
140-200	40-60	25%/15%	SL/Si-L	SF	4,490	4 sheetflood couplets, one dark grungy unit near top
0-40	40-50	25%/15%	SL/Si-L	SF		across drainage from upper 200 cm (coordinates: 42° 04.602N, 113° 42.690W), this unit corresponds to sheetfloods exposed between 140-200 cm on opposite bank, similar surface soil development
40-150	80-120	25%	Si-L	DF		some charcoal present, right side forms sheetflood couplets
150-175	15-25	5%	Si-Cl-L	DF	9,550	very fine-grained debris flow, charcoal rich
175-200	20-30	25%	S/LS	SF		textures for coarse/fine, coarser unit than other sheetfloods at site
200-280	60-100	25%	S/LS	SF	10,290	5 couplets, textures for coarse/fine, upper 25 cm may be thin debris flow, dated sample from continuous darkened charcoal rich thin fine grained SF unit at 260 cm
280-350	50-75	25%	S/LS	SF	10,620	9 well-stratified very thin SF couplets with dated sample from continuous darkened charcoal rich fine grained SF unit, base of exposure
Site C9: Arroyo near South Fork Circle				Elevation: 1848 m		Coordinates: 42° 04.585N, 113° 42.783W
Depth (cm)	Thickness (cm)	Texture (% >2 mm)	Texture (type)[1]	Process[2]	Age (cal yr BP)	Notes
0-25	20-30	15%	LS	SF		weak soil development, A horizon over O horizon, no B horizon, some cc
25-30	3-7	15%	LS	OB	390	fine unit of sheetflood, very charcoal rich
30-112	70-90	40%/10%	S/LS	SF		9 sheetflood couplets, texture done on coarse/fine unit, charcoal present throughout but not abundant
112-145	5-30	15%	LS	DF		organic and wood rich, poorly sorted
145-160	15	10%	LS/SL	SF	490	possible buried soil, charcoal rich
160-210	40-50	40%/5%	S/LS	SF		5 sheetflood couplets that are ~4 cm thick, texture done on coarse/fine units, base of exposure

[1] Texture types: S = sand, Si = silt, Cl = clay, and L = loam.

[2] Process: DF = debris flow, SF = sheetflood, OB = overbank, CF = channel flood, BS = burned surface.

Table A1 continued: Summary of field notes.

Site C10: Active channel on South Circle Crk				Elevation: 1870 m		Coordinates: 42° 04.645N, 113° 42.852W
Depth (cm)	Thickness (cm)	Texture (% >2 mm)	Texture (type)[1]	Process[2]	Age (cal yr BP)	Notes
0-130	50-130	15%	SL/L	DF		charcoal present, surface is riparian willow, aspen, juniper ~50 years old, debris flow originates from an incised arroyo to south, this is the same debris flow as dated (below) from Site C11, pinches out downstream, soil development, mottling, Munsel color for both mottled colors: (wet) 7.5 yr 2.5/1, 2.5 yr 5/2
130-150	20-20	<5%	Si-Cl-L	SF	3640	possibly also burned surface or thin debris flow, hardened unit--2 dark layers separated by coarser unit, continuous downstream for 15 m(where charcoal was actually sampled), charcoal rich
150-250	100-170	40%/5%	S	SF		texture done at 165 cm and 240 cm, sheetflood with no evident couplets, wavy base
250-350	10-100	40%	Si-L	OB	10,720	sample taken from charcoal rich unit at top of overbank deposit, although charcoal throughout unit, base of exposure
Site C11: Arroyo tributary of South Circle Crk				Elevation: 1871 m		Coordinates: 42° 04.599N, 113° 42.884W
Depth (cm)	Thickness (cm)	Texture (% >2 mm)	Texture (type)[1]	Process[2]	Age (cal yr BP)	Notes
0-40	10-40	20%	L/SL	DF		weak soil development, intact micas indicates young soil, Munsel color: (wet) 7.5 yr 2.5/1, A horizon weak B horizon, moderately steep hillslope above exposure, no mature trees, only bunch grasses
40-120	50-75	25%	SL	DF	2,290	charcoal rich debris flow, same debris flow that tops Site C10, inverted age
120-170	50-60	50%	S	CF	2,010	channel flood, maximum clast size is 30 cm, base of exposure, inverted age

[1] Texture types: S = sand, Si = silt, Cl = clay, and L = loam.

[2] Process: DF = debris flow, SF = sheetflood, OB = overbank, CF = channel flood, BS = burned surface.

Table A1 continued: Summary of field notes.

Site C12: Arroyo site near South Circle Crk				Elevation: 1863 m		Coordinates: 42° 04.557N, 113° 42.509W
Depth (cm)	Thickness (cm)	Texture (% >2 mm)	Texture (type)[1]	Process[2]	Age (cal yr BP)	Notes
0-85	75-100	20%/15%	SL	SF	450	3 cm O horizon, weak soil development, A horizon Munsel color: (wet) 10 yr 2/1, 50-75 year old sagebrush at surface, very charcoal rich, sample taken from 50-75, cm depth, texture done for coarse/fine sheetfloods, 10 couplets
85-175	100	30%/<5%	LS/Si-L	SF	610	texture done on coarse/fine sheetflood units, fine component of sheetfloods are very charcoal rich, sample taken at 120 cm
175-200	50-75	15%	Si-L	DF	690	darkened fining upward debris flow deposit, clasts at bottom maximum clast size is 20 cm, sample taken from charcoal rich base of unit, lower boundary forms abrupt boundary between underlying unit
200-260	50-60	20%	S	SF/DF	6,830	2 other fine-grained, undated units above this, black grungy fine-grained continuous debris flow interbedded by sheetfloods, sampled at 250 cm
260-335	60-80	30%/15%	LS	SF/DF	6,950	11 sheetfloods, charcoal sampled from thin, black, grungy continuos debris flow unit interbedded by sheetfloods, texture done on coarse/fine couplets
335-380	40-50	30%/15%	LS	SF/DF	7,210	6 sheetflood couplets, bottom of unit is fine-grained thin debris flow interbedded in sheetfloods, sampled at 380 cm, texture done on coarse/fine couplets
380-425	40-50	30%/15%	LS	SF		5 couplets, no charcoal present
425-500	75	20%	Si-L	SF/DF		similar thin charcoal rich debris flow interbedded by sheetfloods, submitted charcoal sample to lab but sample dissolved, so undated, base of exposure
Site C13: Arroyo site near South Circle Crk				Elevation: 1845 m		Coordinates: 42° 04.743N, 113° 42.448W
Depth (cm)	Thickness (cm)	Texture (% >2 mm)	Texture (type)[1]	Process[2]	Age (cal yr BP)	Notes
0-5	1-5	20%	LS	SF		cored a pinyon on surface = 20 years old, very young soil, weak development thin A horizon, weak B
5-60	40-65	40%/20%	LS	SF		charcoal rich, texture done on coarse/fine, 6-7 sheetflood couplets
60-100	40-50	15%	LS	DF	180	charcoal rich, poorly sorted, base of exposure

[1] Texture types: S = sand, Si = silt, Cl = clay, and L = loam.

[2] Process: DF = debris flow, SF = sheetflood, OB = overbank, CF = channel flood, BS = burned surface.

Table A1 continued: Summary of field notes.

Site C14: Active channel main fork of Circle Crk				Elevation: 1758 m		Coordinates: 42° 04.618N, 113° 40.637W
Depth (cm)	Thickness (cm)	Texture (% >2 mm)	Texture (type)[1]	Process[2]	Age (cal yr BP)	Notes
0-45	40-50	10%	Si-L	DF		Thin O horizon, A horizon at 10 cm Munsel color: (wet) 2.5 y 2.5/1, B horizon at 20 cm B Munsel color: (wet) 10 yr 3/1, very hardened at 20 cm = higher clay content, older soil than most sights
45-105	50-70	30%	SL	DF	4,680	continuous darkened unit at base, sample taken at 80 cm at upstream exposure
105-170	50-75	50%/5%	SL/Si-Cl-L	SF		pinching out sheetfloods alternating coarse/fine, texture done on coarse/fine, charcoal present
170-215	40-50	<5%	Si-Cl-L	OB/SF	6,680	sample taken at 180 cm from upstream location, charcoal rich overbank unit
215-230	10-20	50%	LS	SF	7,080	coarser unit that is very charcoal rich in a thin continuous band
230-350	20-30	50%	LS	SF		probably same unit as above but no charcoal present, base of exposure
Site H15: Arroyo site in upper Heath Canyon				Elevation: 2016 m		Coordinates: 42° 03.985N, 113° 43.730W
Depth (cm)	Thickness (cm)	Texture (% >2 mm)	Texture (type)[1]	Process[2]	Age (cal yr BP)	Notes
0-170	0-180	15%	SL	SF	180	sample taken at 40 cm, ~8 sheetflood couplets, surface is 75-100 year old sagebrush, weak soil development A horizon Munsel color: (wet) 10 yr 3/1, charcoal rich throughout, sheetfloods pinch out
170-330	100-150	15%	L/SL	DF	2,240	buried well developed soil, 170-250 cm Munsel color: (wet) 10 yr 2/1, 250-330 cm Munsel color: (wet) 10 yr 2/2, mottled appearance, lightens in color downward
330-335	5-10	15%	Si-L	DF	6,720	abrupt boundary between upper and lower unit, very thin, fine-grained debris flow
335-420	50-60	30%	LS	SF/DF	7,170	5 couplets with absent charcoal, overlying thin debris flow at 420 cm (sampled unit) with abundant charcoal and abundant obsidian fragments (archeological implications??)
420-480	40-45	30%	LS	SF		2 sheetflood couplets, no charcoal
480-485	2-5	<5%	Si	tephra		rich in glass fragments (examined with handlense and under microscope), unidentified ash unit
485-500	10-20	15%	Si-L	DF	9,970	thin charcoal rich debris flow deposit
500-575	50-75	15%	L	OB	11,540	charcoal rich unit, possibly a debris flow but hard to distinguish process type, base of exposure

[1] Texture types: S = sand, Si = silt, Cl = clay, and L = loam.

[2] Process: DF = debris flow, SF = sheetflood, OB = overbank, CF = channel flood, BS = burned surface